

# **Analyses of the Life Cycle of *TLC1* and the Nuclear RNA Quality Control System in *Saccharomyces cerevisiae***

## **Dissertation**

for the award of the degree

**“Doctor of Philosophy” (Ph.D.)**

Division of Mathematics and Natural Sciences  
of the Georg-August-Universität Göttingen

within the basic program biology  
of the Georg-August University School of Science (GAUSS)



submitted by

**Haijia Wu**

Born in Wuhan, China

**Göttingen, March 2015**

## **Members of the Thesis Committee**

### **Prof. Dr. Heike Krebber**

Department of Molecular Genetics, Institute of Microbiology and Genetics,  
Georg-August University Göttingen

### **PD Dr. Wilfried Kramer**

Department of Molecular Genetics, Institute of Microbiology and Genetics,  
Georg-August University Göttingen

## **Members of the Examination Board**

### **Prof. Dr. Heike Krebber** (1<sup>st</sup> reviewer)

Department of Molecular Genetics, Institute of Microbiology and Genetics,  
Georg-August University Göttingen

### **PD Dr. Wilfried Kramer** (2<sup>nd</sup> reviewer)

Department of Molecular Genetics, Institute of Microbiology and Genetics,  
Georg-August University Göttingen

### **Prof. Dr. Gerhard Braus**

Department of Molecular Microbiology and Genetics, Institute of Microbiology  
and Genetics, Georg-August University Göttingen

### **Prof. Dr. Ralf Ficner**

Department of Molecular Structural Biology, Institute of Microbiology and  
Genetics, Georg-August University Göttingen

### **Prof. Dr. Kai Heimel**

Department of Molecular Microbiology and Genetics, Institute of Microbiology  
and Genetics, Georg-August University Göttingen

### **Prof. Dr. Stefanie Pöggeler**

Department of Genetics of Eukaryotic Microorganisms, Institute of Microbiology  
and Genetics, Georg-August University Göttingen

Date of oral examination: 23. April.2015

## Declaration

I hereby confirm that this thesis entitled:

“Analyses of the Life Cycle of *TLC1* and the Nuclear RNA Quality Control System in *Saccharomyces cerevisiae*”

has been written independently and with no other sources and aids than quoted.

Haijia Wu

Göttingen, March, 2015

Parts of this work were published in:

Wu, H., Becker, D., and Krebber, H. (2014). Telomerase RNA *TLC1* shuttling to the cytoplasm requires mRNA export factors and is important for telomere maintenance. *Cell reports* 8, 1630-1638.

## Table of Contents

1.	Abstract .....	1
2.	Introduction .....	2
2.1	Telomeres and telomerase .....	2
2.1.1	Telomeres .....	2
2.1.1.1	The structure of telomeres.....	2
2.1.1.2	Telomere binding proteins .....	3
2.1.2	Telomerase .....	6
2.1.2.1	Telomerase components .....	6
2.1.2.2	Telomerase function.....	7
2.1.2.3	<i>TLC1</i> and the telomerase life cycle .....	9
2.2	RNA nuclear processing and quality control .....	13
2.2.1	RNA processing and export .....	13
2.2.1.1	Non-coding RNA processing .....	13
2.2.1.2	RNA nuclear export .....	13
2.2.2	RNA nuclear quality control .....	15
2.2.2.1	The TRAMP complex .....	15
2.2.2.2	The nuclear exosome .....	16
3.	Materials and methods .....	18
3.1	Materials .....	18
3.1.1	Chemical and consumables.....	18
3.1.2	Enzymes and antibodies.....	20
3.1.3	Instruments and software .....	21
3.1.4	Strains, plasmids and oligonucleotides .....	22
3.1.4.1	Strains.....	22
3.1.4.2	Plasmids .....	26
3.1.4.3	Oligonucleotides.....	28
3.2	Methods .....	31
3.2.1	General methods.....	31
3.2.1.1	Generation of strains, plasmids and oligonucleotides .....	31
3.2.1.2	Media and plates.....	32
3.2.1.3	Cell cultivation .....	33
3.2.1.4	Yeast sporulation and tetrad analysis.....	35
3.2.1.5	Yeast cell lysis .....	37
3.2.1.6	Preparation of microscope slides .....	39
3.2.1.7	Applications of the microscopes .....	39
3.2.1.8	Signal detection, quantification and statistical analyses .....	40
3.2.2	Biochemical methods.....	41
3.2.2.1	Protein extraction and precipitation .....	41
3.2.2.2	Co-immunoprecipitation (IP or co-IP) .....	41
3.2.2.3	Nucleo-cytoplasmic fractionation .....	43
3.2.2.4	SDS-polyacrylamide gel electrophoresis (SDS-PAGE) and western blot..	44

3.2.3	Molecular biological methods.....	47
3.2.3.1	Polymerase chain reaction (PCR) .....	47
3.2.3.2	DNA gel electrophoresis and gel extraction .....	48
3.2.3.3	Genomic DNA extraction.....	49
3.2.3.4	Acidic phenol RNA extraction.....	50
3.2.3.5	Probe synthesis .....	51
3.2.3.6	Southern blot .....	52
3.2.3.7	RNA-co-immunoprecipitation (RNA-co-IP).....	54
3.2.3.8	Quantitative reverse transcriptase PCR (qRT-PCR).....	55
3.2.4	Cell biological methods .....	57
3.2.4.1	Transformation .....	57
3.2.4.2	Immunofluorescence (IF) .....	59
3.2.4.3	RNA fluorescent <i>in situ</i> hybridization (FISH).....	60
4.	Results.....	63
4.1	<i>TLC1</i> Transport.....	63
4.1.1	<i>TLC1</i> nuclear export.....	63
4.1.1.1	Fluorescent <i>in situ</i> hybridization experiments reveal that the nuclear export of <i>TLC1</i> requires the mRNA export machinery .....	63
4.1.1.2	Nucleo-cytoplasmic fractionation shows decreased cytoplasmic abundance of <i>TLC1</i> upon blocking the mRNA export pathway.....	67
4.1.1.3	The mRNA export factors physically interact with <i>TLC1</i> .....	69
4.1.1.4	The <i>TLC1</i> nuclear export block observed in mRNA export mutants is not due to impaired <i>TLC1</i> transcription or maturation .....	71
4.1.1.5	The <i>TLC1</i> nuclear export is mediated through cooperation of Xpo1/Crm1 and the mRNA export factor .....	74
4.1.2	A <i>TLC1</i> export block affects telomerase formation .....	76
4.1.2.1	<i>TLC1</i> cytoplasmic deficiency leads to impaired localisation of the telomerase components .....	76
4.1.2.2	Less <i>TLC1</i> -Est2 interactions are formed due to the <i>TLC1</i> nuclear retention	81
4.1.2.3	Reduction of the <i>TLC1</i> cytoplasmic presence affects the interaction between the telomerase components.....	83
4.1.3	Analyses of the <i>mex67-5 xpo1-1</i> double mutant on <i>TLC1</i> nuclear export .....	87
4.1.3.1	The <i>mex67-5 xpo1-1</i> double mutant shows a stronger <i>TLC1</i> nuclear accumulation and an increased rate of <i>TLC1</i> processing .....	87
4.1.3.2	The cytoplasmic mislocalisation of a telomerase component is increased in the <i>xpo1-1 mex67-5</i> double mutant.....	91
4.1.3.3	Telomere maintenance is impaired in the double mutant <i>xpo1-1 mex67-5</i>	93
4.1.3.4	Xpo1/Crm1 is directly involved in <i>TLC1</i> nuclear export.....	96
4.2	The processing of <i>TLC1</i> .....	99
4.2.1	The transcription and processing defects of <i>TLC1</i> in the <i>mtr10Δ</i> strain is not due to its effect on <i>TLC1</i> transport.....	99
4.2.2	The factors involved in <i>TLC1</i> processing are identified by qRT-PCR analyses	101

4.2.3	The factors involved in the processing of <i>TLC1</i> are mis-localised in the <i>mtr10Δ</i> mutant	105
4.2.4	Mtr10 physically interacts with factors that are involved in the processing of <i>TLC1</i>	107
4.3	Conclusions	109
5.	Discussion and Perspective	111
5.1	The life cycle of the telomerase complex	111
5.2	RNA nuclear export	114
5.3	Mtr10 and its cargoes	115
6.	References	117
	Acknowledgments	130
	<i>Curriculum Vitae</i>	131

# 1. Abstract

During genome replication, chromosomes undergo a progressive shortening of their ends. To counteract this loss, a complex named telomerase functions as a reverse transcriptase to elongate telomeres. In *Saccharomyces cerevisiae*, telomerase contains a non-coding RNA, *TLC1*, which serves as a scaffold for formation of the telomerase complex and the template for the reverse transcription to elongate the telomeres. Upon its synthesis, *TLC1* undergoes a series of nuclear and cytoplasmic maturation steps.

Here it has been shown that the *TLC1* nuclear export is dependent on the classic mRNA export pathway in addition to the already known Crm1/Xpo1 pathway. The nuclear export defects that occur upon mutation of these pathways impair the formation of the telomerase, as well as its final localisation suggesting an essential role of *TLC1* shuttling in telomerase assembly. Consequently, the *TLC1* nuclear transport defect leads to telomeric shortening indicating a necessity of the *TLC1* shuttling for telomere maintenance. Moreover, the nuclear RNA quality control system, composed of the TRAMP complex and nuclear exosome, might mediate the nuclear maturation of *TLC1*. Finally, it has also been pointed out that the localisation and maturation of the nuclear quality control system might be regulated by a nuclear importer, Mtr10, which is also involved in *TLC1* nuclear import.

## **2. Introduction**

### **2.1 Telomeres and telomerase**

#### **2.1.1 Telomeres**

The genome contains all cellular information important for its own synthesis, cell growth, differentiation and death. This information is transferred from generation to generation through chromosome replication. However, due to the mechanism of DNA replication the linear chromosomes of eukaryotes are not able to be fully duplicated leading to the loss of genomic content during each reproduction cycle (Olovnikov, 1971; Watson, 1972), consequently resulting in cellular defects, aging and death (Harley et al., 1990; Hayflick, 1979; Lundblad and Szostak, 1989). Besides, double-stranded DNA breaks (DSBs) are particularly harmful to the cell due to causing chromosome rearrangements. To distinguish DSBs from authentic chromosome ends is another challenge that an organism must face (Dewar and Lydall, 2012). To solve these critical problems cells evolved variable mechanisms including a special chromosome end nucleoprotein structure named the telomere, which is able to efficiently maintain the stability and integrity of the genome.

##### **2.1.1.1 The structure of telomeres**

Telomeres are conserved on their structure throughout the eukaryotic organisms. The structure of a yeast telomere is shown in figure 2.1A. The yeast chromosome ends consist of two subtelomeric regions, X and Y' elements, and one telomeric region (reviewed in (Kupiec, 2014; Wellinger and Zakian, 2012)).

X elements, containing two subregions: Core X and subtelomeric repeated elements (Louis et al., 1994), are present in almost all chromosome ends with slight differences in size and sequence. Y' elements are separated by telomeric repeats from X elements and present in 0-4 tandem repeats (Chan and Tye, 1983).



The length of the telomeric region varies from yeast (*ca.* 350bp) to mammals (several kb). The yeast telomeric sequence is mainly composed of simple repeats that are usually described as C<sub>1-3</sub>A/TG<sub>1-3</sub>. In addition, these sequence repeats are also found at the border between X and Y' element, as well as Y' and Y' elements. However, compared to those in X and Y' elements, the repeats in the telomeric region are more important because deletion of these sequence results in a high genomic instability and the loss of chromosomes (Lundblad and Szostak, 1989; Shampay et al., 1984; Szostak and Blackburn, 1982). This telomeric region can be extended by a reverse transcriptase complex termed telomerase containing an RNA template. Unlike many other organisms, the telomeres of *Saccharomyces cerevisiae* are irregular and heterogeneous because only a partial RNA template of the telomerase is used for each elongation cycle and diverse short template regions are copied in different elongation rounds (Forstemann and Lingner, 2001). Furthermore, through sequencing it has been shown that the cells from a single colony contain exact identical sequences in the internal half of telomeric region; however, more dynamic combinations are found in the external half, which is therefore thought to be involved in degradation and elongation of the telomeres (Wang and Zakian, 1990). Moreover, a 3'-single strand G-rich tail is present at the very end of the chromosome. These G tails are usually 12-15 nucleotides long throughout the cell cycle except during a short period in late S/G1 phase in which it contains 30-200 nucleotides (Larrivee et al., 2004; Wellinger et al., 1993a, b).

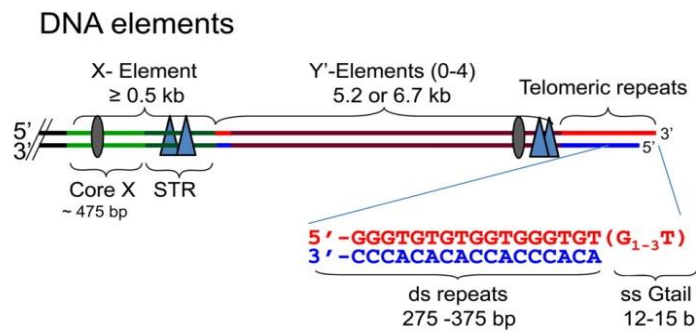
### **2.1.1.2 Telomere binding proteins**

There are a number of proteins that bind to the subtelomeric or telomeric region, directly or indirectly, continuously or transiently, functionally or structurally.

The intrinsic components of the telomeres (figure 2.1B) include Rap1 (Repressor Activator Protein), Rif complex (Rif1 and Rif2, Rap1-Interacting Factor), SIR proteins (Sir2, Sir3 and Sir4, Silent Information Regulator), the CST complex (Cdc13 (Cell Division Cycle), Stn1 (Suppressor of Cdc Thirteen) and Ten1 (Telomeric pathways with STN1)) and the Ku heterodimer (Yku70 and Yku80, Yeast Ku protein).

In wild type cells 15-20 copies of Rap1 bind to each single telomere with the distance of *ca.* 20 base pairs and are the central factors in determining telomere length (Conrad et al., 1990; Gilson et al., 1993; Lustig et al., 1990; Ray and Runge, 1999a, b; Wright and Zakian, 1995). There are key interaction regions for Sir3/4 as well as for Rif1/2 binding present in the C-terminus of Rap1 (Hardy et al., 1992a; Hardy et al., 1992b; Moretti et al., 1994; Wotton and Shore, 1997). Both Rif1 and Rif2 function as negative regulators in telomere elongation (Hardy et al., 1992a; Hardy et al., 1992b; Wotton and Shore, 1997), probably through being involved in the telomere capping, which prevents the access of the double-stranded DNA breaks (DSBs) repair system through covering the telomeres with short telomeric repeats (Ribeyre and Shore, 2012). The SIR complex, composed of Sir2, Sir3 and Sir4, is mainly involved in telomeric silencing by interacting with histones (Gottschling et al., 1990; Pryde and Louis, 1999). Besides, the yeast Ku complex contains two proteins, Yku70 and Yku80, playing the central role in the non-homologous end-joining (NHEJ) machinery and the telomere maintenance (Bonetti et al., 2010a; Bonetti et al., 2010b; Gilson et al., 1993;

### A Telomere Components



### B Main protein components

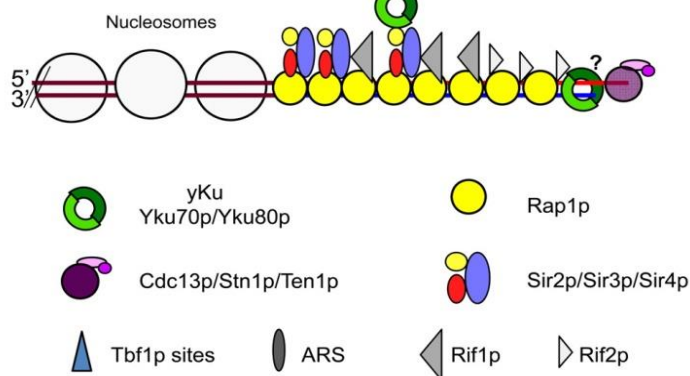


**Figure 2.1 Telomeric DNA structure and protein components in *S. cerevisiae*.**

(A) Schematic representation of the subtelomeric X and Y' elements as well as the telomeric terminal repeat sequences. Red strand: G-rich strand with 3' overhanging end. Blue strand: C-rich strand.

(B) Schematic representation of the telomere bound proteins. Open circles represent nucleosomes.

Figure adapted from (Wellinger and Zakian, 2012).

Palladino et al., 1993; Porter et al., 1996; Vodenicharov and Wellinger, 2007). The Ku complex participates in tethering the telomeres to the perinuclear region (Martin et al., 1999). Furthermore, the Ku complex is able to interact with telomerase RNA (*TLC1*, TeLomerase Component) and assist the localisation of the telomerase in the nucleus (Gravel et al., 1998; Rathmell and Chu, 1994; Roy et al., 2004; Taccioli et al., 1994). However, the Ku complex might not recruit the telomerase onto the telomeres because of the recent study showing a mutually exclusive recruitment of *TLC1* and telomeres by the Ku complex (Pfungsten et al., 2012). Moreover, the other conventional component on telomeres is the CST complex consisting of Cdc13, Stn1 and Ten1. The functions of Stn1 and Ten1 are poorly understood. The core component of the CST complex is Cdc13, which has high affinity and specificity to bind to single-stranded TG<sub>1-3</sub> DNA *in vitro* (Hughes et al., 2000b; Lin and Zakian, 1996; Mitton-Fry et al., 2002; Mitton-Fry et al., 2004; Nugent et al., 1996) and telomeres *in vivo* (Bourns et al., 1998; Tsukamoto et al., 2001) through its DNA binding domain (Hughes et al., 2000b). Besides, Cdc13 contains a recruitment domain on its N-terminal end, which interacts with Est1 of the telomerase complex and recruits it onto telomeres (Nugent et al., 1996; Pennock et al., 2001; Wu and Zakian, 2011).

In addition, some components are present on telomeres only transiently in given cell cycle phases, *e.g.* the telomerase complex. As mentioned above, the telomerase is able to be recruited onto the telomeres via an interaction of one of its components, Est1, with Cdc13 in late S phase of the cell cycle (Evans and Lundblad, 1999; Taggart et al., 2002). Furthermore, some DSB recognition factors are also involved in maintaining the telomere length, *e.g.* Tel1 (TELomere maintenance) and the MRX complex (Mre11 (Meiotic REcombination), Rad50 (RADiation sensitive), Xrs2 (X-Ray Sensitive)). Tel1 is recruited onto DSBs and telomeres via the MRX complex (Nakada et al., 2003; Shima et al., 2005). Lacking of Tel1 or of MRX components leads to short, however stable telomeres (Boulton and Jackson, 1998; Kironmai and Muniyappa, 1997; Tsukamoto et al., 2001). The functions of these factors are proposed to be to participate in the telomerase recruitment (Bianchi and Shore, 2007; Hector et al., 2007; Mantiero et al., 2007; Sabourin et al., 2007).

## 2.1.2 Telomerase

During DNA replication in eukaryotic cells, DNA polymerases extend short RNA primers composed of 8-12 nucleotides through adding nucleotides to their 3'-end. DNA polymerases extend one DNA strand in the direction of the growing replication fork (leading strand) and the other strand in a discontinuous fashion which requires many RNA primed Okazaki fragments (lagging strand). The RNA primers subsequently are removed and the gaps are filled and ligated (Olovnikov, 1971; Watson, 1972). However, this leaves two end-replication problems: first, removal of the very start RNA primers results in a shorter newly synthesised product (Watson, 1972); second, although there is an essentiality of 3' single-stranded G-tails at the end of eukaryotic chromosomes, which is important for distinguishing the DSBs and chromosome ends, DNA polymerases generate 3'-blunt ends on the chromosomes created by the leading strands (Lingner et al., 1995). The telomerase has been evolved to solve the first problem through using its integrated RNA template to elongate the chromosome ends by a reverse transcription.

### 2.1.2.1 Telomerase components

The telomerase holoenzyme is composed of Est1, Est2, Est3 and the *TLC1* RNA (Dandjinou et al., 2004; Hughes et al., 2000a; Zappulla and Cech, 2004). The name EST is an abbreviation of “ever shorter telomeres” from a screen for defective telomere function (Lundblad and Szostak, 1989).

Est1 is a protein predicted with 699 amino acids in length (Lundblad and Szostak, 1989) and has the ability to bind both RNA and TG<sub>1-3</sub> single strand DNA that contain 3'-OH ends *in vitro* (DeZwaan and Freeman, 2009; Virta-Pearlman et al., 1996). In its sequence three nuclear localisation signals have been identified that might interact with importin alpha, Srp1 (Hawkins and Friedman, 2014). The expression level of *EST1* is cell cycle regulated: it is low in the telomerase inactive G1 phase (*ca.* 20 molecules/cell) and high in the telomerase active late S/G2 phase (*ca.* 110 molecules/cell) (Taggart et al., 2002; Wu and Zakian, 2011).

Although the telomerase activity is independent of Est1 *in vitro* (Cohn and Blackburn, 1995), Est1 directly binds to a *TLC1* stem loop (Seto et al., 2002) and contributes to the telomeric localisation of the telomerase (Chan et al., 2008) as well as to the telomerase-telomere recruitment via direct interaction with Cdc13 *in vivo* (Evans and Lundblad, 1999; Qi and Zakian, 2000; Wu and Zakian, 2011). In addition, Est1 is predicted to activate telomerase through recruiting Est3 onto the complex (Tuzon et al., 2011).

Est2 confers the activity of the reverse transcriptase to the telomerase (Lingner et al., 1997). Est2 is composed of 884 amino acids and contains a long basic N-terminal region that includes three conserved aspartate residues essential for its activity (Friedman and Cech, 1999; Lingner et al., 1997). In addition, the N-terminus of Est2 bears the ability to interact with *TLC1* and Est3 (Friedman and Cech, 1999; Friedman et al., 2003; Talley et al., 2011). The expression level of *EST2* is quite low (<40 molecules/cell) and *TLC1* dependent (only *ca.* 50% in *tlc1Δ* strain) (Taggart et al., 2002).

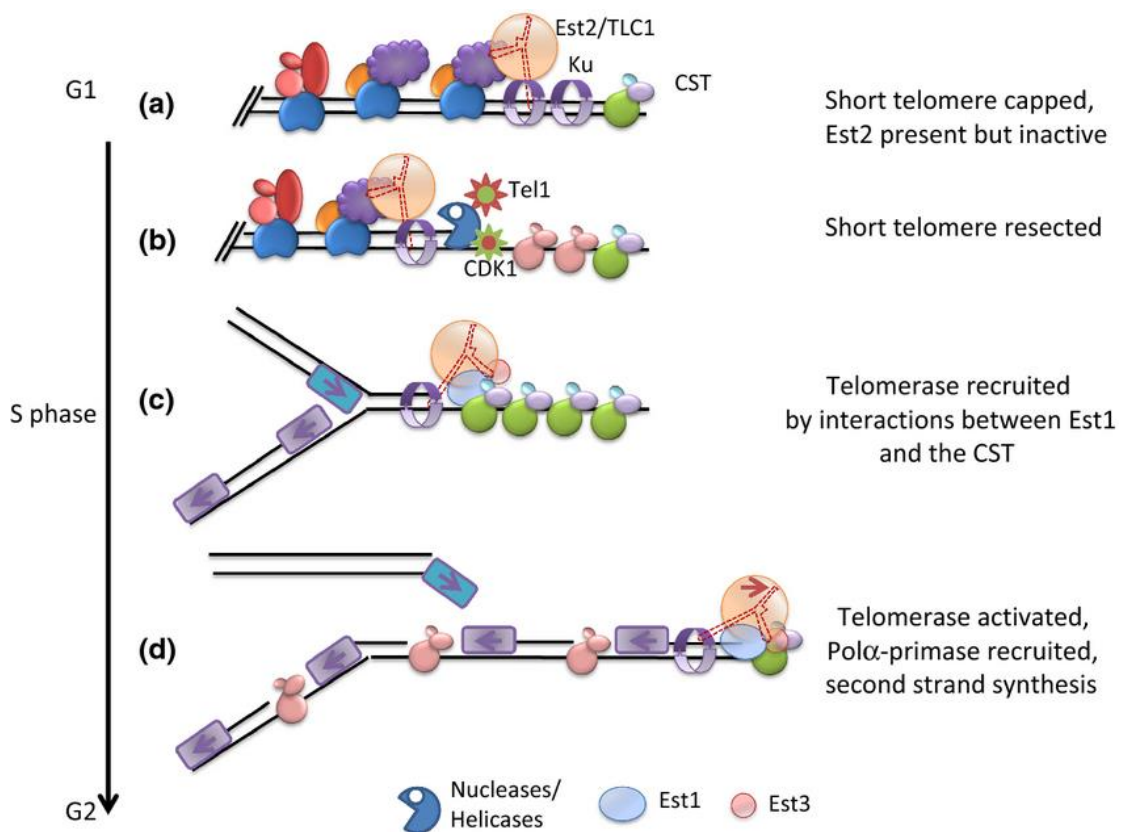
Unlike Est1 and Est2, synthesis of the functional Est3 protein needs a programmed translational frameshift (Morris and Lundblad, 1997). The functional, full-length Est3 is a protein with 181 amino acids; a truncated Est3 of 93 amino acids can be formed without the frameshift and its function has not been found yet (Morris and Lundblad, 1997). The full length Est2 interacts with Est1 directly and associates with the telomerase in an Est1 dependent manner (Osterhage et al., 2006; Tuzon et al., 2011). Est3 has also the ability to bind to the long basic N-terminus of Est2 (Friedman et al., 2003; Talley et al., 2011) and to telomeres in G1 phase with yet unknown functions (Tuzon et al., 2011).

*TLC1* (Telomerase Component) is a low abundant RNA (*ca.* 30 molecules/cell) longer than 1000 nucleotides; *TLC1* is utilised as a template for reverse transcription and a scaffold for the formation of the telomerase complex (Mozdy and Cech, 2006; Singer and Gottschling, 1994).

### **2.1.2.2 Telomerase function**

The telomerase carries out the addition of the telomere repeats using its reverse

transcriptase activity at the end of the S phase of the cell cycle (Raghuraman et al., 2001). The recruitment of the telomerase onto telomeres is shown in figure 2.2. During G1 and early S phase, only an Est2-*TLC1* complex is recruited via the interaction between the Ku complex and a 48 bp stem loop on *TLC1*; however, this incomplete telomerase is inactive and elimination of the engagement of this complex to telomeres leads to only little telomere shortening (Fisher et al., 2004). Besides, this association is located at >100bp from the end of the chromosomes rather than at the very end of the chromosomes (Sabourin et al., 2007). The active telomerase holoenzyme associates with the telomeres in late S/G2 phase of the cell cycle (Chan et al., 2008). The association of this active telomerase with telomeres is



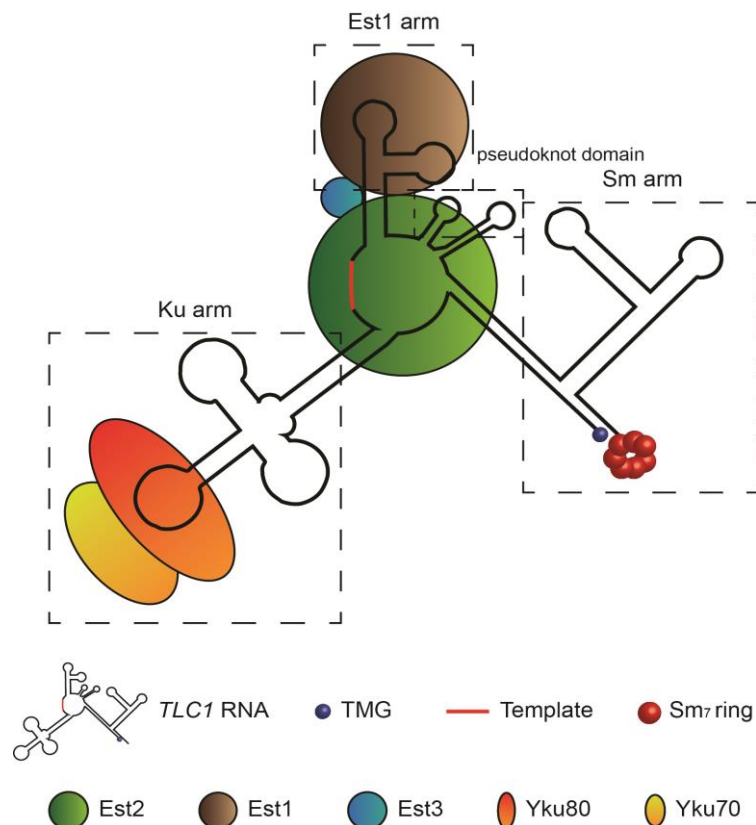
**Figure 2.2 Telomere replication.** (a) In G1 phase, Est2-*TLC1*, an incomplete telomerase complex, is inactively present at the telomeres. (b) The chromosome end resection is performed by nucleases and helicases, which are activated by CDK1 and Tel1, to create single strand DNA platforms for association of the CST complex. (c) The telomerase holoenzyme is loaded via interactions between Est1 and the CST complex. (d) The active telomerase holoenzyme elongates the G-rich strand and the CST complex recruits the DNA polymerase alpha-primase, a subunit of the DNA polymerase alpha, to complete the DNA replication.

Figure adapted from (Kupiec, 2014).

related to the interaction between Est1 and Cdc13. In late S/G2 phase the telomeric binding level of Cdc13 is dramatically increased for facilitating an enhanced recruitment of the telomerase holoenzyme onto the telomeres (Chan et al., 2008; Taggart et al., 2002). Upon association, the telomerase uses short stretches within the sequence 5'-CACACACCCACACCAC-3' in *TLC1* as templates to elongate telomeres in a heterogeneous fashion (Forstemann and Lingner, 2001; Lin et al., 2004).

### 2.1.2.3 *TLC1* and the telomerase life cycle

Around 90% of *TLC1* is non-polyadenylated and consists of 1157 nucleotides (poly(A)<sup>-</sup> *TLC1*);



**Figure 2.3 *TLC1* is a scaffold in constructing the telomerase.** Yku80, Est2 and Est1 bind to *TLC1*. Est3 is involved in telomerase formation through interaction with Est2. However, Est3 is also able to interact with Est1. The Sm<sub>7</sub> ring binds to the 3'-end of *TLC1* important for its processing and stabilization. Besides, *TLC1* contains a TMG Cap structure, which is common in RNA polymerase II produced non-coding RNA, and a core sequence (red part of *TLC1*), which is utilised as the template for reverse transcription.

however, 5-10% of *TLC1* exists in longer polyadenylated forms that differ in the length of the 3'-parts and polyadenylation tails (poly(A)<sup>+</sup> *TLC1*) (Bosoy et al., 2003; Chapon et al., 1997; Noel et al., 2012). Only the form of poly(A)<sup>-</sup> *TLC1* is incorporated in the mature telomerase (Bosoy et al., 2003).

The active poly(A)<sup>-</sup> *TLC1* is the scaffold for composition of the telomerase (figure 2.3). In addition to the core region, which includes the template for reverse transcription, *TLC1* contains a domain for association of the reverse transcriptase Est2 and a conserved pseudoknot domain with yet unknown function, which is however usually thought to be important for maintaining the secondary structure (Dandjinou et al., 2004; Lin et al., 2004; Livengood et al., 2002; Qiao and Cech, 2008; Zappulla and Cech, 2004). Furthermore, *TLC1* possesses three other duplex arms, termed Est1 arm, Ku arm and Sm arm. The Est1 arm is the interaction region of Est1, which is essential for the telomerase activity *in vivo* (Seto et al., 2002). The Ku complex binds to the Ku arm and this interaction is essential for nuclear localisation of the telomerase and its telomeric recruitment in the G1 phase of the cell cycle (Fisher et al., 2004; Gallardo et al., 2008; Stellwagen et al., 2003; Vega et al., 2007). Nevertheless, compared to the telomerase RNA in ciliates (ca. 160 nucleotides) or mammalian cells (ca. 450 nucleotides), the size of the *TLC1* of *Saccharomyces cerevisiae* is much larger (Singer and Gottschling, 1994) and an artificial 384-nucleotide *TLC1* lacking most non-protein-binding regions is still able to maintain stable telomeres *in vivo* (Zappulla et al., 2005).

The life cycle of *TLC1* and the telomerase is demonstrated in figure 2.4. *TLC1* shares many features with some classes of small nuclear RNAs (snRNAs), which are involved in mRNA splicing. Similar to other RNA polymerase II products, *e.g.* mRNAs, snRNAs, *etc.*, *TLC1* is initially capped with 7-monomethyl guanosine (m<sup>7</sup>G) and tailed with poly-adenylates (Abou Elela and Ares, 1998; Chapon et al., 1997; Seipelt et al., 1999). However, like some classes of snRNAs but unlike mRNAs, the poly-adenylated *TLC1* receives a seven-Sm protein (Smb1, Smd1, Smd2, Smd3, Sme1, Smx2 and Smx3, *abbr.* Sm<sub>7</sub>) ring that binds near its 3' end and this association triggers two subsequent events: 5' hypermethylation and 3' degradation (Seto et al., 1999). In budding yeast, the hypermethylation converts the m<sup>7</sup>G cap into a



2,2,7-trimethylguanosin (TMG) cap in the nucleolus through the methyltransferase Tgs1 (TrimethylGuanosine Synthase), which is also involved in the cap hypermethylation of snRNAs and small nucleolar RNAs (snoRNAs) (Franke et al., 2008). It must be noted that in higher eukaryotes snRNAs shuttle to the cytoplasm to acquire the Sm<sub>7</sub> ring and to be hypermethylated due to the cytoplasmic localisation of the Sm proteins and Tgs1 and subsequently these modifications promote the nuclear re-import of snRNAs (reviewed in (Matera et al., 2007)). Also similar to snRNAs, in the 3' end region of poly(A)<sup>+</sup> *TLC1* a Nab3 (Nuclear polyAdenylated RNA-Binding) and an Nrd1 (Nuclear pre-mRNA Down-regulation) binding site have been identified (Noel et al., 2012) indicating that *TLC1* undergoes 3' modification through the Nrd1-Nab3-Sen1 pathway, which is one of the pathways that mediates RNA polymerase II transcription termination (Steinmetz et al., 2001; Vasiljeva et al., 2008). This pathway is thought to trigger the nuclear RNA exosome to remove the poly(A)<sup>+</sup> tail of *TLC1* under the protection of the Sm<sub>7</sub> complex (Coy et al., 2013; Noel et al., 2012). *TLC1* undergoes a nucleo-cytoplasmic shuttling supposed to be important for maturation of the telomerase complex (Ferrezuelo et al., 2002; Gallardo et al., 2008). Similar to the snRNA transport in metazoan (reviewed in (Hopper, 2006)), the nuclear export of *TLC1* has been identified to be mediated by the Crm1/Xpo1 pathway (Gallardo et al., 2008), which mainly uses the Ran/GTPase dependent exportin Xpo1 (EXPORTIN)/Crm1 (Chromosome Region Maintenance) to transport large macromolecules from the nucleus to cytoplasm (Neville et al., 1997; Stade et al., 1997). *TLC1* cytoplasmic presence is thought to be important for the telomerase formation, where *TLC1* assembles with the Est protein components (reviewed in (Gallardo and Chartrand, 2008)). After assembly of the Est proteins in the cytoplasm, *TLC1* is re-imported into the nucleus via nuclear import receptors, Mtr10 (Mrna TRansport defective) and Pdr6/Kap122 (KARYOPherin) (Ferrezuelo et al., 2002; Gallardo et al., 2008). Interestingly, recent data show an unexpected Mtr10-independent nuclear import pathway for Est1, which is mediated by the importin alpha, Srp1 (Suppressor of RPB1), and these data suggest an alternative nuclear import pathway for telomerase components (Hawkins and Friedman, 2014).

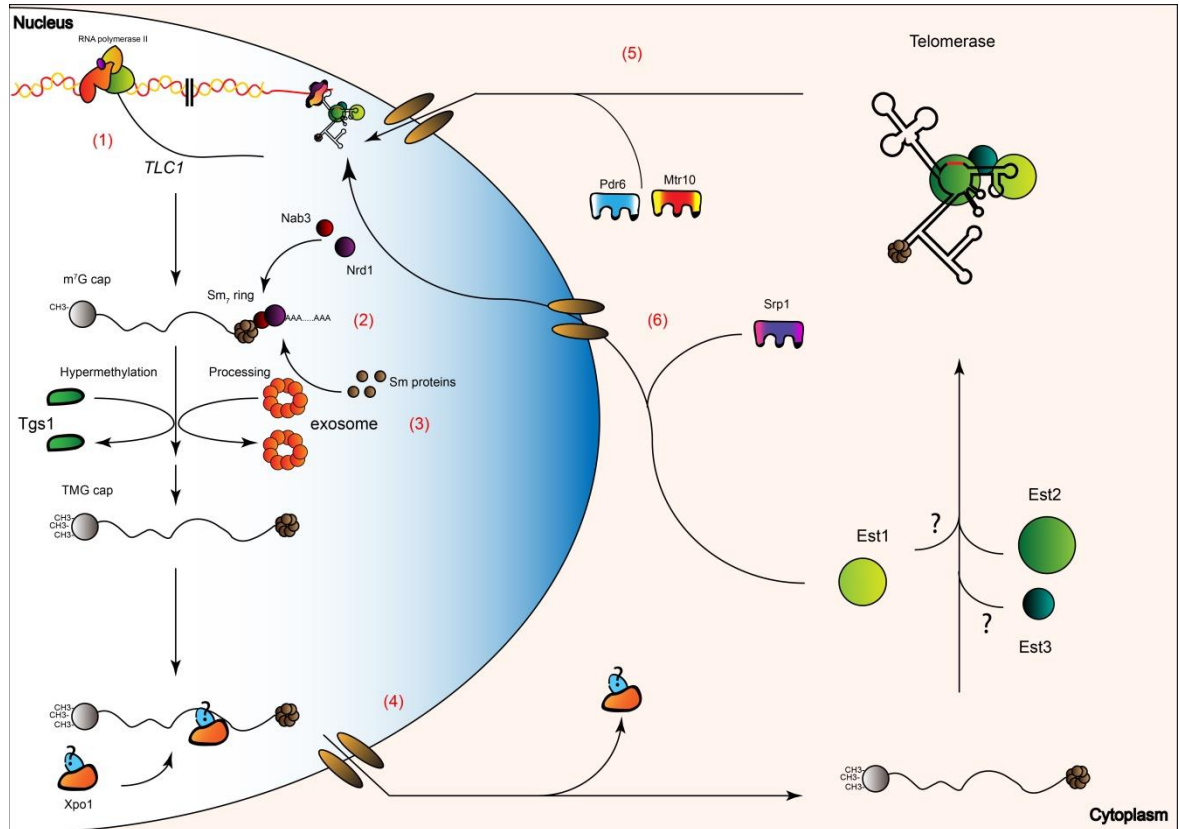


**Figure 2.4 The life cycle of *TLC1* and the telomerase.** (1) *TLC1* is synthesised by RNA polymerase II. (2) Immature *TLC1* contains a poly(A)<sup>+</sup> tail and m<sup>7</sup>G cap. On its 3' part its Sm, Nab3 and Nrd1 binding sites are recognised by the Sm<sub>7</sub> ring complex, Nab3 and Nrd1, respectively. (3) The association of the Sm<sub>7</sub> complex and Nab1-Nrd1 transcription termination complex on *TLC1* triggers a hypermethylation of the 5'-m<sup>7</sup>G cap by Tgs1 and a trimming of the 3'-poly(A)<sup>+</sup> tail by the nuclear exosome. (4) Modified *TLC1* is exported into the cytoplasm via the Crm1/Xpo1 pathway, which is mediated by the exportin Xpo1/Crm1 with a so far unknown adaptor. (5) In the cytoplasm *TLC1* associates with Est proteins and the complex is subsequently re-imported into the nucleus by Mtr10 and Pdr6/Kap122. (6) Est1 is also supposed to be independently re-imported by Srp1.

## 2.2 RNA nuclear processing and quality control

### 2.2.1 RNA processing and export

#### 2.2.1.1 Non-coding RNA processing

In yeast, the non-coding RNAs transcribed by RNA polymerase II have several classes including, small nuclear RNA (snRNA), small nucleolar RNA (snoRNA), stable unannotated transcripts (SUTs), cryptic unstable transcripts (CUTs), Xrn1 stabilised transcripts (XUTs), telomerase RNA (*TLC1*), *etc.* In contrast to the differentiation between non-coding RNA and mRNA in their promoter regions in mammalian cells (de Vegvar et al., 1986; Hernandez and Weiner, 1986; Richard and Manley, 2009), in yeast one of the differentiations between the non-coding RNA produced by RNA polymerase II and mRNA is in the way of how transcription termination takes place. Predominantly, snRNA, snoRNA, CUTs and *TLC1* use an Nrd-Nab3-Sen1 pathway (also referred to NRD pathway) to mediate their termination and processing (Arigo et al., 2006; Noel et al., 2012; Steinmetz et al., 2001). Although only partially understood, these RNA are co-transcriptionally protected and stabilised by recruitment of the specific protein components: H/ACA or C/D-box proteins for snoRNA and Sm family proteins for snRNA and *TLC1*. Besides, the multi-heterodimer Nrd1 (Nuclear pre-mRNA Down-regulation)-Nab3 (Nuclear polyAdenylated RNA-Binding) complexes also bind to their recognition sites, the 5'-UCUUG-3' motif for Nab3 and the 5'-(U/A)GUA(A/G)-3' motif for Nrd1 (Carroll et al., 2004; Creamer et al., 2011; Morlando et al., 2002). This binding leads to a shortening of the 5'-end by Lsm2-8 (Kufel et al., 2004) and Rat1 and the 3'-end by the exosome (reviewed in (Slomovic and Schuster, 2011)).

#### 2.2.1.2 RNA nuclear export

The nucleus is separated from the cytoplasm by the nuclear envelope. Nuclear transport occurs through the nuclear pore complex (NPC). RNA is packaged into a large

ribonucleoprotein complex (RNP) and leaves the nucleus through a series of interactions.

Although in mammalian cells snRNA and snoRNA are exported to the cytoplasm via the CRM1 pathway (Hamm and Mattaj, 1990; Izaurralde et al., 1995; Ohno et al., 2000), whether these non-coding RNA do so in yeast still remains mysterious.

Furthermore, in *Saccharomyces cerevisiae*, mRNA nuclear export is primarily mediated by the export receptor heterodimer Mex67 (MRNA EXport factor of 67 kDa)-Mtr2 (Mrna TRansport) (Segref et al., 1997), which is able to interact with the phenylalanine-glycine (FG) repeats in the NPC-proteins (Bachi et al., 2000; Grant et al., 2002; Gwizdek et al., 2006; Hobeika et al., 2009; Katahira et al., 1999; Suyama et al., 2000). On its N-terminus, Mex67 possesses an RNP domain and next to it a leucine-rich region, both of which are required for its interactions with RNA and RNA adaptor proteins (Kang and Cullen, 1999; Liker et al., 2000). The proper transcript-protein complexes pass through the NPC and reach its cytoplasmic side. At the cytoplasmic face of the NPC, Rat7 (Ribonucleic Acid Trafficking)/Nup159 (NUclear Pore) docks the ATP-dependent RNA helicase, Rat8/Dbp5 (Dead Box Protein), at the NPC (Del Priore et al., 1997; Hodge et al., 1999; Weirich et al., 2004). Both of Rat7/Nup150 and Rat8/Dbp5 are important for dissociation of mRNP factors, e.g. Mex67, from the mRNA and this dissociation is thought to create the directionality for mRNA export (reviewed in (Tieg and Krebber, 2013)).

## 2.2.2 RNA nuclear quality control

Through investigation of the model organism, *Saccharomyces cerevisiae*, two complexes have been identified that are involved in the degradation of faulty mRNAs in the nucleus (LaCava et al., 2005; Van Hoof et al., 2000a; Vanacova et al., 2005), the TRAMP complex (LaCava et al., 2005) and the RNA exosome (Mitchell et al., 1997). In addition, these two complexes have been shown to contribute to the maturation of many non-coding RNAs (Allmang et al., 2000; Coy et al., 2013; Van Hoof et al., 2000a).

### 2.2.2.1 The TRAMP complex

In *Saccharomyces cerevisiae*, the TRAMP complex is composed of a nuclear 3'-5' RNA helicase (Mtr4, MRNA TRansport), a protein containing zinc knuckle domains (Air1 or Air2, Arginine methyltransferase-Interacting RING finger protein) and a non-canonical poly(A) polymerase (Trf4 or Trf5, Topoisomerase one-Related Function), which gives the name of TRAMP4 or TRAMP5; the TRAMP complexes mark faulty RNAs by adding short poly(A)<sup>+</sup> sequences on their 3' tail and this polyadenylation supplies an extended single strand platform to load the nuclear exosome and trigger degradation (Dez et al., 2007; Egecioglu et al., 2006; Houseley and Tollervy, 2006; Kadaba et al., 2004; Kadaba et al., 2006; Paolo et al., 2009; Wyers et al., 2005).

Like the canonical poly(A) polymerase Pap1 (Poly(A) Polymerase), Trf4/5 contains a similar catalytic central domain (Vanacova et al., 2005), which allows an addition of 10-50 adenosine residues at the end of RNA that is shorter than the 60-80 nucleotides poly(A)<sup>+</sup> tail obtained from Pap1 (reviewed in (Eckmann et al., 2011)). Mtr4 is a 3'-5' RNA helicase that consists of an ATPase core of DExH helicase, which is defined by six conserved peptide motifs (de la Cruz et al., 1999), and a unique arch domain similar to some ribosomal proteins (Jackson et al., 2010; LaCava et al., 2005; Weir et al., 2010). In the presence of Mtr4, the polymerase activity of Trf4/5 is suppressed and the poly(A)<sup>+</sup> tail is limited to 3-5 adenosine residues (Jia et al., 2011). Although Trf4/5 marks RNA with this short poly(A)<sup>+</sup> tail, these proteins are lack of the

ability to associate with RNA, which is however supplied by Air1/2 in the TRAMP complex (Holub et al., 2012; van Hoof et al., 2000b). Air1/2 contains 5 conserved Zinc knuckle motifs, which are involved in both protein-protein and protein-RNA interaction (Fasken et al., 2011). These interactions bridge recognition and polyadenylation on the RNAs and facilitate the degradation of these substrates by the exosome (Fasken et al., 2011; Hamill et al., 2010; Holub et al., 2012). Strikingly, the interaction between Trf4/5 and Mtr4 is Air-independent but requires the helicase core of Mtr4 (Jackson et al., 2010; LaCava et al., 2005; Weir et al., 2010). With this interaction, Trf4/5 is also able to promote the activity of Mtr4 to unwind the highly structured RNA and expose a 3'-ssRNA tail, which can be captured by the exosome (Vanacova et al., 2005).

In addition to RNA degradation, the TRAMP complex has also been proposed to participate in some non-coding RNA transcription termination, e.g. *SNR65* and *SNR13* (Small Nucleolar RNA), by connecting the RNAs to the NRD pathway (Grzechnik and Kufel, 2008; Tudek et al., 2014).

Furthermore, although compositions vary, the differentiation between TRAMP4 and TRAMP5 remains still unclear. Since there are slight differences in their localisations, TRAMP4 and TRAMP5 are proposed to preferentially work on the surveillance of diverse classes of substrates (Fasken et al., 2011; Huh et al., 2003; Paolo et al., 2009).

Finally, some components of the TRAMP complex are able to function apart from the complex, e.g. Mtr4. Its association with the exosome leads to the processing of some non-coding RNA independently of the TRAMP complex (de la Cruz et al., 1998; Kadaba et al., 2006; LaCava et al., 2005; Van Hoof et al., 2000a).

### **2.2.2.2 The nuclear exosome**

The core RNA exosome complex contains 10 subunits, Csl4 (Cep1 Synthetic Lethal), Ski6 (Super Killer), Rrp4, Rrp40, Rrp42, Rrp43, Rrp45, Rrp46 (Ribosomal RNA Processing), Mtr3 and Dis3 (chromosome DISjunction). Six of them (Ski6, Rrp42, Rrp43, Rrp45, Rrp46 and Mtr3)

form a hexameric ring structure and three of them (Csl4, Rrp4 and Rrp40) constitute a trimeric cap, which is positioned on top of the hexameric ring and together termed Exo-9 (Liu et al., 2006). Exo-9 possesses catalytic activity only if Dis3 is associated with the hexameric ring on the opposite side of the trimeric cap. Exo-9 together with associated Dis3 is named Exo-10 (reviewed in (Das and Das, 2013)). Dis3 is the only catalytic unit in the core RNA exosome and contains both endo- and exo-ribonuclease activity (Mitchell et al., 1997). In the nucleus the core exosome complex associates with Rrp6, Lrp1 (Like RrP6) and Mpp6 (M-Phase Phosphoprotein) to form the nuclear RNA exosome (Synowsky et al., 2009). The targets of the exosome include a quite wide spectrum of RNAs, comprising both coding and non-coding RNA produced by all three RNA polymerase I, II and III (Gudipati et al., 2012; Schneider et al., 2012). The exosome has been found to degrade most RNA substrates, *e.g.* mRNA, rRNA, snRNA, snoRNA, tRNA and CUT, *etc.*, and this degradation occurs always together with an oligoadenylation (Schneider et al., 2012). Especially in the nuclear mRNA quality control, the nuclear exosome (Exo-10 with Rrp6, Lrp1 and Mpp6) participates in removing aberrant mRNAs, together with additional factors, *e.g.* Rat1, a nuclear 5'-3' exoribonuclease (Bousquet-Antonelli et al., 2000; Burkard and Butler, 2000; Libri et al., 2002; Torchet et al., 2002; Zenklusen et al., 2002).

# 3. Materials and methods

## 3.1 Materials

### 3.1.1 Chemical and consumables

All chemicals, solutions and consumables in this thesis were obtained from the following companies if not stated otherwise:

AppliChem (Munich/Germany), BD Biosciences (Heidelberg/Germany), Carl Roth (Karlsruhe/Germany), GE Healthcare (Freiburg/Germany), Invitrogen (Frankfurt am Main/Germany), Macherey-Nagel (Dueren/Germany), Merck (Darmstadt/Germany), New England Biolabs (Frankfurt am Main/Germany), OMNILAB GmbH (Bremen/Germany), Promega (Mannheim/Germany), Peqlab (Erlangen/Germany), Roche Diagnostics (Mannheim/Germany), Sarstedt (Nuernbrecht/Germany), Serva Feinbiochemika (Heidelberg/Germany), Sigma-Aldrich (Munich/Germany), Thermo Fisher Scientific (Schwerte/Germany), Th. Geyer (Renningen/Germany), VWR International (Darmstadt/ Germany)

<b>Chemical, Consumables</b>	<b>Source</b>
Agarose NEEO Ultra	Carl Roth, Karlsruhe/Germany
Amersham Hybond-N+ Membran	GE Healthcare, Freiburg/Germany
Bacto Yeast nitrogen base	Becton Dickinson, Franklin Lakes/USA
Cy3-Oligo-dT <sub>50</sub>	Biospring, Frankfurt/Germany
DAPI	Merck, Darmstadt/Germany
Deionised Formamide	AppliChem, Munich/Germany
DIG RNA labeling mix, 10x	Roche Diagnostics, Mannheim/Germany
dNTPs	Thermo Fisher Scientific, Schwerte/Germany
5-Fluoroorotic Acid (5-FOA)	ApolloScientific, Stockport/UK
Formaldehyde 37% (ACS reagent)	Sigma-Aldrich, Taufkirchen/Germany
Galactose	Acros Organics, Geel/Belgium
GFP-Trap_A	ChromoTek, Martinsried/Germany
Glass beads 0.2-0.5 mm	Carl Roth, Karlsruhe/Germany
IgG-Sepharose™ beads	GE Healthcare, Freiburg/Germany
Nitrocellulose Membran (Protran)	PerkinElmer, Waltham/USA
Poly-L-Lysine	Sigma-Aldrich, Taufkirchen/Germany
cOmplete Protease Inhibitor cocktail	Roche Diagnostics, Mannheim/Germany
Protease inhibitor cocktail for yeast	Sigma-Aldrich, Taufkirchen/Germany
Protein G Sepharose	Applied Biosystems, Foster City/USA
Raffinose	Serva, Heidelberg/Germany
Rotiphorese Gel 30	Carl Roth, Karlsruhe/Germany
Sucrose	Carl Roth, Karlsruhe/Germany



Salmon sperm DNA	Sigma-Aldrich, Taufkirchen/Germany
Sorbitol	Carl Roth, Karlsruhe/Germany
12-well microscope slide	Thermo Fisher Scientific, Schwerte/Germany
CSPD	Roche Diagnostics, Mannheim/Germany
Hoechst 33342	Sigma-Aldrich, Taufkirchen/Germany
IgG Sepharose	GE Healthcare, Freiburg/Germany
tRNA	Sigma-Aldrich, Taufkirchen/Germany
Yeast extract	Carl Roth, Karlsruhe/Germany
Ribonucleoside vanadyl complexes	Sigma-Aldrich, Taufkirchen/Germany
Fujifilm Super RX	Fujifilm, Tokyo/Japan
<b>Kits</b>	<b>Source</b>
ECL Prime Western Blotting Detection Kit	GE Healthcare, Freiburg/Germany
DIG-High Prime DNA Labeling and Detection Starter Kit II	Roche Diagnostics, Mannheim/Germany
NucleoBond PC 100	Macherey-Nagel, Dueren/Germany
NucleoSpin Plasmid	Macherey-Nagel, Dueren/Germany
peqGOLD Gel Extraction kit	Peqlab, Erlangen/Germany
GoTaq qPCR Master Mix	Promega, Mannheim/Germany
pGEM-T vector system	Promega, Mannheim/Germany
<b>Size Standards</b>	<b>Source</b>
Lambda DNA/EcoRI+HindIII DNA Ladder	Thermo Fisher Scientific, Schwerte/Germany
GeneRuler 1 kb DNA Ladder	Thermo Fisher Scientific, Schwerte/Germany
PageRuler Prestained Protein Ladder	Thermo Fisher Scientific, Schwerte/Germany
PageRuler Unstained Protein Ladder	Thermo Fisher Scientific, Schwerte/Germany

### 3.1.2 Enzymes and antibodies

All enzymes were used with the appropriate buffers according to the protocols of the manufactures.

To be used in western blot (WB) analyses all antibodies were diluted in 1-2% milk powder/TBST. To be used in immunofluorescence (IF) or fluorescence *in situ* hybridization (FISH) experiments all antibodies were diluted in antibody blocking buffer (5-10% heat inactivated fetal bovine serum/PBST). To be used in southern blot (SB) analyses the antibody was diluted in 1xBlocking reagent (1% blocking reagent in 1xMaleic acid buffer)

Enzymes	Source	
DreamTaq DNA Polymerase	Thermo Fisher Scientific, Schwerte/Germany	
FastAP Alkaline Phosphatase	Thermo Fisher Scientific, Schwerte/Germany	
Phusion High-Fidelity DNA Polymerase	New England Biolabs, Frankfurt /Germany	
KAPAHiFi Polymerase	Peqlab, Erlangen/Germany	
Restriction enzymes	Thermo Fisher Scientific, Schwerte/Germany New England Biolabs, Frankfurt /Germany	
RiboLock Rnase Inhibitor	Thermo Fisher Scientific, Schwerte/Germany	
RNase A	AppliChem, Munich/Germany	
T4 DNA Ligase	Thermo Fisher Scientific, Schwerte/Germany	
T7 RNA Polymerase	Thermo Fisher Scientific, Schwerte/Germany	
Zymolase	Seikagaku Corporation, Tokyo/Japan	
Antibodies	Dilution	Source
Anti-mouse-HRP (goat)	1:5000-1:10000 (WB)	Dianova, Hamburg/Germany
Anti-rabbit-HRP (goat)	1:10000-1:20000 (WB)	Dianova, Hamburg/Germany
Anti-mouse AlexaFluor 488 (sheep)	1:1000 (IF)	Invitrogen, Frankfurt/Germany
Anti-rabbit AlexaFluor 488 (sheep)	1:1000 (IF)	Invitrogen, Frankfurt/Germany
Anti-GFP (mouse)	1:250 (IF), 1:1000 (WB)	Santa Cruz, Heidelberg/Germany
Anti-GFP (rabbit)	1:250 (IF), 1:1000 (WB)	Santa Cruz, Heidelberg/Germany
Anti-myc (mouse)	1:250 (IF), 1:1000 (WB)	Santa Cruz, Heidelberg/Germany
Anti-myc (rabbit)	1:250 (IF), 1:1000 (WB)	Santa Cruz, Heidelberg/Germany
Anti-Nop1 (rabbit)	1:5000 (IF and WB)	
Anti-Hem15 (rabbit)	1:5000 (WB)	Gift from Roland Lill, Marburg
Anti-Zwf1 (rabbit)	1:2500 (WB)	Gift from Roland Lill, Marburg
Anti-Mtr4 (rabbit)	1:1000 (WB)	
Anti-Digoxigenin-FITC	1:200 (FISH)	Roche Diagnostics, Mannheim/ Germany
Anti-Digoxigenin-AP	1:10000 (NB)	Roche Diagnostics, Mannheim/ Germany

### 3.1.3 Instruments and software

<b>Instrument</b>	<b>Company</b>
Fusion FX7	Peqlab, Erlangen/Germany
FastPrep-24	MP Biomedicals, Illkirch/France
Leitz Biomed Typ 020-507-010	Leica, Wetzlar/Germany
Leica DMI6000B	Leica, Wetzlar/Germany
Leica DFC360FX	Leica, Wetzlar/Germany
Hamamatsu 1394 ORCA-ERA camera	Leica, Wetzlar/Germany
Rotor Gene Q	Qiagen, Hilden/Germany
Nikon Eclipse E400	Nikon, Duesseldorf/Germany
Heraeus Pico 21 centrifuge	Thermo Fisher Scientific, Schwerte/Germany
Heraeus Fresco 21 centrifuge	Thermo Fisher Scientific, Schwerte/Germany
Heraeus Multifuge X3R centrifuge	Thermo Fisher Scientific, Schwerte/Germany
Heraeus B6060	Heraeus, Hanau/Germany
Heraeus B6420	Heraeus, Hanau/Germany
Optimax X-Ray Film Processor	PROTEC, Oberstenfeld/Germany
Vacuum Blot	ITF, Marl/Germany
Cross Linker Bio Link BLX 365	Peqlab, Erlangen/Germany
Perfect Blue Semi dry Electroblotter	Peqlab, Erlangen/Germany
Gilson Pipetman P2/P10/P100/P1000	Gilson, Inc., Middleton/USA
Intelli Scan 1600	Quato Technology, Braunschweig/Germany
INTAS UV-system	Intas, Göttingen/Germany
MyCycler Thermal Cycler	BioRad, München/Germany
NanoDrop2000	Thermo Fisher Scientific, Schwerte/Germany
Milli-Q water purification	Millipore, Eschborn/Germany
<b>Software</b>	<b>Source</b>
Bio 1D	Peqlab, Erlangen/Germany
Image J	<a href="http://imagej.net/">http://imagej.net/</a>
Leica LAS AF	Leica, Wetzlar/Deutschland
SilverFast v3.1.1	LaserSoft Imaging AG, Kiel/Germany
Adobe Creative Suite Design Standard	Adobe, San Jose/USA
Microsoft office	Microsoft, Redmond/USA
ApE editor	<a href="http://biologylabs.utah.edu/jorgensen/wayned/ape/">biologylabs.utah.edu/jorgensen/wayned/ape/</a>
FileMaker	FileMaker, Inc.

### 3.1.4 Strains, plasmids and oligonucleotides

#### 3.1.4.1 Strains

<i>E. coli</i> strain		
Name	Genotype	Source
DH5 $\alpha$	<i>fhuA2 lac(del)U169 phoA glnV44 <math>\Phi</math>80' lacZ(del)M15 gyrA96 recA1 relA1 endA1 thi-1 hsdR17</i>	Krebber lab
Yeast strains		
Number	Genotype	Source
HKY36	Mata <i>ura3-52 leu2<math>\Delta</math>1 his3<math>\Delta</math>200</i>	(Winston et al., 1995)
HKY46	Mata <i>mtr10-1 ura3-52 lys2-301 ade2</i>	(Liu et al., 1999)
HKY82	Mata <i>mtr10::HIS3 ura3 leu2 trp his3 ade2 + pURA-MTR10</i>	(Senger et al., 1998)
HKY97	Mata <i>mtr10::HIS3 ura3 leu2 trp his3 ade2 + pURA-MTR10</i>	Krebber lab
HKY124	Mata <i>rat7-1 ura3-52 leu2<math>\Delta</math>1 his3<math>\Delta</math>200</i>	(Gorsch et al., 1995)
HKY128	Mata <i>rat8::HIS3 ura3-52 leu2<math>\Delta</math>1 trp1<math>\Delta</math>63 his3<math>\Delta</math>200 + pCS543 (YCplac33 rat8-3) LEU2</i>	(Snay-Hodge et al., 1998)
HKY130	Mata <i>rat8-2 ura3-52 leu2<math>\Delta</math>1 trp1<math>\Delta</math>63</i>	(Snay-Hodge et al., 1998)
HKY145	Mata <i>XPO1-GFP-TRP1 ura3 leu2 his3</i>	Krebber lab
HKY206	Mata <i>xpo1::LEU2 ade2-1 his leu trp1-1 ura3-1 ade2-1 + pCEN TRP1 xpo1-1</i>	(Taura et al., 1998)
HKY209	Mata <i>pdr6::HIS3 lys2 trp1 ura3-52 leu2<math>\Delta</math>1</i>	Krebber lab
HKY280	Mata <i>PAB1-GFP-KAN leu2 trp1 ura3-52 pep4-3 pre1-407 prb1-1122</i>	(Zenklusen et al., 2001)
HKY305	Mata <i>prp4-1 ura1 trp1 his7 ade1 ade2</i>	Krebber lab
HKY306	Mata <i>prp16-2 ura3-53 lys2-801 his3<math>\Delta</math>200 ade2-101 tyr1</i>	Krebber lab
HKY316	Mata <i>MTR10-9xMYC-TRP1 ura3-52 leu2<math>\Delta</math>1 trp1<math>\Delta</math>63</i>	Krebber lab

HKY380	Mata <i>npl3::kanMX4 his3Δ1 leu2Δ0 met15Δ0 ura3Δ0 TRP LYS</i>	Euroscarf
HKY381	Mata <i>his3Δ1 leu2Δ0 ura3Δ0 lys2Δ0</i>	Euroscarf
HKY382	Mata <i>rat8::HIS3 ura3-52 leu2Δ1 trp1Δ63 + pRAT8-MYC 2μ LEU2</i>	Krebber lab
HKY428	Mata <i>mtr4-G677D ura3-52 leu2Δ1 his3Δ200 + pCEN-gbp2-S15A URA3</i>	Krebber lab
HKY446	Mata <i>sup45-2 ura3-1 ade2-1 his5-2 can1-100</i>	(Stansfield et al., 1997)
HKY578	Mata <i>TIF4631-3xMYC-HIS3 ura leu trp his ade</i>	(Knop et al., 1999)
HKY644	Mata <i>mex67::HIS3 ade2 his3 leu2 trp1 ura3 + pUN100-mex67-5 LEU2 CEN</i>	(Segref et al., 1997)
HKY648	Mata <i>mex67::HIS3 ade2 his3 leu2 trp1 ura3 + pUN100-MEX67-GFP LEU2 CEN</i>	(Segref et al., 1997)
HKY661	Mata <i>mex67::HIS3 ade2 his3 leu2 trp1 ura3 + pUN100-mex67-5 LEU2 CEN</i>	Krebber lab
HKY948	Mata <i>prp18::kanMX4 his3Δ1 leu2Δ0 met15Δ0 ura3Δ0 TRP LYS</i>	Euroscarf
HKY1008	Mata <i>prp8 908_909 ura3-52 his3Δ200 leu2Δ1</i>	Krebber lab
HKY1028	Mata <i>rrp6::kanMX4 his3Δ1 leu2Δ0 met15Δ0 ura3Δ0 TRP LYS</i>	Euroscarf
HKY1072	Mata <i>est2::kanMX4 his3Δ1 leu2Δ0 met15Δ0 ura3Δ0 TRP LYS</i>	Euroscarf
HKY1073	Mata <i>yku70::kanMX4 his3Δ1 leu2Δ0 met15Δ0 ura3Δ0 TRP LYS</i>	Euroscarf
HKY1074	Mata <i>est1::kanMX4 his3Δ1 leu2Δ0 met15Δ0 ura3Δ0 TRP LYS</i>	Euroscarf
HKY1075	Mata <i>tel1::kanMX4 his3Δ1 leu2Δ0 met15Δ0 ura3Δ0 TRP LYS</i>	Euroscarf
HKY1076	Mata <i>est3::kanMX4 his3Δ1 leu2Δ0 met15Δ0 ura3Δ0 TRP LYS</i>	Euroscarf
HKY1077	Mata <i>mre11::kanMX4 his3Δ1 leu2Δ0 met15Δ0 ura3Δ0 TRP LYS</i>	Euroscarf
HKY1078	Mata <i>YKU70-GFP-HIS3MX6 his3Δ1 leu2Δ0 met15Δ0 ura3Δ0</i>	(Huh et al., 2003)
HKY1079	Mata <i>RAP1-GFP-HIS3MX6 his3Δ1 leu2Δ0 met15Δ0 ura3Δ0</i>	(Huh et al., 2003)
HKY1081	Diploid <i>TLC1/tlc1::LEU2 RAD52/rad52::TRP ura3-1 leu2-3 his3-11 trp1-1 ade2-1</i>	(Gallardo et al., 2008)
HKY1082	Mata <i>RAP1-13xMYC-HIS3 ura3-1 leu2-3 his3-11 trp1-1 ade2-1</i>	(Gallardo et al., 2008)
HKY1094	Mata <i>exo1::kanMX4 his3Δ1 leu2Δ0 met15Δ0 ura3Δ0 TRP LYS</i>	Euroscarf
HKY1111	Mata <i>swt1::kanMX4 his3Δ1 leu2Δ0 met15Δ0 ura3Δ0 TRP LYS</i>	Euroscarf
HKY1112	Mata <i>trf4::kanMX4 his3Δ1 leu2Δ0 met15Δ0 ura3Δ0 TRP LYS</i>	Euroscarf
HKY1136	Mata <i>RRP6-GFP-HIS3MX6 his3Δ1 leu2Δ0 met15Δ0 ura3Δ0</i>	(Huh et al., 2003)
HKY1171	Mata <i>TRF4-GFP-HIS3MX6 his3Δ1 leu2Δ0 met15Δ0 ura3Δ0</i>	(Huh et al., 2003)

HKY1172	Mata <i>RRP44-GFP-HIS3MX6 his3Δ1 leu2Δ0 met15Δ0 ura3Δ0</i>	(Huh et al., 2003)
HKY1236	Mata <i>trf5::kanMX4 his3Δ1 leu2Δ0 met15Δ0 ura3Δ0 TRP LYS</i>	Euroscarf
HKY1237	Mata <i>air1::kanMX4 his3Δ1 leu2Δ0 met15Δ0 ura3Δ0 TRP LYS</i>	Euroscarf
HKY1238	Mata <i>air2::kanMX4 his3Δ1 leu2Δ0 met15Δ0 ura3Δ0 TRP LYS</i>	Euroscarf
HKY1240	Mata <i>xrn1::kanMX4 his3Δ1 leu2Δ0 met15Δ0 ura3Δ0 TRP LYS</i>	Euroscarf
HKY1242	Mata <i>DBP5-GFP-HIS3MX6 his3Δ1 leu2Δ0 met15Δ0 ura3Δ0</i>	(Huh et al., 2003)
HKY1266	Mata <i>MEX67-GFP-HIS3MX6 his3Δ1 leu2Δ0 met15Δ0 ura3Δ0</i>	(Huh et al., 2003)
HKY1267	Mata <i>MTR4-GFP-HIS3MX6 his3Δ1 leu2Δ0 met15Δ0 ura3Δ0</i>	(Huh et al., 2003)
HKY1290	Mata <i>pGAL-3xHA-RRP44-HIS3MX6 his3Δ1 leu2Δ0 met15Δ0 ura3Δ0</i>	(Schneider et al., 2009)
HKY1291	Mata <i>rrp44::kanMX4 his3Δ1 leu2Δ0 met15Δ0 ura3Δ0 TRP LYS + pRS316/RRP44-szz URA</i>	(Schneider et al., 2009)
HKY1292	Mata <i>EST1-6xGLY-12xMYC 3xFLAG-12xMYC-6xGLY-Est2 leu2 trp1 ura3-52 prb<sup>-</sup> prc<sup>-</sup> pep4-3</i>	(Lubin et al., 2012)
HKY1293	Mata <i>tlc1::HIS ura3-52 lys2-801 trp-Δ1 his3-Δ200 leu2-Δ1 + pCEN URA3 TLC1</i>	(Lubin et al., 2012)
HKY1294	Mata <i>α EST1-6xGLY-12xMYC 3xFLAG-12xMYC-6xGLY-Est2 tlc1::HIS leu2 trp1 ura3-52 prb<sup>-</sup> prc<sup>-</sup> pep4-3 + pCEN URA3 TLC1</i>	(Lubin et al., 2012)
HKY1302	Mata <i>α EST1-6xGLY-12xMYC 3xFLAG-12xMYC-6xGLY-Est2 xpo1::LEU2 leu2 trp1 ura3-52 prb<sup>-</sup> prc<sup>-</sup> pep4-3 + pCEN TRP xpo1-1</i>	This study
HKY1304	Mata <i>TRF5-GFP-HIS3MX6 his3Δ1 leu2Δ0 met15Δ0 ura3Δ0</i>	(Huh et al., 2003)
HKY1332	Mata <i>EST1-6xGLY-12xMYC 3xFLAG-12xMYC-6xGLY-Est2 rat7-1 leu2 trp1 ura3-52 prb<sup>-</sup> prc<sup>-</sup> pep4-3</i>	This study
HKY1334	Mata <i>α EST1-6xGLY-12xMYC 3xFLAG-12xMYC-6xGLY-Est2 rat8-2 leu2 trp1 ura3-52 prb<sup>-</sup> prc<sup>-</sup> pep4-3</i>	This study
HKY1336	Mata <i>α EST1-6xGLY-12xMYC 3xFLAG-12xMYC-6xGLY-Est2 mex67::HIS leu2 trp1 ura3-52 + pUN100-mex67-5 LEU2 CEN</i>	This study
HKY1353	Mata <i>mex67::HIS3 xpo1::TRP1 ura + pUN100-mex67-5 LEU2 CEN + pxpo1-1::HIS3</i>	(Brune et al., 2005)
HKY1377	Mata <i>XPO1-GFP-HIS3MX6 his3Δ1 leu2Δ0 met15Δ0 ura3Δ0</i>	(Huh et al., 2003)
HKY1396	Mata <i>α rat8-2 yku70::kanMX4 ura leu trp</i>	This study
HKY1397	Mata <i>α mex67::HIS3 yku70::kanMX4 ura leu trp + pUN100-mex67-5 LEU2 CEN</i>	This study
HKY1398	Mata <i>α rat7-1 yku70::kanMX4 ura leu trp</i>	This study
HKY1399	Mata <i>α mtr4-G677D- ura3-52 leu2Δ1 his3Δ200</i>	Krebber lab
HKY1444	Mata <i>α xpo1::LEU2 yku70::kanMX4 ade2-1 his leu trp1-1 ura3-1 + pCEN TRP1 xpo1-1</i>	This study
HKY1445	Mata <i>mex67::HIS3 xpo1::TRP1 yku70::kanMX4 ura + pUN100-mex67-5 LEU2 CEN + pxpo1-1::HIS3</i>	This study
HKY1463	Mata <i>α EST1-3xMYC-kanMX4 his3Δ1 leu2Δ0 ura3Δ0 lys2Δ0</i>	This study

HKY1464	Mata <i>xpo1::LEU2 EST1-3xMYC-kanMX4 ade2-1 his leu trp1-1 ura3-1 + pCEN TRP1 xpo1-1</i>	This study
HKY1465	Mata <i>mex67::HIS3 EST1-3xMYC-kanMX4 ade2 his3 leu2 trp1 ura3 + pUN100-mex67-5 LEU2 CEN</i>	This study
HKY1466	Mata <i>mex67::HIS3 xpo1::TRP1 EST1-3xMYC-kanMX4 ura + pUN100-mex67-5 LEU2 CEN + pxpo1-1::HIS3</i>	This study
HKY1467	Mat <i>EST2-3xMYC-kanMX4 his3Δ1 leu2Δ0 ura3Δ0 lys2Δ0</i>	This study
HKY1468	Mata <i>xpo1::LEU2 EST2-3xMYC-kanMX4 ade2-1 his leu trp1-1 ura3-1 + pCEN TRP1 xpo1-1</i>	This study
HKY1469	Mata <i>mex67::HIS3 EST2-3xMYC-kanMX4 ade2 his3 leu2 trp1 ura3 + pUN100-mex67-5 LEU2 CEN</i>	This study
HKY1470	Mata <i>mex67::HIS3 xpo1::TRP1 EST2-3xMYC-kanMX4 ura + pUN100-mex67-5 LEU2 CEN + pxpo1-1::HIS3</i>	This study
HKY1471	<i>tlc1::LEU2 rad52::TRP EST2-3xMYC-KanMX4 ura3-1 leu2-3 his3-11 trp1-1 ade2-1</i>	This study
HKY1472	<i>tlc1::LEU2 rad52::TRP EST1-3xMYC-KanMX4 ura3-1 leu2-3 his3-11 trp1-1 ade2-1</i>	This study

### 3.1.4.2 Plasmids

Number	Construct	Source
pHK12	<i>CEN URA3 pADH-NLS-NES-GFP-GFP</i>	Krebber lab
pHK20	<i>CEN LEU2 pUN100-MEX67-GFP</i>	(Segref et al., 1997)
pHK40	<i>CEN HIS3 XPO1</i>	Krebber lab
pHK43	<i>CEN URA3 XPO1-GFP</i>	Krebber lab
pHK85	<i>CEN pRS313-HIS3</i>	(Sikorski and Hieter, 1989)
pHK86	<i>CEN pRS314-TRP1</i>	(Sikorski and Hieter, 1989)
pHK87	<i>CEN pRS315-LEU2</i>	(Sikorski and Hieter, 1989)
pHK88	<i>CEN pRS316-URA3</i>	(Sikorski and Hieter, 1989)
pHK260	<i>2μ LEU2 RAT8-MYC</i>	(Snay-Hodge et al., 1998)
pHK413	<i>LEU2 ProtA-TEV-MTR10</i>	(Senger et al., 1998)
pHK453	<i>CEN TRP1 mtr10-7</i>	(Senger et al., 1998)
pHK475	<i>2μ URA3 pGAL1-GBP2-S13,15,17A-GFP</i>	Krebber lab
pHK491	<i>3xMYC-kanMX6</i>	(Knop et al., 1999)
pHK492	<i>3xMYC-HIS3MX6</i>	(Knop et al., 1999)
pHK636	<i>2μ LEU2 pGAL1-MYC-RAT8</i>	Krebber lab
pHK637	<i>2μ TRP1 RAT8</i>	Krebber lab
pHK643	<i>CBP-TEV-ProtA K.I.TRP1</i>	(Puig et al., 2001)
pHK644	<i>CBP-TEV-ProtA K.I.URA3</i>	(Puig et al., 2001)
pHK645	<i>pGal1-ProtA-TEV-CBP K.I.TRP1</i>	(Puig et al., 2001)
pHK648	<i>2μ TRP1 pGAL1-RAT8-MYC</i>	Krebber lab
pHK649	<i>2μ URA3 pGAL1-RAT8-MYC</i>	Krebber lab
pHK670	<i>9xMYC kanMX4</i>	(Gauss et al., 2005)
pHK1238	<i>2μ URA3 TRF4-2xMYC</i>	(Fasken et al., 2011)



pHK1239	<i>2μ URA3 TRF5-2xMYC</i>	(Fasken et al., 2011)
pHK1240	<i>2μ URA3 MTR4-2xMYC</i>	(Fasken et al., 2011)
pHK1336	<i>2μ URA3 NLS-TRF4-2xMYC</i>	This study
pHK1337	<i>2μ URA3 NLS-MTR4-2xMYC</i>	This study
pHK1351	<i>URA3 RRP44-szz</i>	(Schneider et al., 2009)
pHK1352	<i>LEU2 RRP44-szz</i>	(Schneider et al., 2009)
pHK1353	<i>LEU2 RRP44-exo</i>	(Schneider et al., 2009)
pHK1354	<i>LEU2 RRP44-endo</i>	(Schneider et al., 2009)
pHK1355	<i>LEU2 RRP44-exo-endo</i>	(Schneider et al., 2009)
pHK1411	<i>URA3 NLS-RRP44-szz</i>	Krebber lab
pHK1412	<i>LEU2 NLS-RRP44-szz</i>	Krebber lab

### 3.1.4.3 Oligonucleotides

The gene sequences are depicted in upper case letters, other regions, *e.g.* restriction sites, transcription sites, are indicated in lower case letters

Number	Sequence	Description
HK743	5'-TTTCGGCGCCTGAGCACCAT-3'	<i>TAP</i> reverse
HK744	5'-GTGGACAACAAATTCACAAAGAACAACAA-3'	<i>TAP</i> forward
HK754	5'-ccgctcgagctATGGGTTCCAAAAGAAGATTCTC-3'	XhoI+ <i>PRP43</i> forward
HK755	5'-cgggatccCTATTTCTTGAGTGCTTACTCT-3'	BamHI+ <i>PRP43</i> reverse
HK756	5'-ccgctcgagctATGGGTGAACAAAAGTTGATTTC-3'	XhoI+9x <i>MYC</i> forward
HK757	5'-cgggatccTTATCCGTTCAAGTCTTCTCTGAGA-3'	BamHI+9x <i>MYC</i> reverse
HK804	5'-ccgctcgagctAATAAACTAGAGAGGAAGATAGGT-3'	XhoI+ <i>TLC1</i> forward
HK805	5'-cgggatccTAAATATTAAGAGGCATACCTCCG-3'	BamHI+ <i>TLC1</i> reverse
HK890	5'-ggactagtAATAAACTAGAGAGGAAGATAGGT-3'	SpeI+ <i>TLC1</i> forward
HK891	5'-ccggaattcTAAATATTAAGAGGCATACCTCCG-3'	EcoRI+ <i>TLC1</i> reverse
HK936	5'-CGTTTGAGTTTTCCATCATGC-3'	<i>TLC1</i> forward
HK937	5'-taatacactcactatagggCAGGCTATCAACTGAAAGATCA-5'	T7 transcription site+ <i>TLC1</i> reverse
HK938	5'-TTCCTGTTATTCTTCTTCGTAC-3'	<i>TLC1</i> forward
HK939	5'-taatacactcactatagggGCTGTAACATTTGTGTGTGG-3'	T7 transcription site + <i>TLC1</i> reverse
HK940	5'-ATGTGCCCCGTACATCG-3'	<i>TLC1</i> forward
HK941	5'-taatacactcactatagggCGCAAACCTAACCGATGC-3'	T7 transcription site + <i>TLC1</i> reverse
HK942	5'-TGTATTGTAGAAATCGCGCG-3'	<i>TLC1</i> forward
HK943	5'-taatacactcactatagggGGCATACCTCCGCCTAT-3'	T7 transcription site + <i>TLC1</i> reverse
HK1138	5'-AGGTAGGAGTACCCGCTGAA-3'	25S rRNA genes forward
HK1139	5'-taatacactcactatagggATGGAATTTACCACCCACTTAGAGC-3'	T7 transcription site +25S rRNA genes reverse
HK1140	5'-GTGAAACTGCGAATGGCTCATTAAAT-3'	18S rRNA genes forward

HK1141	5'-taatacactcactatagggAATCGAACCCCTTATCCCCGTTA-3'	T7 transcription site +18S rRNA genes reverse
HK1142	5'-AAACTTTCAACAACGGATCTCTTGG-3'	5.8S rRNA genes forward
HK1143	5'-taatacactcactatagggAAATGACGCTCAAACAGGCATG-3'	T7 transcription site +5.8S rRNA genes reverse
HK1379	5'-CTTGATGTATATTTTTGTATTGTA-3'	<i>TLC1</i> forward
HK1380	5'-taatacactcactatagggCAATTTAAAGCGCTTATAAAG-3'	T7 transcription site + <i>TLC1</i> reverse
HK1396	5'-CATGGCCGTTCTTAGTTGGTGG-3'	18S rRNA genes forward
HK1397	5'-ATTGCCTCAAACCTCCATCGGC-3'	18S rRNA genes reverse
HK1404	5'-TCGCGAAGTAACCCTTCGTG-3'	<i>SNR6</i> forward
HK1405	5'-AAACGGTTCATCCTTATGCAGG-3'	<i>SNR6</i> reverse
HK1467	5'-ccaaaaaagaaaagaaaagttGATTCTACTGATCTGTTTCGATGTTTTTC-3'	<i>NLS</i> + <i>MTR4</i> forward
HK1468	5'-aacttttcttttctttttggCATCCTTCGTATATAATCTATATTTCTTGCAG-3'	<i>NLS</i> + <i>MTR4</i> reverse
HK1469	5'-ccaaaaaagaaaagaaaagttGGGGCAAAGAGTGAACAGC-3'	<i>NLS</i> + <i>TRF4</i> forward
HK1470	5'-aacttttcttttctttttggCATATTTCAAGTATAGTTCCTTGCTTATTCA-3'	<i>NLS</i> + <i>TRF4</i> reverse
HK1483	5'-ATGCCAAAAAAGAAAAGAAAAGTT-3'	<i>NLS</i> forward
HK1492	5'-taataggactcactatagggAAATAAATCTCTTTGTAAAACGGTTCATCC-3'	T7 transcription site+ <i>SNR6</i> reverse
HK1517	5'-ccaaaaaagaaaagaaaagttTCAGTCCCGCTATCGCC-3'	<i>NLS</i> sequence+ <i>DIS3</i> forward
HK1518	5'-aacttttcttttctttttggCATGTTGTTTTGGCCTGTATGATG-3'	<i>NLS</i> sequence+ <i>DIS3</i> reverse
HK1539	5'- <b>DIG</b> -CCACCACACACACCCACACCC-3'	DIG labelled Telomere probe
HK1742	5'-TGATTTGTTAAGTGACTCTAAGCCTGATTTTAAAACGGGAATATTATG-3'	<i>YKU70</i> forward
HK1743	5'-AAATATTGTATGTAACGTTATAGATATGAAGGATTTCAATCGTCTTTA-3'	<i>YKU70</i> reverse
HK1761	5'- <b>Cy3</b> -GCGCACACACAAGCATCTACACTGACACCAGCATACTCGAAATTCTTTGG- <b>Cy3</b> -3'	Cy3 labelled <i>TLC1</i> probe
HK1787	5'- <b>Cy5</b> -CAATTTAAAGCGCTTATAAAGCGATATACAAGTAC- <b>Cy5</b> -3'	Cy5 labelled <i>TLC1</i> probe
HK1788	5'- <b>Cy5</b> -CGCGCGATTCTACAATACAAAAAATATACATCAAG- <b>Cy5</b> -3'	Cy5 labelled <i>TLC1</i> probe
HK1789	5'- <b>Cy3</b> -CGATAAGATAGACATAAAGTGACAGCGCTTAGCACCGTCTGTTTGC- <b>Cy3</b> -3'	Cy3 labelled <i>TLC1</i> probe
Hk1790	5'- <b>Cy3</b> -CCTACTCGTATTTTTCTCTGTACATCGTTTCGATGTACGGGGCACATTTGG- <b>Cy3</b> -5'	Cy3 labelled <i>TLC1</i> probe
HK1830	5'-CAATTGATGCTGATGAGGACATCACCGTCCAAGTGCCAGATACTCTACTcgtacgtcaggtcgac-3'	pHK491+ <i>EST1</i> forward
HK1831	5'-TAATATATTTTCAATTATGATTTTTCCCTCACCATTACTTGTCTCTCAatcgtatgaattcgagctcg-3'	pHK491+ <i>EST1</i> reverse

HK1845	5'-AAATTCAACACTTGCAAGCATATATATATATATATACATATAGTTAATcgtacgctgcaggtcgac-3'	pHK491+EST2 forward
HK1846	5'-TTCCTTATCAGCATCATAAGCTGTCAGTATTCATGTATTATTAGTACTAatcgatgaattcgagctcg-3'	pHK491+EST2 reverse

## 3.2 Methods

### 3.2.1 General methods

#### 3.2.1.1 Generation of strains, plasmids and oligonucleotides

All *S. cerevisiae* and *E. coli* strains, plasmids, oligonucleotides used in this study are listed in the material part (see section 3.1.4).

The plasmids pHK1336 and pHK1337 were created directly through PCR reactions, with which the gene sequence of the nuclear localisation signal (NLS) was incorporated into the plasmids with the specific primers that contain the NLS sequence. In the PCR reactions for generating pHK1336, pHK1238 was used as the template and HK1469 and HK1470 were used as the primer pair. In the PCR reactions for generating pHK1337, pHK1240 was used as the template and HK1467 and HK1468 were used as the primer pair. A routine PCR reaction was described in **Polymerase chain reaction (PCR)** (section 3.2.3.1). Subsequently, 1µl DpnI (10u/µl, Thermo Fisher Scientific) was directly added to the PCR reaction mixture and the mixture was incubated at 37°C for 1 hour and then used for *E. coli* transformation (see **Transformation**, section 3.2.4.1). DpnI recognized and digested 5'-G<sup>M</sup>A<sup>T</sup>C-3' sites, which existed only in the template plasmids that were isolated from DH5α strain. Therefore, after transformation, only the transformed cells containing newly synthesized plasmids were able to grow on the selective plates.

The yeast strains were generated by strains crossing or transformation. Strain crossing was described in **Yeast sporulation and tetrad analysis** (section 3.2.1.4). Homologous recombination was achieved through **Transformation** (section 3.2.4.1) of cells with 1ng PCR products (e.g. *KanMX4*, *3xMYC*) that contained a homologous sequence of approximate 50 nucleotides in length of the target genes on each side.

The yeast strains HKY1302, HKY1332, HKY1334, HKY1336 were generated by crossing HKY206+HKY1292, HKY124+HKY1292, HKY582+HKY1292, HKY661+HKY1292, respectively. The haploid cells showing both temperature sensitivities (mutations) and expression of

*EST1-MYC* and *EST2-MYC* (detection see **SDS-polyacrylamide gel electrophoresis (SDS-PAGE) and western blot**, section 3.2.2.4) were selected.

The yeast strains HKY1396, HK1397, HK1398 were generated by crossing HKY582+HKY1073, HKY644+HKY1073, HKY124+HKY1073, respectively. The haploid cells showing both temperature sensitivities (mutations) and geneticin (200µg/ml used in medium or plate) resistance (*KanMX4* marker) were selected.

The yeast strains HKY1444 and HKY1445 were created by transformation of HKY206 and HKY1353, respectively, with the PCR products that were generated from the gDNA of HKY1073 with the primer pair HK1742+HK1743. Through homologous recombination the *YKU70* gene was replaced by the *KanMX4* gene. Desired *YKU70* knock-out strains showing geneticin resistance were selected.

The yeast strains HKY1463, HKY1464, HKY1465, HKY1466, HKY1472 were created through transforming HKY381, HKY206, HKY644, HKY1353, HKY1081 respectively, with the PCR products that were generated from the plasmid pHK491 with the primer pair HK1830+HK1831. Through homologous recombination the *3xMYC:KanMX4* sequence was incorporated upstream of the stop codon of the *EST1* gene. Desired *MYC*-tagged *EST1* strains that showed geneticin resistance were selected.

The yeast strains HKY1467, HKY1468, HKY1469, HKY1470, HKY1471 were created through transforming HKY381, HKY206, HKY644, HKY1353, HKY 1081 respectively, with the PCR products that were generated from the plasmid pHK491 with the primer pair HK1845+HK1846. Through homologous recombination the *3xMYC:KanMX4* sequence was incorporated upstream of the stop codon of *EST2* gene. Desired *MYC*-tagged *EST2* strains that showed geneticin resistance were selected.

### **3.2.1.2 Media and plates**

All media were autoclaved before usage. Heat sensitive materials (antibiotics, some carbon sources and 5'-FOA, etc.) were filter-sterilised before being added to the autoclaved media.

Solid agar plates were made by adding 1.5% agar (for *E. coli*) or 1.8% agar (for yeast) to the autoclaved corresponding media.

### 3.2.1.3 Cell cultivation

Cells were grown in YPD, YP or selective media. YP medium is a full medium without a carbon source to which the carbon source (glucose, raffinose or galactose, *etc.*) is added separately. The selective media lack one or several amino acids or nucleobases, which allow the growth of the yeast strains that contain select markers in plasmids or in the genomes. Yeast cells were cultivated in the medium at 25°C and the cells were harvested at the middle-logarithmic phase (cell concentration:  $1 \times 10^7$  to  $3 \times 10^7$  cells/ml) if not indicated otherwise. Yeast cells were harvested through centrifugation at 2000-4000×g and 4°C (Heraeus Multifuge X3R centrifuge) for 10 minutes (the cell culture volume ≥ 5ml) or centrifugation at 10000-20000×g and 4°C (Heraeus Fresco 21 centrifuge) or room temperature (Heraeus Pico 21 centrifuge) for 1 minute (the cell culture volume < 5ml).

#### YPD medium:

1% (w/v) Yeast extract

2% (w/v) Peptone

2% (w/v) Glucose

#### YP medium:

1% (w/v) Yeast extract

2% (w/v) Yeast extract

1% (w/v) Peptone

#### Selective media:

2% (w/v) Drop-out mix

0.17% (w/v) Nitrogen base

0.51% (w/v) Ammonium sulfate

2% (w/v) Glucose

Additional desired amino acids/bases

Drop-out mix (-Ura -Leu -His -Lys -Ade -Trp):

2g/l each of the following components: Alanine, Arginine, Asparagine, Aspartic acid, Cysteine, Glutamine, Glutamic acid, Glycine, Inositol, Isoleucine, Methionine, Phenylalanine, Proline, Serine, Threonine, Tyrosine, Valine.

0.2g/l Para-aminobenzoic acid

The following components were selectively added as desired:

0.5g/l Adenine

2g/l Histidine

10g/l Leucine

2g/l Lysine

2g/l Tryptophan

2g/l Uracil

B-plates:

0.17% (w/v) Nitrogen base

0.51% (w/v) Ammonium sulfate

0.3% (w/v) Agar

2% (w/v) Glucose

FOA plates (5'-Fluoro-orotic-acid):

0.17% (w/v) Nitrogen base

0.51% (w/v) Ammonium sulfate

0.2% (w/v) Drop-out mix (all amino acids and bases included)

0.3% (w/v) Agar



2% (w/v) Glucose

0.1% (w/v) FOA

LB medium is a standard nutrient-rich medium used for cultivating *E. coli* cells. *E. coli* cells were grown overnight at 37°C in LB medium with or without antibiotics. The addition of antibiotics allows the growth of the *E. coli* cells with the specific antibiotic resistances from the plasmids. *E. coli* cells were harvested through centrifugation at 4000×g (Heraeus Fresco 21 centrifuge) for 10 minutes (cell culture volume ≥ 5ml) or at 10000-20000×g and room temperature (Heraeus Pico 21 centrifuge) for 1 minutes (cell culture volume <5ml).

LB medium (pH7.5):

1% (w/v) Tryptone

0.5% (w/v) Yeast extract

0.5% (w/v) NaCl

Antibiotics:

As desired, one or some of the following antibiotics are added :

100µg/ml Ampicillin

20µg/ml Kanamycin

### **3.2.1.4 Yeast sporulation and tetrad analysis**

In *Saccharomyces cerevisiae*, diploid strains can be created by mating two haploid strains with different mating types (mating type a or  $\alpha$ ). Under the condition of nitrogen starvation and poor carbon source the yeast diploid cells undergo meiosis, sporulation and form asci. The genotypes of single spores (tetrads) were analysed through a series of genetic, biochemical and molecular biological methods.

Two haploid strains with different mating types (a or  $\alpha$ ) were mixed and incubated on YPD

plates at 25°C for 2-3 days. The diploid cells were selected from the selectable markers (*URA3*, *LEU2*, *KanMX4*, etc.) or the phenotypes (temperature-sensitivity, etc.) from the haploid strains. The diploid strains were cultivated in 2ml SuperSpo medium for 3 days at 25°C until the asci became visible. The asci were collected by centrifugation at 10000×g and room temperature for 1 minute. After washing once in 100µl sterile H<sub>2</sub>O and centrifugation at 10000×g and room temperature for 30 seconds, the cells were resuspended in 50µl P-solution. The cell walls of the spores were digested by adding 2.5µl zymolyase (10mg/ml, Sigma) at room temperature and the digestion was monitored under the microscope. After the cell walls were digested (around 5-10 minutes at room temperature), the spores were harvested by centrifugation at 10000×g and room temperature for 30 seconds and washed in 100µl P-solution. The spores were again collected through centrifugation at 10000×g and room temperature for 30 seconds and finally resuspended in 200µl P-solution. 2.5µl of cells were diluted in 100µl sterile H<sub>2</sub>O and plated on YPD plates. By using the tetrad microscope with a micromanipulator (Nikon Eclipse E400) the four spores from a tetrad were separated. The spores were grown on YPD plates for 2-5 days at 25°C. The phenotype of the spores were identified through analyses of their select makers (*URA3*, *LEU2*, *KanMX4*, etc.) by incubating them on selective plates, or through verification of their protein tags (myc, GFP, etc.) by western blot, or through identification of their genome content (mutations, truncated genes, knock-out genes, etc.) by PCR, etc.

SuperSpo medium:

5g/l Yeast extract

30g/l Potassium acetate

1g/l Glucose

80mg/l Adenine

80mg/l Uracil

80mg/l Tyrosine

40mg/l Histidine

40mg/l Leucine

40mg/l Lysine

40mg/l Tryptophan

40mg/l Methionine

40mg/l Arginine

200mg/l Phenylalanine

700mg/l Threonine

0.1M Potassium phosphate buffer (pH 6.5)

3.3% (v/v) 1M K<sub>2</sub>HPO<sub>4</sub>

6.7% (v/v) 1M KH<sub>2</sub>PO<sub>4</sub>

P-solution (pH 6.5):

0.1M Potassium phosphate buffer pH6.5

1.2M Sorbitol

### **3.2.1.5 Yeast cell lysis**

Cells were collected from 10ml-1000ml cell culture, which was grown to the middle-logarithmic phase if not indicated otherwise, by centrifugation at 4000×g and 4°C for 10 minute. The cells were washed once with 1ml sterile H<sub>2</sub>O and transferred to 2ml screw-cap tubes. The cells were washed once with the ice-cold appropriate buffer (according to applications, *e.g.* 1×SDS sample buffer for western blot, PBSKMT for co-immunoprecipitation, RNA co-IP buffer for RNA co-immunoprecipitation). The cells were mixed with the same cell pellet volume of glass beads and double cell pellet volume of the ice-cold buffer. The mixture was vigorously shaken 2-3 times with the Fastprep machine (MP Biomedicals) at a speed of 4.0m/s for 20 seconds. The samples were cooled down on ice between shaking intervals. The cracked cells were finally centrifuged at 20000×g for 5 minutes at 4°C. The supernatants were carefully transferred to fresh 1.5ml or 2ml reaction

tubes and used in following experiments (Western blot analyses, protein precipitation, co-immunoprecipitation or RNA co-immunoprecipitation).

1×SDS sample buffer:

33% (v/v) 3×SDS sample buffer

2.5% (v/v) β-Mercaptoethanol

3×SDS sample buffer:

0.3M Tris pH6.8

30% (v/v) Glycerol

6% (w/v) SDS

0.01% (w/v) Brome phenol blue

10×PBS (pH7.4):

137mM NaCl

2.7mM KCl

1.8mM KH<sub>2</sub>PO<sub>4</sub>

10mM Na<sub>2</sub>HPO<sub>4</sub>

Adjust pH to 7.4

PBSKMT:

1×PBS

3mM KCl

2.5mM MgCl<sub>2</sub>

0.1-0.5% (v/v) Triton-X100

Before usage freshly add:

1× cOMplete Protease inhibitor cocktail (Roche)

RNA co-IP buffer:

150mM KCl

25mM Tris pH7.0

2mM EDTA

0.1-0.5% (v/v) Triton-x100

Before usage freshly add:

1× cOmplete Protease inhibitor cocktail (Roche)

1mM DTT

0.01% (v/v) Ribonucleoside vanadyl complexes (Sigma)

### 3.2.1.6 Preparation of microscope slides

12-well slides (Thermo Fisher Scientific) were used in immunofluorescence or fluorescent *in situ* hybridization experiments. The wells were incubated with 3 µl poly-L-lysine (100µg/ml, Sigma) for 5 minutes and were air-dried at 42°C. Poly-L-lysine is positively charged and is able to enhance the attachment of negatively charged cell wall to the well surface. The wells were washed three times with sterile H<sub>2</sub>O and were air-dried at 42°C. The slides were stored at 4°C for weeks.

### 3.2.1.7 Applications of the microscopes

The light microscope (Leitz Biomed Typ 020-507-010) was used for counting the cell number and monitoring cell wall digestions (see **Yeast sporulation and tetrad analysis**, section 3.2.1.4; **Nucleo-cytoplasmic fractionation**, section 3.2.2.3; **Immuno-fluorescence (IF)**, section 3.2.4.2; **RNA fluorescent *in situ* hybridization (FISH)**, section 3.2.4.3) .

The tetrad microscope with a micromanipulator (Nikon Eclipse E400) was used to separate single spores from tetrads.

The Fluorescence microscopes (Leica DMI6000B with Leica DFC360FX camera or Hamamatsu 1394 ORCA-ERA camera) were used for capturing and analysing the fluorescent signals in

immunofluorescence or fluorescent *in situ* hybridisation experiments. If necessary, deconvolution was applied by using the Leica LAS AF software to acquire images with sharper contrast and higher intensity. In these cases cells were imaged through 6-10 z-stacks (0.2 $\mu$ m/stack) followed by the blind deconvolution.

### 3.2.1.8 Signal detection, quantification and statistical analyses

The fluorescent signals from immunofluorescence and fluorescent *in situ* hybridization experiments were captured by the fluorescence microscopes as described in **Applications of the microscopes** (section 3.2.1.7). The chemiluminescent signals from western blot and southern blot analyses were detected by the Fusion FX7 system (Peqlab) or Super RX X-ray films (Fujifilm) and Optimax X-Ray Film Processor (PROTEC). Ethidium bromide incorporated nucleic acids were detected by the 312nm UV-light with the INTAS UV-system (INTAS).

The intensity of chemiluminescent signals (western blot signals from protein expression analyses or co-immunoprecipitation experiments) was quantified by using the Bio1D software (Peqlab) or ImageJ software (<http://imageJ.net>). The intensity of fluorescent signals (immunofluorescence or fluorescent *in situ* hybridization) was quantified by using ImageJ software (<http://imageJ.net>). The intensity of the fluorescent signals from qRT-PCR experiments was quantified by the Rotor Gene Q system (Qiagen).

In each case of this thesis at least three independent experiments were performed. Western signals were quantified from at least three independent experiments. Fluorescent signals were quantified from 20 to 50 cells. Figures in this thesis represent one experiment. All quantifications are the mean values  $\pm$  standard deviations of at least 3 independent experiments. Error bars represent the standard deviations. The mean values and standard deviations were calculated by using Microsoft Excel. The p-values were calculated through paired or unpaired, two tailed t-test by using the Microsoft Excel (\*:  $0.01 \leq p < 0.05$ ; \*\*:  $0.001 \leq p < 0.01$ ; \*\*\*:  $0.0001 \leq p < 0.001$ ; \*\*\*\*:  $0.00001 \leq p < 0.0001$ ).

## 3.2.2 Biochemical methods

### 3.2.2.1 Protein extraction and precipitation

According to the protocol **Yeast lysis** (section 3.2.1.5), cells of interest were lysed and centrifuged and the clear supernatants were obtained. The same volume 20% (w/v) Trichloroacetic acid (TCA) was added to the supernatants. After vigorously mixing (5-10 seconds), the mixture was incubated on ice for 30 minutes. The mixture was further centrifuged at 20000×g and room temperature for 15 minutes. After discarding the supernatant, the pellet was washed twice with 1ml 80% (v/v) acetone. After centrifugation at 20000×g and room temperature for 2 minutes, the supernatant was discarded and the pellet was air-dried. The pellet was dissolved in 1×SDS sample buffer (recipe in section 3.1.5). The samples were either further used in western blot analyses or stored at -80°C

### 3.2.2.2 Co-immunoprecipitation (IP or co-IP)

Co-immunoprecipitation experiments were used to study interactions among proteins. In these assays proteins of interest were precipitated by using specific antibodies and immobilised beads. The interaction partners of target proteins were co-precipitated and analysed through western blot analyses (**SDS-polyacrylamide gel electrophoresis (SDS-PAGE) and western blot**, section 3.2.2.4). To precipitate proteinA tagged (TAP, SZZ, *etc.*) proteins, IgG Sepharose™ 6 Fast Flow (Roche) beads were used. To precipitate GFP tagged proteins, GFP-Trap\_A beads (Chromotek), on which GFP antibodies were covalently bound, were used. To precipitate untagged or the other tagged (*e.g.* myc, HA, *etc.*) proteins, the appropriate antibodies (*e.g.* direct antibodies for untagged proteins, anti-myc for myc tagged proteins, *etc.*) and Protein G Plus agarose beads (Applied Biosystems) were used.

Before co-immunoprecipitation experiments the beads (10µl IgG Sepharose 6 Fast Flow, 8µl GFP-Trap\_A beads or 15µl Protein G Plus agarose beads for one sample) were pre-washed with 1ml ice-cold PBSKMT buffer for 5 times, each time with centrifugation at 500×g and 4°C

for 5 minutes. The beads were resuspended in 20µl buffer and stored on ice until usage.

Cells from 200-500ml cell cultures (middle-logarithmic phase) were lysed in ice-cold PBSKMT buffer as described in **Yeast lysis** (section 3.2.1.5). To prevent proteins from digestion, the protease inhibitor cocktail (25×, Roche) was added with a final concentration of 1×.

25-50µl of the clear lysates was mixed with the same volume of the 2×SDS sample buffer and used in western analyses as input controls. The rest of the clear lysates were incubated with corresponding beads and antibodies at 4°C for 3 hours to overnight on a rotator. If necessary, during the incubations 10mg/ml RNaseA was added to a final concentration of 50µg/ml to remove potential RNA-bridged indirect protein-protein interactions. Subsequently, the beads were precipitated by a centrifugation at 500×g and 4°C for 5 minutes. The beads were washed 5 times with 1ml cold PBSKMT and between washes a centrifugation at 500×g and 4°C for 5 minutes was used to precipitate beads and to remove the buffer. After the last wash, the supernatants were carefully removed and the beads (samples) were resuspended in 20-50µl 2×SDS sample buffer.

The input controls and samples were either stored at -20°C or used in western blot experiments.

RNaseA:

10mg/ml RNaseA

10mM Tris pH7.5

15mM NaCl

Incubate at 100°C for 15 minutes

PBSKMT: see section 3.2.1.5

SDS Sample buffer: see section 3.2.1.5



### 3.2.2.3 Nucleo-cytoplasmic fractionation

Cells from 200-500ml cell cultures (middle-logarithmic phase) were harvested through centrifugation at 4000×g and 4°C for 10 minutes. The cell pellets were washed once with YPD/1M Sorbitol/2mM DTT. To digest cell walls, the cells were spheroplasted in 1-2ml YPD/1M Sorbitol with 0.1mg zymolyase per gram of cells at room temperature. The cell wall digestion was monitored under the phase contrast light microscope (Leitz Biomed Typ 020-507-010). When 50% of the cells became dark, the cells were harvested with centrifugation at 1000×g and 4°C for 5 minutes. After washing once with 1-2ml YPD/1M Sorbitol, the cells were recovered in 50-100ml YPD/1M Sorbitol for 30 minutes at 25°C. After recovery, the cells were shifted to the desired temperature for the indicated time if necessary. The cells were harvested again with centrifugation at 1000×g and 4°C for 10 minutes. 1/10 volume of the cell pellets were lysed (**Yeast lysis**, section 3.2.1.5) and the lysates were used as input controls. The rest of the cells were resuspended in cell lysis buffer with a volume of 0.5ml buffer/g cell pellets. To release the cell contents, cell buffer A was added with a volume of 1ml buffer/g cell pellets. The mixture was incubated for 5-10 minutes at 4°C. Afterwards, the mixture was centrifuged at 1500×g and 4°C for 15 minutes. The supernatant was carefully taken as the cytosolic extract. RNAs were obtained from the cytosolic extracts (**Acidic phenol extraction**, section 3.2.3.4) and used for qRT-PCR. Proteins were obtained from the extracts (**Protein extraction and precipitation**, section 3.2.2.1) and used for western blot analyses.

YPD medium: see section 3.2.1.3

Cell lysis buffer:

18% (w/v) Ficoll 400

10mM HEPES pH6.0

Cell buffer A:

50mM NaCl

1 mM MgCl<sub>2</sub>

10mM HEPES pH6.0

### **3.2.2.4 SDS-polyacrylamide gel electrophoresis (SDS-PAGE) and western blot**

Protein samples from protein precipitation, western blot, co-immunoprecipitation or RNA co-immunoprecipitation experiments were dissolved in 1×SDS sample buffer. The samples were incubated at 95°C for 5 minutes followed by centrifugation at 20000×g and room temperature for 1 minute. The clear supernatants were loaded onto the stacking gel. Protein ladders (5µl pre-stained or 10µl unstained PageRuler Protein ladder, Thermo Fisher Scientific) were loaded to indicate the protein size. SDS-PAGE was performed in 1×SDS running buffer at 25mA for the stacking gel and 35mA for the resolving gel. Alternatively, a constant 6-8mA was used overnight.

After SDS-PAGE, proteins were electrically transferred from the gel onto a nitrocellulose membrane. Western blot was performed by using a semi-dry electroblotter (Perfect Blue Semi dry Electroblotter, Peqlab). The SDS-polyacrylamide gel, a nitrocellulose membrane and four pieces of whatmann paper were presoaked with the transfer buffer. The transfer sandwich was assembled as follows (from the negative pole to the positive pole): two pieces of whatmann paper, the SDS-polyacrylamide gel, the nitrocellulose membrane, two pieces of whatmann paper. After removing the bubbles in the transfer sandwich, the western blot was performed at 0.8-1.2mA/cm<sup>2</sup> for 90 to 105 minutes. After blotting, the transferred membrane was stained in the Ponceau S for 3 minutes followed by a washing step in H<sub>2</sub>O. The Ponceau S staining stained the blotted proteins and the unstained protein ladder, which was marked. After removing residual Ponceau S staining with 1×TBST, the membrane was blocked in 5% (w/v) milk powder/1×TBST at room temperature for 1 hour. Subsequently, the membrane was incubated with the primary antibodies (*e.g.* mouse anti-myc antibody, rabbit

anti-GFP antibody, rabbit anti-Mtr4 antibody, *etc.*) diluted in 2% (w/v) milk powder/1×TBST for 2 hours at room temperature or overnight at 4°C. After four times over 15 minutes washing with 1×TBST, the membrane was incubated with the secondary antibodies (*e.g.* goat anti-mouse-HRP, goat anti-rabbit-HRP, *etc.*) diluted in 2% (w/v) milk powder/1×TBST for 1.5 to 2 hours at room temperature. Chemiluminescent signals were generated by using the Amersham ECL prime Western Blotting Detection reagents (GE Healthcare) according to the manufacture's instruction. The signals were detected by using the Fusion FX7 detection system (Peqlab).

1×SDS Sample buffer: see section 3.2.1.5

5% Stacking gel:

16.7% (v/v) Rotiphorese Gel 30

(aqueous 30 % acrylamide and bisacrylamide stock solution at a ratio of 37.5:1)

0.125M Tris pH6.8 (recipe in section 3.1.5)

0.1% (w/v) SDS (sodium dodecyl sulfate)

0.1% (w/v) APS (ammonium persulfate)

0.01% (v/v) TEMED (N,N,N,N'-Tetramethylenediamine)

8-12% Resolving gel:

26.4%-39.6% (v/v) Rotiphorese Gel 30

0.375M Tris pH8.8 (recipe in section 3.1.5)

0.1% (w/v) SDS

0.1% (w/v) APS

0.04-0.08% (v/v) TEMED

1×SDS running buffer:

25mM Tris Base

0.1% (w/v) SDS

192mM Glycin

Transfer buffer:

192mM glycine

25mM Tris Base

10%-20% methanol

0.03%-0.05% SDS added if 10% methanol was used

Ponceau S solution:

0.2% (w/v) Ponceau S

5% (v/v) acetic acid

20×TBS:

1M Tris pH7.4

3M NaCl

1×TBST:

1× TBS

0.1% (v/v) Tween-20

### 3.2.3 Molecular biological methods

#### 3.2.3.1 Polymerase chain reaction (PCR)

PCR reaction parameters vary according to templates, products, and polymerases. The PCR reactions were usually set up as below:

Component		Final concentration
Template	Plasmid	100pg-10ng for 50-100µl reaction
	or Genomic DNA	1µg for 50-100µl reaction
10×reaction buffer (polymerase specific)		1×
dNTP		0.2mM
DNA polymerase		1unit for 50µl reaction
Forward primer		1µM
Reverse primer		1µM

To generate desired products, different DNA polymerases were used. For routine PCR reactions, DreamTaq DNA Polymerase (without proof-reading ability, Thermo Fisher Scientific) was used. For proof-reading PCRs (products used for *e.g.* sequencing, molecular cloning, *etc.*) either the Phusion High-Fidelity DNA Polymerase (New England Biolabs) or KAPAHiFi Polymerase (Peqlab) was used.

The PCR procedures were set as below:

Step		Temperature	Time
Initial denaturation		95-98°C	30 seconds to 3 minutes
20-40 cycles	Denaturation	95-98°C	10-30 seconds
	Annealing	0-5°C below the T <sub>m</sub> (DNA melting temperature) of the primers	15-60 seconds
	Extension	68°C or 72°C	30-120seconds/kb
Final extension		68°C or 72°C	5-10 minutes
Hold		4°C	

### 3.2.3.2 DNA gel electrophoresis and gel extraction

To prepare agarose gel 0.8%-1.2% agarose (w/v) was dissolved in 1×TAE buffer by cooking and mixing. Subsequently, once the agarose gels were cooled down to around 60°C, ethidium bromide was added to a final concentration of 0.5µg/ml.

6×DNA loading dye was added to DNA samples to a final concentration of 1×. To indicate the DNA size, 5-7 µl DNA marker (0.5µg/µl, Lambda DNA/EcoRI+HindIII DNA Ladder or GeneRuler 1 kb DNA Ladder, Thermo Fisher Scientific) was also loaded. The DNAs were separated by agarose gelelectrophoresis at 100-120 Volts and room temperature for 20-30 minutes. DNAs were detected by the 312nm UV-light with INTAS UV-system (INTAS).

To obtain specific DNA samples, the DNA bands were cut from the gels. Desired DNAs were extracted from the gel by using the peqGOLD Gel Extraction Kit (Pqlab) according to the manufacture's instruction.

#### 1×TAE buffer (pH8.5):

40mM Tris Base

1mM EDTA

0.114% (v/v) Acetic acid

Adjust pH to 8.5

#### 6×DNA loading dye:

10mM Tris pH7.6

0.03% (w/v) Bromophenol blue

0.03% (w/v) Xylene carbol blue

60% (v/v) Glycerol

60mM EDTA

### 3.2.3.3 Genomic DNA extraction

10ml yeast culture was grown to a concentration of  $>1 \times 10^8$  cell/ml. The cells were harvested through centrifugation at  $4000 \times g$  and room temperature for 10 minutes. The cells were mixed with 500  $\mu$ l detergent lysis buffer, 500  $\mu$ l phenol and 300  $\mu$ l glass beads and lysed by two vigorous shakes on the Fastprep machine at 6.0m/s for 20 seconds.

The mixture was centrifuged at  $20000 \times g$  and room temperature for 5 minutes. The upper layer was carefully transferred to a fresh tube and the same volume of phenol was added. The mixture was shaken vigorously by vortexing and centrifuged at  $20000 \times g$  and room temperature for 5 minutes. This step was repeated twice, once replacing phenol with phenol/chloroform/isoamyl alcohol (25:24:1, Carl Roth) and once with chloroform/isoamyl alcohol (24:1, Carl Roth). Afterwards, 1/10 volume 3M sodium acetate pH5.3 and 3 times the volume of 100% ethanol were added to the extract and the mixture was incubated at  $-20^\circ\text{C}$  for 15 minutes for precipitation. Genomic DNA (gDNA) pellet was obtained by a centrifugation at  $20000 \times g$  and  $4^\circ\text{C}$  for 20 minutes. The pellet was washed with 75% ethanol and centrifuged at  $20000 \times g$  and  $4^\circ\text{C}$  for 5 minutes. The gDNA pellet was air-dried at room temperature or  $37^\circ\text{C}$  and finally dissolved in nuclease-free  $\text{H}_2\text{O}$  or TE buffer pH8.0. The gDNAs were either stored at  $-20^\circ\text{C}$  or used for PCR or southern blot experiments.

#### Detergent lysis buffer :

2% (v/v) Triton X-100

1% (w/v) SDS

100mM NaCl

10mM Tris Cl

1mM EDTA

#### TE buffer (pH7.5 or 8.0):

10mM Tris pH7.5 or 8.0

1mM EDTA

### 3.2.3.4 Acidic phenol RNA extraction

Cells from 20-50ml cell cultures (logarithmic phase) were harvested through centrifugation at 4000×g and 4°C for 10 minutes. The cells were mixed with 400µl AE buffer, 40µl 10% SDS, 440µl aqua-phenol and incubated at 65°C for 5 minutes with occasional inversions. The mixture was frozen at -80°C for more than 30 minutes and subsequently centrifuged at 20000×g at room temperature for 5 minutes. The upper phase was carefully transferred to a fresh tube.

The samples for RNA extraction were the extracts obtained as mentioned above or from the nucleo-cytoplasmic fractionation or RNA co-immunoprecipitation experiments. The same volume of aqua-phenol was added to the extract and the mixture was shaken vigorously by hand and centrifuged at 20000×g and room temperature for 5 minutes. This step was repeated twice, once replacing aqua-phenol with aqua-phenol/chloroform /isoamyl alcohol (25:24:1, Carl Roth) and once with chloroform/isoamyl alcohol (24:1, Carl Roth). 1/10 the volume of 3M sodium acetate pH5.3 or 1/4 the volume of 4M DEPC treated lithium chloride and 3-time the volume of 100% ethanol were added to the extract and the mixture was incubated at -80°C for 30 minutes or at -20°C overnight for precipitation. RNA pellet was obtained by centrifugation at 20000×g and 4°C for 30 minutes. The pellet was washed with 75% -20°C ethanol made with DEPC-H<sub>2</sub>O and centrifuged at 20000×g and 4°C for 15 minutes. The RNA pellet was air-dried on ice and finally dissolved in DEPC-H<sub>2</sub>O or TE buffer pH7.5 made with DEPC-H<sub>2</sub>O. The RNAs were either stored at -20°C for weeks and at -80°C for months or used in qRT-PCR experiments.

#### Diethylpyrocarbonate (DEPC) treated solution:

Add DEPC in solution with final concentration of 0.1%. Mix overnight and autoclave.

Alternatively, prepare solution with DEPC-treated H<sub>2</sub>O

#### AE buffer (pH 5.2):

50 mM sodium acetate



10 mM EDTA

Adjust pH to 5.2

TE buffer (pH7.5): see section 3.2.3.3

### 3.2.3.5 Probe synthesis

A nucleic acid probe can be a DNA or an RNA molecule that is labeled with *e.g.* the fluorescent tag Cy3 or special chemicals like digoxigenin (DIG), *etc.*

3'-end DIG-labelled single-strand DNA oligonucleotide probes (*e.g.* HK1539) for southern blot experiments were ordered from Sigma. The oligo probes were diluted in sterile H<sub>2</sub>O or TE buffer pH7.5 with a concentration of 100mM as stock solutions and stored at -20°C.

The Cy3-labelled single-strand DNA oligonucleotide probes that were labelled at both the 3' and the 5' ends (*e.g.* HK 1761, HK1789, HK1790) for fluorescent *in situ* hybridisation were purchased from Sigma. The oligonucleotide probes were diluted in sterile H<sub>2</sub>O or TE buffer pH7.5 with a concentration of 10mM as stock solutions and stored at -20°C under light protection.

DIG labeled RNA probes for fluorescent *in situ* hybridisation were produced through *in vitro* transcription. The templates were PCR products that contained T7 transcription sites upstream of the anti-sense strands of target genes and were generated by **PCR** (section 3.2.3.1) and purified via **DNA gel electrophoresis and gel extraction** (section 3.2.3.2). The *TLC1* probes were generated from the PCR products of primer pairs HK936+HK937, HK938+HK939, HK940+HK941, HK942+HK943 as templates. The 25S rRNA probes were generated from the PCR products of HK1138+HK1139. The 18S rRNA probes were generated from the PCR products of HK1140+HK1141. The U6 RNA probes were generated from the PCR products of HK1404+HK1492. To synthesize probes, 200-250ng of the PCR products were mixed with 1× T7 transcription buffer (Thermo Fisher Scientific), 1u RNase inhibitor (40u/μl, Thermo Fisher Scientific), 5u T7 RNA polymerase (20u/μl, Thermo Fisher Scientific) and 1× DIG RNA labeling mix (Roche) in a total volume of 20μl. The 20μl-mixture was

incubated at 37°C for 1.5-2 hours. Subsequently, the reaction was stopped by adding 1µl 0.5M EDTA pH8.0. The transcripts were precipitated by adding 10µl tRNA (10mg/ml), 1/4 volume 4M DEPC treated lithium chloride and 3× volume 100% ethanol. The mixture was incubated at -20°C overnight or at -80°C for at least 30 minutes. The RNAs were pelleted by a centrifugation at 20000×g and 4°C for 30-60 minutes. The pellet was washed for 10 second by using 75% -20°C ethanol (made by DEPC-H<sub>2</sub>O) and centrifuged again at 20000×g and 4°C for 15 minutes. The pellet was air-dried on ice. The RNAs were dissolved in 100µl DEPC-H<sub>2</sub>O and stored at -20°C for weeks and at -80°C for months.

TE buffer (pH7.5): see section 3.2.3.3

### 3.2.3.6 Southern blot

Genomic DNAs were extracted (**genomic DNA extraction**, section 3.2.3.3). To perform the southern blot experiments that detected telomeres, gDNAs were mixed with 1× buffer R (Thermo Fisher Scientific) and 10u XhoI (10u/µl, Thermo Fisher Scientific) and incubated at 37°C overnight. Digested gDNAs were separated overnight on 1.0-1.2% agarose gels (**gel electrophoresis**, section 3.2.3.2) at 2 volts/cm. Subsequently the DNA gels were depurinated in 0.25N HCl for 15 minutes, denatured in 0.5M NaOH/1.5M NaCl for 30 minutes, neutralized in 0.5M Tris pH7.5/1.5M NaCl for 30 minutes and equilibrated in 20×SSC for 15 minutes. A capillary transfer (dry blot) was performed as follows (from bottom to top): a glass plate (supporter), the agarose gel facing down, a dry Hybond-N+ membran (GE Healthcare), three dry whatmann papers, 5-cm-thick paper-tower and 1kg weight on the top. Alternatively, a vacuum transfer was set from bottom to top: supporter, a 20×SSC pre-soaked whatmann paper, a 20×SSC pre-soaked nylon membrane, the gel facing up and the sealing frame. The capillary transfer usually took 4 hours to overnight and the vacuum transfer took 1-2 hours. After blotting, the membranes were cross-linked under UV light (312nm, Cross Linker Bio Link BLX 365) for 5 minutes and further baked at 80°C for 2 hours. The membranes were

pre-hybridised at 37°C for 1 hour in 10ml hybridization buffer. Subsequently, 0.1-1.0nmol probes (HK1539, 100mM) were added and the membranes were hybridised at 37°C for 4 hours to overnight. After hybridization, the membranes were washed once with 2×SSC/0.1% (w/v) SDS, 1×SSC/0.1% (w/v) SDS at room temperature, twice with 0.5×SSC/0.1% (w/v) SDS at 37°C, each for 15 minutes, respectively. The membranes were further washed with DIG washing buffer for 5 minutes and blocked in DIG blocking solution for 30 minutes at room temperature. The membranes were incubated with anti-DIG-alkaline phosphatase (Roche) diluted 1:10000 in DIG blocking solution for 30 minutes at room temperature. The membranes were washed twice with DIG washing buffer, each for 15 minutes at room temperature. The membranes were equilibrated in DIG detection buffer for 5 minutes at room temperature and incubated with the chemiluminescent substrate CSPD (Roche, 1:100 diluted in DIG detection buffer) for 5 minute at room temperature. The CSPD was removed from the membranes and the membranes were sealed in autoclave bags and incubated at 37°C for 15 minutes. The chemiluminescent signals were detected by using the Fusion FX7 detection system (Pqlab) (if detection time ≤30 minutes) or Super RX films (Fujifilm) followed by being developed with Optimax X-Ray Film Processor (Protec) (if detection time >30 minutes).

20×SSC:

3M NaCl

300mM Sodium citrate

Adjust pH to 7.0

1M Sodium phosphate buffer (pH7.2):

68.4% (v/v) 1M Na<sub>2</sub>HPO<sub>4</sub>

31.6% (v/v) 1M NaH<sub>2</sub>PO<sub>4</sub>

The hybridization buffer (pH7.2) for southern blot:

0.5M sodium phosphate buffer pH7.2 (recipe in section 3.1.5)

7% (w/v) SDS

1mM EDTA

5×Maleic acid buffer (pH7.5):

0.5M Maleic acid

0.75M NaCl

Adjust pH to 7.5

DIG washing buffer:

1×Maleic acid buffer

0.3% (v/v) tween-20

10×DIG blocking buffer:

1×Maleic acid buffer

10% (w/v) blocking reagent (Roche)

DIG blocking buffer:

1:10 dilute 10×DIG blocking buffer in 1×Maleic acid buffer

DIG Detection buffer:

0.1M Tris pH9.5

0.1M NaCl

### **3.2.3.7 RNA-co-immunoprecipitation (RNA-co-IP)**

The procedures of harvesting cells, lysing cells, precipitating desired proteins were similar as described in **co-immunoprecipitation** (section 3.2.2.2) but the PBSKMT buffer was replaced with the RNA co-IP buffer.

After the last washing step, the beads were divided into two portions. 1/10 volume of the beads were mixed with 10 $\mu$ l 2 $\times$ SDS sample buffer and used for SDS-polyacrylamide gel electrophoresis (SDS-PAGE) and western blot experiments as protein controls. The RNA was extracted from the rest 9/10 volume of the beads by using **acidic phenol-chloroform extraction** protocol (section 3.2.3.4). The extracted RNA was stored at -20°C for weeks or -80°C for months or was directly used for qRT-PCR experiments.

RNA co-IP buffer: see section 3.2.1.5

SDS sample buffer: see section 3.2.1.5

### **3.2.3.8 Quantitative reverse transcriptase PCR (qRT-PCR)**

To synthesize cDNA, 1 $\mu$ g RNA, 1 $\times$ random hexamer primer (from 20 $\times$ random hexamer primer, Thermo Fisher Scientific), and nuclease-free H<sub>2</sub>O were mixed in a total volume of 11.5 $\mu$ l. The mixtures were incubated at 65°C for 5 minutes and then chilled on ice for 5 minutes. 200u Maxima reverse transcriptase (Thermo Fisher Scientific), 10u RNase inhibitor (Thermo Fisher Scientific), 1 $\times$  reverse transcription buffer (Thermo Fisher Scientific) and 1 mM dNTP (Thermo Fisher Scientific) were added to the mixture to a final volume of 20 $\mu$ l and the mixture was incubated at 50-60°C for 30-45 minutes. The reaction was stopped by incubation at 95°C for 5 minutes. The cDNA samples were either directly used in the qPCR reaction or stored at -20°C for days and -80°C for months.

The 25 $\mu$ l qPCR sample was composed of 5 $\mu$ l 1:50 diluted cDNA, 0.2 $\mu$ l 10mM reverse and forward primers, 12.5 $\mu$ l 2 $\times$  GoTaq PCR master mix (Promega) and nuclease-free H<sub>2</sub>O. The primers (HPLC purification level) were purchased from Sigma. The primers were diluted in nuclease-free H<sub>2</sub>O to 10mM and stored at -20°C. The primer pair HK1382+HK1384 was used to quantify the immature *TLC1*; the primer pair HK1385+HK1386 was used to quantify the total amount of *TLC1*; the primer pair HK1404+HK1405 was used to quantify the U6 snRNA; the primer pair HK1396+HK1397 was used to quantify the 18S rRNA. The PCR reactions were

performed on the Rotor Gene Q (Qiagen). The PCR reaction was initiated with one 95°C 5-minute denature step. Afterwards, 40-50 cycles of two-step PCR reaction, which was composed of one 95°C 5-second denature step and one 60°C 20-second annealing and elongating step, were performed. A final melting step rising the temperature from 60°C to 95°C was used to determine the specificity of the PCR products.

Results output by Rotor Gene Q software (Qiagen) represented the Ct (cycle threshold) values, which meant the cycle number required for the fluorescent signal to cross the threshold (*e.g.* background level).  $Ct_{average}$  values were calculated from three PCR reaction replicates.  $\Delta Ct$  values represented the difference of transcription level between RNAs and were calculated according to " $\Delta Ct = Ct_{averageRNA1} - Ct_{averageRNA2}$ ". Usually RNA1 indicated the transcripts of interest (*e.g.* total *TLC1*, immature *TLC1*) and RNA2 indicated the reference transcripts (*e.g.* 18S rRNA, U6 snRNA).  $\Delta\Delta Ct$  values represented the different RNA transcription level between strains and were calculated according to " $\Delta\Delta Ct = \Delta Ct_{strain1} - \Delta Ct_{strain2}$ ". Usually strain1 indicated the strain of interest (*e.g.* mutants, gene-tagged strains) and strain2 indicated the reference strain (*e.g.* wild type, non-tagged strains). A relative fold enrichment of target RNA transcription level of target strains compared to reference strains was finally calculated according to " $fold\ change = 2^{(-\Delta\Delta Ct)}$ ". All these calculations were performed in Microsoft Excel (Microsoft). Calculations of standard deviations and P-values were described in **Signal detection, quantification and statistical analyses** (section 3.2.1.8).

## 3.2.4 Cell biological methods

### 3.2.4.1 Transformation

To prepare competent *E.coli* cells (DH5 $\alpha$ ), a single *E.coli* colony was grown in 10ml LB medium at 37°C for overnight. Subsequently the pre-culture was further diluted in 250ml SOB medium and grown until the OD<sub>600</sub> reached 0.6. The culture was aliquoted into 50ml falcons and the aliquots were incubated on ice for 10 minutes. The *E.coli* cells were harvested through centrifugation at 4000 $\times$ g and 4°C for 15 minutes. The cells were washed once in 80ml ice-cold transformation buffer, incubated 10 minutes on ice and harvested through centrifugation at 4000 $\times$ g and 4°C for 15 minutes. The cells were resuspended in 20ml ice-cold transformation buffer/7.5% (v/v) DMSO. The mixtures were incubated on ice for 10 minutes and aliquoted to 500 $\mu$ l before they were frozen in liquid nitrogen. These ultracompetent *E.coli* cells were stored at -80°C.

To transform *E.coli* cells, plasmids were incubated with the ultracompetent cells on ice for 30 minutes followed by a 2-minute heat shock at 42°C. The *E.coli* cells were subsequently shaken in 1ml LB medium for 45 minutes to 1.5 hours at 37°C. The cells were finally harvested at 20000 $\times$ g and room temperature for 1 minute and were grown on specific selective plates (*e.g.* LB plate containing ampicillin, *etc.*).

LB medium: see section 3.2.1.3

SOB medium:

0.5% (w/v) Yeast extract

2% (w/v) Peptone

10mM NaCl

2.5mM KCl

10mM MgCl<sub>2</sub>

10mM MgSO<sub>4</sub>

Transformation buffer:

10mM HEPES pH 6.3

15mM CaCl<sub>2</sub>

55mM MnCl<sub>2</sub>

250mM KCl

To transform yeast cells, the cells from 10-20 ml cell culture (logarithmic phase) were harvested by a centrifugation at 4000×g and room temperature for 10 minutes. The cells were washed once with 1ml sterile H<sub>2</sub>O and resuspended to 1×10<sup>9</sup> cells/ml in lithium acetate (LiOAc)/TE buffer. 50μl yeast cells were mixed with 1μg DNA and 50μg SS-carrier DNA, which was boiled at 95°C for 5minutes and chilled on ice for 2 minutes before usage. 300μl PEG400/LiOAc/TE buffer was added to the mixtures and the mixtures were incubated at 25°C for 30 minutes to 2 hours. The cells were heat-shocked at 42°C for 15 minutes and washed in 1ml sterile H<sub>2</sub>O. The cells were harvested with centrifugation at 10000×g and room temperature for 1 minute and resuspended in 100μl H<sub>2</sub>O. The transformed cells were grown on the selective plates (e.g. URA- plates, LEU- plates according to the select markers).

Lithium acetate (LiOAc)/TE buffer (pH7.5):

100mM Lithium acetate

10mM Tris pH7.5

1mM EDTA

PEG/ Lithium acetate (LiOAc)/TE buffe (pH7.5)r:

40% (v/v) PEG4000

100mM Lithium acetate

10mM Tris pH7.5

1mM EDTA



### 3.2.4.2 Immunofluorescence (IF)

Cells were grown to the middle-logarithmic phase if not indicated otherwise. If necessary, the cells were shifted to the desired temperature (*e.g.* 16°C for some cold sensitive strains, 37°C for some heat sensitive strains, *etc.*) for the indicated time (usually 30 to 60 minutes). The cells were subsequently fixed by adding formaldehyde (37%) to a final concentration of 4% (v/v). After fixation for 30 to 60 minutes, the cells were washed once with 1ml potassium phosphate buffer pH6.5 and twice with 1ml P-solution. The cells were resuspended and incubated in 100µl P-solution/10mM DTT for 10 minutes. Furthermore, the cell walls were digested by adding 5µl 10mg/ml zymolyase (Sigma). The cell wall digestion was monitored under the phase contrast microscope (Leitz Biomed Typ 020-507-010). When over 70% cells became dark, the spheroplasts were harvested by centrifugation at 500×g and 4°C for 5 minutes. The cells were washed twice with 500 µl P-solution and resuspended in P-solution with a concentration of around  $1 \times 10^9$  cell/ml. On poly-L-lysine coated slides 30 µl cells suspensions were incubated with the wells for 20 to 30 minutes at room temperature. After the cells were permeabilised in P-solution/0.5% (v/v) triton-X100, the cells were blocked in antibody blocking buffer for 1 hour at room temperature. Subsequently, the cells were incubated with the indicated primary antibodies (*e.g.* mouse anti-GFP antibody, rabbit anti-myc antibody, *etc.*), which were diluted in an appropriate concentration in antibody blocking buffer, for 2 hours at room temperature or overnight at 4°C. The primary antibodies were removed by washing for four times over 15 minutes with antibody blocking buffer. The cells were incubated with indicated secondary antibodies (*e.g.* sheep anti-mouse-AlexaFluor488 antibody, sheep anti-rabbit-AlexaFluor488 antibody, *etc.*), which were diluted to the appropriate concentration in antibody blocking buffer, at room temperature for 1.5-2 hours. Afterwards, the slides were washed with antibody blocking buffer for four times 15 minutes followed by washing twice for 30 minutes with 1×PBT. The cells were incubated with hoechst 33342 (1:10000 diluted in 1×PBS, Sigma) for 2-3 minutes to stain the DNA. Finally the slides were washed with 1×PBS for 3 times 5 minutes and covered with mounting solution (recipe in section 3.1.5) and coverslips. The slides were

either immediately analysed under microscope or were stored at -20°C for months.

Potassium phosphate buffer (pH6.5): see section 3.2.1.4

P-solution: see section 3.2.1.4

10×PBS: see section 3.2.1.5

1×PBT:

1×PBS

0.1% (v/v) Tween-20

Antibody Blocking Buffer:

5-10% (v/v) heat inactive fetal bovine serum

1×PBT

Mounting solution:

2% (w/v) n-Propyl gallate

80% (v/v) Glycerol

1×PBS

### **3.2.4.3 RNA fluorescent *in situ* hybridization (FISH)**

Cells were fixed, washed, zymolyase digested, immobilized on poly-L-lysine coated slides and permeabilized as described in **immunofluorescence** (section 3.2.4.2). The cells were pre-hybridised in hybridisation buffer at 37°C for 1 hour. After pre-hybridisation, the appropriate probes were diluted (1:20-1:40 for DIG labeled RNA probes, 1:400-1:4000 for Cy3 labeled oligo probes) in hybridisation buffer and were incubated on the cells at 37°C overnight. The cells were washed once with 2×SSC for 1 hour at room temperature, once with 1×SSC for 1 hour at room temperature, once with 0.5×SSC for 30 minutes at 37°C and

once with 0.5×SSC for 30 minutes at room temperature.

If Cy3 labeled oligo probes were used, the cells were incubated with hoechst33342 (Sigma) diluted 1:10000 in 1×PBS for 2-3 minutes and washed 3 times with 1×PBS, each for 5 minutes.

Alternatively, if DIG labeled RNA probes were used, the cells were blocked in antibody blocking buffer for 1 hour at room temperature. The cells were incubated with anti-DIG-FITC antibodies (Roche), which were diluted 1:200 in antibody blocking buffer, at 4°C for overnight. Afterwards, the unbound antibodies were removed by washing the cells twice with antibody blocking buffer for 15 minutes, once with antibody blocking buffer for 30 minutes and once with PBT for 30 minutes. The cells were incubated with hoechst33342 (Sigma) diluted 1:10000 in 1×PBS for 2-3 minutes and were washed 3 times with 1×PBS, each for 5 minutes.

The slides were finally covered with the mounting solution and coverslips and were either stored at -20°C or analysed under microscope.

50×Denhardt's:

1% (w/v) Ficoll

1% (w/v) Polyvinylpyrrolidone

1% (w/v) BSA

20×SSC: see section 3.2.3.6

hybridisation buffer:

50% (v/v) deionised formamide

5× DEPC treated SSC

1× Dehardt's

0.1mg/ml Heparin

Made by DEPC treated H<sub>2</sub>O

1×PBS: see section 3.2.1.5

1×PBT: see section 3.2.4.2

Antibody Blocking Buffer: see section 3.2.4.2

Mounting solution: see section 3.2.4.2

## 4. Results

### 4.1 *TLC1* Transport

#### 4.1.1 *TLC1* nuclear export

##### 4.1.1.1 Fluorescent *in situ* hybridization experiments reveal that the nuclear export of *TLC1* requires the mRNA export machinery

As a non-coding RNA (ncRNA) and a product of the RNA polymerase II, *TLC1* shares many features with the other ncRNAs from RNA polymerase II, e.g. snRNAs, snoRNAs etc. In mammalian cells, RNA polymerase II synthesised ncRNAs utilise CRM1 for their nuclear export (Kohler and Hurt, 2007). In *Saccharomyces cerevisiae*, *TLC1* also utilises the Crm1/Xpo1 export receptor for its export (Gallardo et al., 2008). However, whether there are other factors involved in *TLC1* nuclear export still remains unknown. Since an mRNA export factor, Mex67, is involved in rRNA export together with Crm1/Xpo1 (Faza et al., 2012; Gadai et al., 2001; Ho et al., 2000; Hurt et al., 1999; Stage-Zimmermann et al., 2000; Yao et al., 2007), it is unclear whether this is the same case for *TLC1* export. To further investigate *TLC1* nuclear export, fluorescent *in situ* hybridisation experiments were performed to identify *TLC1* localisation in the mRNA export mutants *mex67-5*, *rat7-1* and *rat8-2* (figure 4.1.1).

Prior to fluorescent *in situ* hybridisation experiments, the cell cultures of wild type (HKY381), *xpo1-1* (HKY206), *mex67-5* (HKY644), *rat7-1* (HKY124) and *rat8-2* (HKY130) strains were grown to the middle-logarithmic phase and the cells were shifted to 37°C for 1 hour. After the cells were spheroplasted, permeabilized and immobilized on slides, the cells were pre-hybridised. Afterwards, DIG labelled specific *TLC1* RNA probes were applied and the hybridised *TLC1* RNAs were subsequently detected by FITC conjugated anti-DIG antibodies.

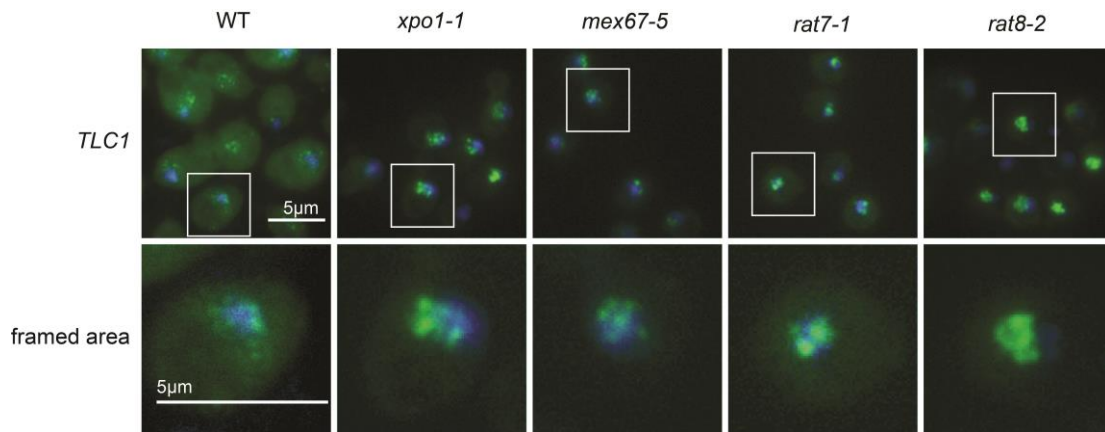


**Figure 4.1.1 *TLC1* localization patterns in the mRNA export defective mutants are similar to that seen in the *xpo1-1* cells.** To identify *TLC1* localisation in mRNA export mutants, fluorescent *in situ* hybridization (FISH) experiments were performed in the indicated strains. All cells were grown to the logarithmic phase and shifted to 37°C for 1 hour. Subsequently, *in-situ* hybridisation was performed by using specific DIG labeled anti-sense RNA probes against *TLC1* and the hybridised *TLC1* molecules were detected with FITC labeled anti-DIG antibodies (green). The nuclei were stained with hoechst33342 (blue). The framed areas show enlarged single cells in the figures below. At least three independent experiments were done, one of which is shown here. Scale bars: 5µm.

The results (figure 4.1.1) show that in wild type cells, *TLC1* signals are clustered in 8-10 foci around the nucleus as shown in previously published data (Gallardo et al., 2008) but the cytoplasmic background is relatively high, reflecting a low abundance of *TLC1* in the cytoplasm due to its nucleo-cytoplasmic trafficking (Ferrezuelo et al., 2002; Gallardo et al., 2008). Differently, the *xpo1-1* mutant, in which *TLC1* export is inhibited (Gallardo et al., 2008), shows a more concentrated *TLC1* nuclear accumulation and the cytoplasmic signals are much weaker than those in wild type cells. Strikingly, in the mRNA export mutants, *mex67-5*, *rat7-1* and *rat8-2*, the phenotypes of *TLC1* localisation are more similar to that in *xpo1-1* than in wild type cells, suggesting a potential role of the mRNA transport pathway in *TLC1* nuclear export.

Nevertheless, due to the nature of the nucleo-cytoplasmic trafficking of *TLC1* (Ferrezuelo et al., 2002; Gallardo et al., 2008), the localisation patterns of *TLC1* in *mex67-5*, *rat7-1* and *rat8-2* cells can also be due to enhanced *TLC1* nuclear re-import. To distinguish whether the nuclear accumulation of *TLC1* in these mutants was due to nuclear export block or increased nuclear re-import, these mRNA export defective mutants were crossed with the *yku70Δ* strain. In this background, *TLC1* is retained in the cytoplasm after its nuclear export (Gallardo

et al., 2008).

Fluorescent *in situ* hybridisation experiments were performed as described above in wild type (HKY381), *xpo1-1* (HKY206), *yku70Δ* (HKY1073), *mex67-5 yku70Δ* (HKY1397), *rat7-1 yku70Δ* (HKY1398) and *rat8-2 yku70Δ* (HKY1396), to detect the localisation of *TLC1* (figure 4.1.2). Additionally, a Cy3 labelled oligo-d(T)<sub>50</sub> probe was used to identify the localisation of poly(A)<sup>+</sup> containing RNAs in these strains. Since the probes were labelled with the fluorescent dye Cy3, the fluorescent *in situ* hybridisation experiments without the antibody detection step were performed.

Compared to the *TLC1* distribution in the cytoplasm of the *yku70Δ* strain, *TLC1* accumulates in the nuclei of the mRNA export mutants (HKY1397, HKY1398, HKY1396) (*TLC1* in figure 4.1.2). Besides, the localisation patterns of *TLC1* in these mutants remained comparable to that seen in *xpo1-1*, confirming *TLC1* nuclear export impairment in the mRNA export mutants. Besides, the fluorescent *in situ* hybridisation experiments that detect poly(A)<sup>+</sup>

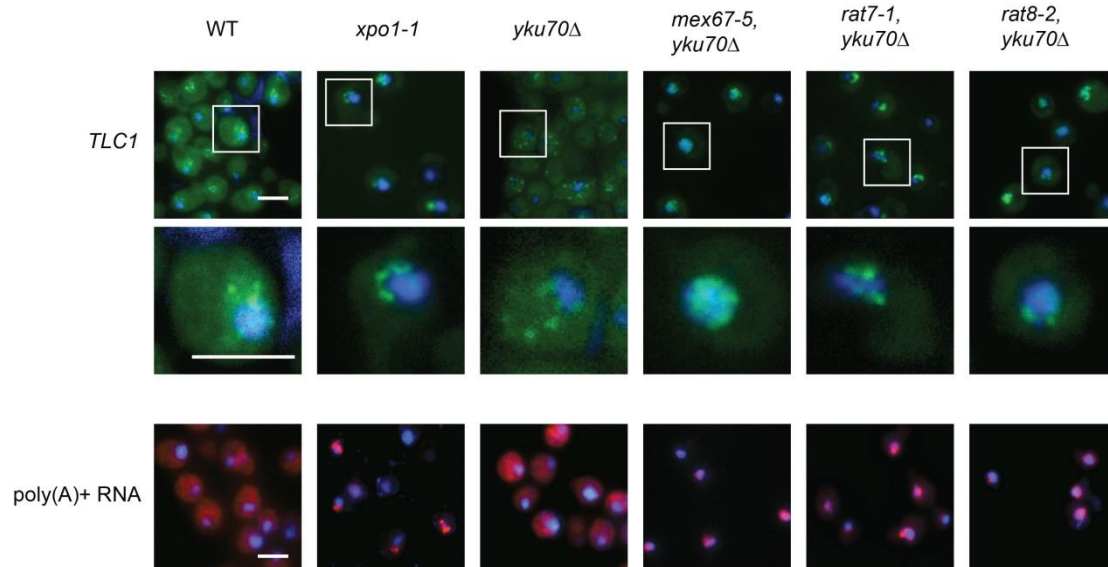


**Figure 4.1.2 No *TLC1* cytoplasmic retention is observed in the mRNA export defective mutants that contain the *yku70Δ* background.** Fluorescent *in situ* hybridization (FISH) experiments were performed in the indicated strains. All strains were grown to the logarithmic phase and shifted to 37°C for 1 hour. Subsequently, *in-situ* hybridisation was performed by using specific DIG labeled anti-sense RNA probes against *TLC1* and the hybridised *TLC1* molecules were detected with FITC labeled anti-DIG antibodies (green). Poly(A)<sup>+</sup> RNA was detected by using a CY3 labeled oligo d(T)<sub>50</sub> probe (red). The nuclei were stained with hoechst33342 (blue). The framed areas show enlarged single cells in the figures below. At least three independent experiments were done, one of which is shown here. Scale bars: 5µm.

RNAs (poly(A)<sup>+</sup> RNA in figure 4.1.2) showed that the poly(A)<sup>+</sup> RNAs accumulate in the mRNA export mutants. Surprisingly, in the *xpo1-1* mutant, poly(A)<sup>+</sup> RNA nuclear export defect was observed. This phenotype was also mentioned in earlier published literature and was proposed as an indirect effect of the defective Xpo1 (AskjaerStade et al., 1997).

Summed up, these results extend the previous knowledge that *TLC1* is exported via Crm1/Xpo1 and suggest a possibility of *TLC1* nuclear export via the mRNA export machinery.



#### **4.1.1.2 Nucleo-cytoplasmic fractionation shows decreased cytoplasmic abundance of *TLC1* upon blocking the mRNA export pathway**

Due to the *TLC1* nucleo-cytoplasmic movement (Ferrezuelo et al., 2002; Gallardo et al., 2008), its export block in the export mutants was proposed to reduce the amount of cytoplasmic *TLC1*. To examine this hypothesis, a cytoplasmic cell fractionation was performed and the amount of the cytoplasmic *TLC1* was measured via qRT-PCR (figure 4.1.3).

The strains wild type (HKY381), *sup45-2* (HKY446), *xpo1-1* (HKY206), *mex67-5* (HKY644), *rat7-1* (HKY124) and *rat8-2* (HKY130) were grown to the logarithmic phase. The cells were spheroplasted and further split into two equal portions. One portion was incubated at 25°C and the other portion was shifted to 37°C for 1 hour. Cells were lysed and subsequently fractionated. Zwf1 and Nop1 were used as the indicators of the cytoplasmic and nuclear fraction, respectively. Zwf1, a cytoplasmic glucose-6-phosphate dehydrogenase, and Nop1, a nucleolar histone glutamine methyltransferase, were detected through western blot analyses by using anti-Zwf1 or anti-Nop1 antibodies, respectively. The cytoplasmic RNAs were extracted from the cellular cytoplasmic fractions. *TLC1* was quantified using a specific *TLC1* primer pair (HK1385+HK1386) through qRT-PCR. Wild type and the *sup45-2* strain, a translation termination mutant that should not be involved in non-coding RNA transport, were used as the reference strains in these experiments. To evaluate the level of cytoplasmic *TLC1*, the amount of the cytoplasmic *TLC1* was compared to that of the total *TLC1*. These ratios were set into relation to that of wild type at 25°C.

The western blot analyses show an exclusive detection of Zwf1 but not Nop1 in the cytoplasmic fractions (C in figure 4.1.3 upper panel) confirming a successful isolation of the cytoplasmic fractions. Furthermore, the qRT-PCR analyses show that in *xpo1-1* and in the mRNA export defective mutants, the cytoplasmic *TLC1* levels are as stable as those in

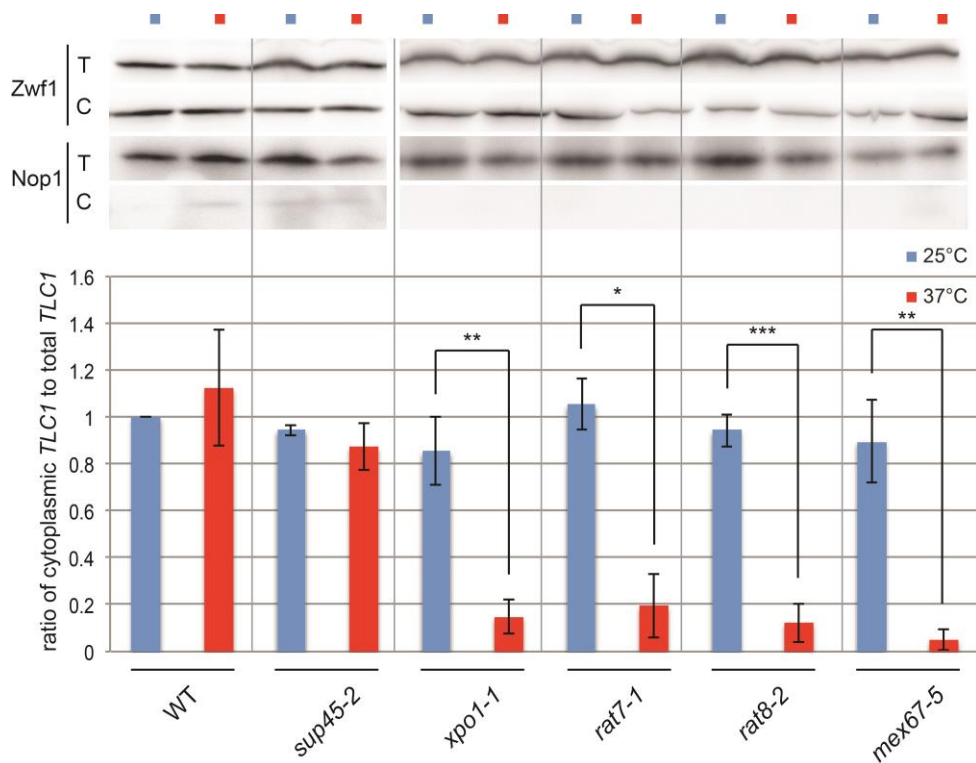


**Figure 4.1.3 Analyses of the cytoplasmic fraction show a reduction of the cytoplasmic *TLC1* level in the export defective mutants.** The indicated strains were grown to the logarithmic phase. Half of the cells were shifted to 37°C for 1 hour and the other half was kept at 25°C for 1 hour. The cytoplasmic fractions were extracted and confirmed through western blot analyses by detecting the cytoplasmic protein Zwf1 and the nuclear protein Nop1 (C in upper panel). The total cell lysates were used as the loading controls (T in upper panel). After RNA was extracted from the cytoplasmic fractions and the total cell lysates, cytoplasmic *TLC1* and total *TLC1* were measured through qRT-PCR by using the primer pair HK1385+HK1386. The amount of cytoplasmic *TLC1* was compared to that of the total *TLC1*. These ratios were set into relation with that of wild type at 25°C and shown in the diagram (25°C: blue column/dot; 37°C: red column/dot). At least three independent experiments were done. Error bars indicate the standard deviation. P-value was calculated using two-tailed, paired t-test (\*: 0.01≤p≤0.05; \*\*: 0.001≤p≤0.01; \*\*\*: 0.0001≤p≤0.001)

wild type and *sup45-2* at 25°C (blue columns in figure 4.1.3). Nevertheless, compared to wild type and *sup45-2*, the cytoplasmic amount of *TLC1* was largely reduced (~80%-90%) in *xpo1-1* and in the mRNA export defective mutants at 37°C (red columns in figure 4.1.3). These results provide a direct evidence that in the mRNA export mutants, nuclear export of *TLC1* is also impaired, further suggesting the involvement of the mRNA export factors in *TLC1* nuclear export.

### 4.1.1.3 The mRNA export factors physically interact with *TLC1*

If the mRNA export factors were involved in *TLC1* nuclear export, these factors should also physically interact with *TLC1*. To test this hypothesis, RNA co-IP experiments were performed (figure 4.1.4).

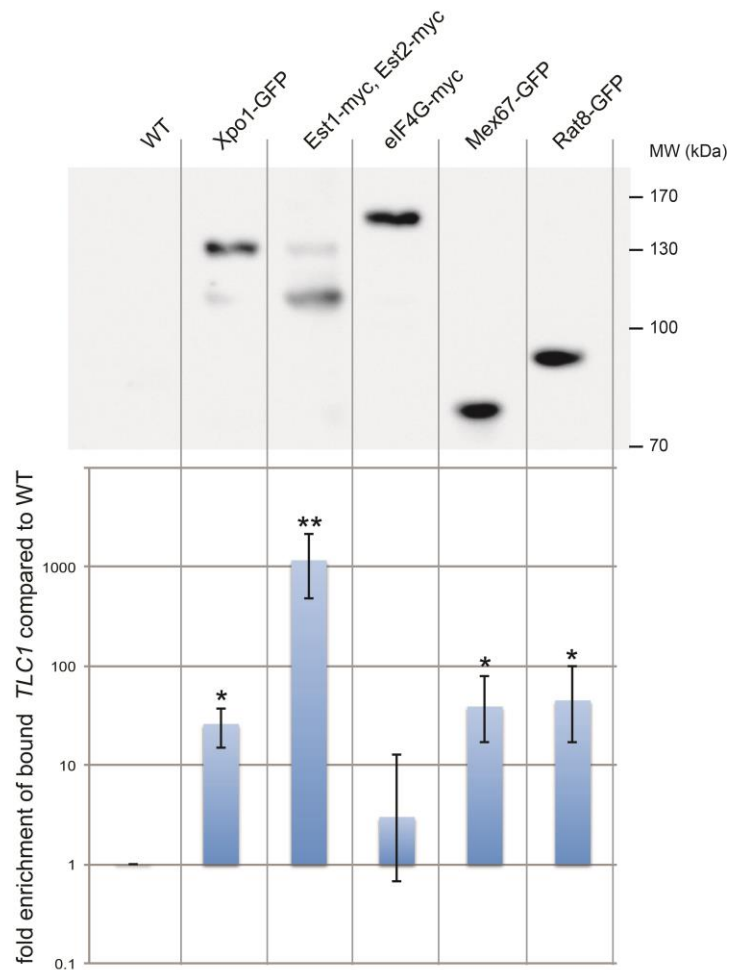


**Figure 4.1.4 *TLC1* physically interacts with the mRNA export factors.** All strains wild type (HK381), *XPO1/CRM1-GFP* (HKY145), *EST1-MYC EST2-MYC* (HKY1292), *TIF4631/EIF4G-MYC* (HKY578), *MEX67-GFP* (HKY1266) and *RAT8/DBP5-GFP* (HKY1242) were grown to the logarithmic phase. Proteins of interest were immuno-precipitated by using the mixture of anti-myc and anti-GFP antibodies and confirmed through western blot analyses (top panel). RNA bound to these proteins and the total RNA were extracted. *TLC1* was quantified through qRT-PCR using the specific *TLC1* primer pair (HK1385+HK1386). The amount of protein bound *TLC1* was compared to that of the total *TLC1*. These ratios were set into relation to that of wild type and shown in the diagram (bottom panel). At least three independent experiments were done. Error bars indicate the standard deviation. P-value was calculated according to two tailed, paired t-test (\*:  $0.01 \leq p \leq 0.05$ ; \*\*:  $0.001 \leq p \leq 0.01$ ).

In these experiments the strain wild type (HKY381) and the genomically tagged strains *XPO1/CRM1-GFP* (HKY145), *EST1-MYC EST2-MYC* (HKY1292), *TIF4631/EIF4G-MYC* (HKY578), *MEX67-GFP* (HKY1266) and *RAT8/DBP5-GFP* (HKY1242) were cultivated to the middle-logarithmic phase. The cells were harvested and lysed. The myc or GFP tagged proteins were precipitated using specific antibodies (anti-myc or anti-GFP). The RNA bound to these proteins was eluted. Subsequently, *TLC1* was quantified through qRT-PCR analyses (primer pair HK1385+HK1386) to reveal the physical interaction between *TLC1* and the analysed factors. To evaluate the interaction levels between the factors and *TLC1*, the amount of *TLC1* bound to these factors was compared to that of the total *TLC1* and the ratios were set into relation to that of wild type. The precipitated proteins were controlled via western blot analyses. (figure 4.1.4 upper panel).

As demonstrated in figure 4.1.4, Est1 and Est2 show a strongly enriched *TLC1* binding (~1000 fold) compared to the non-tagged background control, wild type (set as baseline 1). This suggests a specific and enduring interaction between the telomerase components and *TLC1*. On the other side, eIF4G, a translation initiation factor that is proposed to have no connection with non-coding RNA transport, shows an expected low *TLC1* binding ability that is similar to the non-tagged wild type control. Furthermore, similar to Xpo1 (~26 fold enrichment compared to the non-tagged wild type), two mRNA export factors, Mex67 as well as Dbp5/Rat8, showed a significantly enhanced *TLC1* binding (~39 fold for Mex67 and ~37 fold for Dbp5/Rat8), suggesting an interaction between *TLC1* and these factors. Although there is no evidence for a direct interaction, the results suggest an involvement of the mRNA export factors in *TLC1* nuclear export. Besides, together with previous results showing that *TLC1* molecules accumulate in the nuclei of the mRNA export mutants, *mex67-5*, *rat7-1* and *rat8-2*, it can also be concluded that *TLC1* nuclear export does not only depend on a single factor, e.g. Mex67, but rather require several proteins, including Mex67, Rat8/Dbp5 and Rat7.

#### **4.1.1.4 The *TLC1* nuclear export block observed in mRNA export mutants is not due to impaired *TLC1* transcription or maturation**

*TLC1* needs a series of processing steps to reach maturation and some of these processing failures lead to a *TLC1* nuclear mislocalisation, e.g. defect in hypermethylation of the m<sup>7</sup>G cap structure of *TLC1* (Gallardo et al., 2008). Therefore, the nuclear accumulation of *TLC1* might also be caused by defective *TLC1* transcription or processing. To exclude this possibility, qRT-PCR experiments were performed to examine *TLC1* transcription and processing in these mRNA export mutants.

The strains wild type (WT, HKY381), *xpo1-1* (HKY206), *rat7-1* (HKY124), *rat8-2* (HKY130) and *mex67-5* (HKY644) were grown to the logarithmic phase and subsequently shifted to 37°C for 1 hour. Total RNA was extracted from the cells. Specific primer pairs that detect unprocessed *TLC1* (HK1382+HK1384) and total *TLC1* (both processed and unprocessed, HK1385+HK1386) were designed as shown in figure 4.1.5A. As demonstrated in the figure, the primer pair for the total *TLC1* (HK1385+HK1386) flanks the region that includes the template of reverse transcription for telomere elongation and a part of the Est2 binding domain. The products of the primer pair for unprocessed *TLC1* (HK1382+HK1384) contain a part of the sequence, which will be post-transcriptionally removed during *TLC1* maturation, and a part of the matured *TLC1*, which bears the Sm<sub>7</sub> binding site. Besides, the primer pair HK1404+HK1405 was used to quantify the U6 snRNA, an RNA Polymerase III product, as a reference for the qRT-PCR experiments. To evaluate the transcription levels of *TLC1*, the amount of total *TLC1* was compared to that of the snRNA U6 and the ratios were set into relation to that of the wild type. To evaluate *TLC1* processing, the amount of unprocessed *TLC1* was compared to that of the total *TLC1* and the ratios were set into relation to that of the wild type.

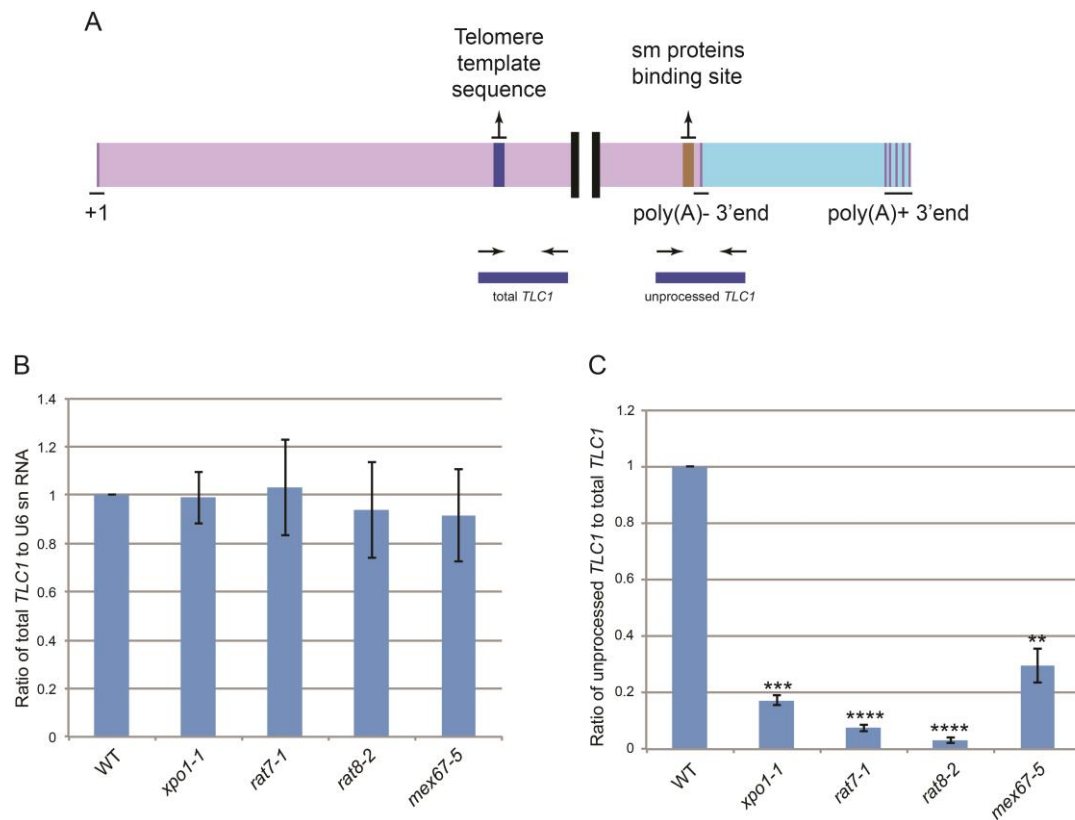


**Figure 4.1.5 *TLC1* nuclear export defect in mRNA export mutants is not due to impairments on its transcription and processing.** (A) A brief illustration of the *TLC1* structure and the schematic demonstration of the primer pairs. The primer pair (HKY1385+HK1386) for detecting total *TLC1* covers the *TLC1* core region including the telomere template sequence. The primer pair (HK1382+HK1384) for detecting immature *TLC1* flanks the 3'-end of mature *TLC1* and the 5'-part of the region that is removed from immature *TLC1* during processing steps. (B,C) All indicated strains were shifted to 37°C for 1 hour. Subsequently, total RNA was extracted from the cells. Total *TLC1* and unprocessed *TLC1* were quantified through qRT-PCR using their specific primer pair (HK1385+HK1386 and HK1382+ HK1394), respectively. The U6 snRNA, as the reference RNA, was quantified by using the specific primer pair (HK1404+HK1405). The amount of the total *TLC1* was compared to that of the snRNA U6 and the ratios were set into relation to that of the wild type (B). The amount of the unprocessed *TLC1* was compared to that of the total *TLC1* and the ratios were set into relation to that of the wild type (C). At least three independent experiments were done. Error bars indicate the standard deviation. P value was calculated via two-tailed, paired t-test (\*\*: 0.001≤p≤0.01; \*\*\*: 0.0001≤p≤0.001; \*\*\*\*: p<0.0001).

The results show that the relative transcription levels of *TLC1* compared to the U6 snRNA remain unchanged in all export defective mutants compared to the wild type (figure 4.1.5B). Furthermore, although the rates of unprocessed *TLC1* show unexpected reductions in the mRNA export defective mutants (figure 4.1.5C), these reductions are similar within the mRNA export mutants and the known *TLC1* export mutant, *xpo1-1*. These identical

phenotypes in the mRNA export mutants and *xpo1-1* further suggest that these factors might possess similar functions on *TLC1* in mediating its nuclear export. Moreover, these results are consistent with previous findings that the maturation of *TLC1*, including hypermethylation and 3'-trimming, occurs in the nucleus via the nuclear RNA modification machinery, *e.g.* Tgs1 (Franke et al., 2008) and the NRD pathway (Coy et al., 2013; Noel et al., 2012). In addition, fluorescent *in situ* hybridisation experiments showing that *TLC1* does not co-localise with the nucleolus in the export defective mutants (Daniel Becker and Heike Krebber) suggest an exit from the processing sites. All of these results support a model in which *TLC1* undergoes the maturation steps prior to its nuclear export.

#### 4.1.1.5 The *TLC1* nuclear export is mediated through cooperation of Xpo1/Crm1 and the mRNA export factor

The results above show that the *TLC1* nuclear export is mediated not only by the Crm1/Xpo1 export receptor, but also by the mRNA export factors. However, the relationship between these two pathways in the role of *TLC1* translocation is still unclear. To determine whether

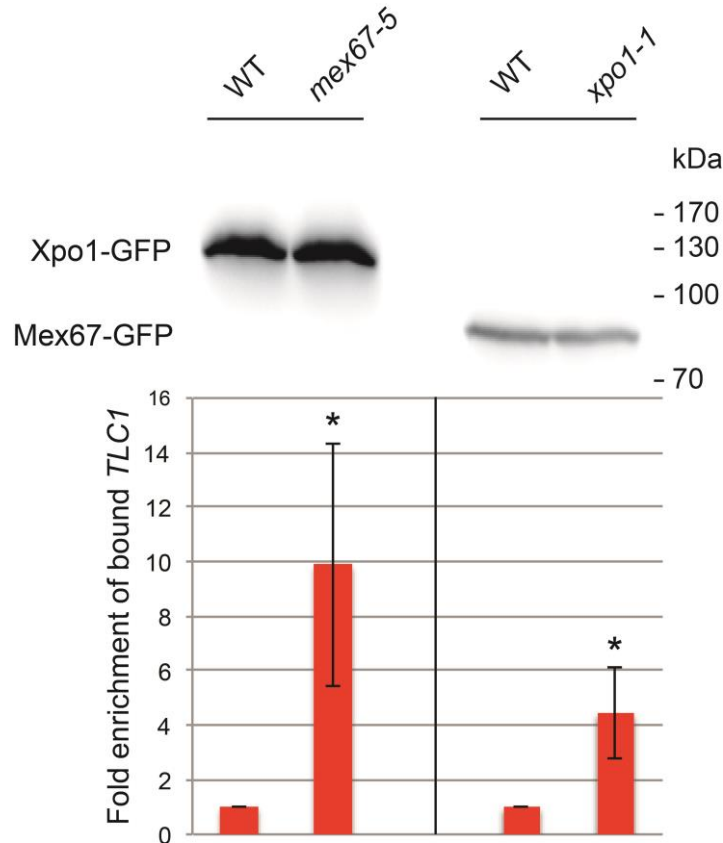


**Figure 4.1.6 The *TLC1* export activities of Xpo1/Crm1 and Mex67 are connected.** Wild type (HKY381) and the *mex67-5* (HKY644) cells were transformed with a *XPO1-GFP* containing plasmid (*pCEN URA3 XPO1-GFP*, pHK43). Additionally, wild type (HKY381) and the *xpo1-1* (HKY206) cells were transformed with a *MEX67-GFP* containing plasmid (*pCEN LEU2 pUN100-MEX67-GFP*, pHK20). All strains (HKY380+pHK43, HKY644+pHK43, HKY381+pHK20, HKY206+pHK20) were grown to the logarithmic phase and shifted to 37°C for 1 hour. Xpo1-GFP and Mex67-GFP were immuno-precipitated by using anti-GFP antibodies and identified by using western blot analyses (top panel). The RNA bound to these proteins and the total RNA were extracted. RNA was used to quantify the *TLC1* amount with the primer pair HK1385+HK1386 by qRT-PCR. The protein bound *TLC1* was compared to the total *TLC1* and these ratios were set into relation to that of wild type (*mex67-5*+pXPO1-GFP vs wild type+pXPO1-GFP, or *xpo1-1*+pMEX67-GFP vs wild type+pMEX67-GFP) (bottom panel). At least three independent experiments were done. Error bars indicate the standard deviation. P-value was calculated using two tailed, paired t-test (\*:0.01≤p≤0.05).



these two machineries function independently or coordinately, RNA co-immunoprecipitation experiments were performed. With the experiments, the *TLC1* recruitment was analysed on either Mex67 or Xpo1 in the genetic background of mutating the genes of the opposite factors (*mex67-5 + pXPO1-GFP* or *xpo1-1 + pMEX67-GFP*) (figure 4.1.6).

Wild type (HKY381) and the *mex67-5* (HKY644) cells were transformed with a *XPO1-GFP* containing plasmid (*pXPO1-GFP*, pHK43). Additionally, wild type (HKY381) and the *xpo1-1* (HKY206) cells were transformed with a *MEX67-GFP* containing plasmid (*pMEX67-GFP*, pHK20). All strains (HKY380+pHK43, HKY644+pHK43, HKY381+pHK20, HKY206+pHK20) were grown to the logarithmic phase and shifted to 37°C for 1 hour. GFP tagged Xpo1 or Mex67 was precipitated by using anti-GFP antibodies. The precipitated proteins were identified through western blot analyses (figure 4.1.6 upper panel). The bound RNA was eluted from the precipitated proteins and the total RNA was extracted from the whole cell lysates. The RNA was used for qRT-PCR analyses and *TLC1* was quantified from the RNA by using the primer pair HK1385+HK1386. To evaluate the interaction between the factors and *TLC1*, the protein bound *TLC1* was compared to the total *TLC1* and the ratios were set into relation to that of wild type (*mex67-5+pXPO1-GFP* vs wild type+*pXPO1-GFP*, or *xpo1-1+pMEX67-GFP* vs wild type+ *pMEX67-GFP*).

The results (figure 4.1.6 bottom panel) show an enriched *TLC1* binding to one factor in the case of the defect of the other RNA transport factor. This observation suggests that Xpo1/Crm1 and Mex67 are connected through *TLC1* and defect of one export factor will affect binding of the other one. Therefore, together with the fluorescent *in situ* hybridisation experiments showing that defects of either of these two pathways lead to a *TLC1* export block (figure 4.1.1 and 4.1.2), the results suggest a cooperative manner of these two factors in transporting *TLC1*.

Taken together, these results clearly indicate an important role of the mRNA export pathway in *TLC1* nuclear export. Besides, both the mRNA export factor and Crm1/Xpo1 work cooperatively on this RNA translocation. Finally, it also suggests that although the nuclear export pathway is blocked in the export mutants, *TLC1* appears to undergo maturation.

## 4.1.2 A *TLC1* export block affects telomerase formation

### 4.1.2.1 *TLC1* cytoplasmic deficiency leads to impaired localisation of the telomerase components

The results shown above allow the conclusion that *TLC1* utilises the mRNA export pathway for its export. Further experiments were performed to uncover the effects of impaired *TLC1* nuclear export on telomerase formation. Due to *TLC1* nucleo-cytoplasmic trafficking and the telomerase formation in the cytoplasm (Ferrezuelo et al., 2002; Gallardo et al., 2008), it can be proposed that the cytoplasmic presence of *TLC1* would be important for formation and localisation of the telomerase complex. To directly address the effects of the *TLC1* nuclear retention on the telomerase formation and localisation, immunofluorescence experiments were performed to track the localisation of the telomerase components, Est1 and Est2 (figure 4.1.7).

The immunofluorescence experiments were carried out in strains producing myc tagged Est1 and Est2 in the background of wild type, *xpo1-1* or the mRNA export defective mutants (figure 4.1.7A). The strains *EST1-12xMYC 3xFLAG-12xMYC-EST2* (wild type, HKY1292), *EST1-12xMYC 3xFLAG-12xMYC-EST2 tlc1::HIS* (*tlc1*Δ, HKY1294), *EST1-12xMYC 3xFLAG-12xMYC-EST2 xpo1::LEU2+pxpo1-1* (*xpo1-1*, HKY 1302), *EST1-12xMYC 3xFLAG-12xMYC-EST2 rat7-1* (*rat7-1*, HKY1332), *EST1-12xMYC 3xFLAG-12xMYC-EST2 rat8-2* (*rat8-2*, HKY1334) and *EST1-12xMYC 3xFLAG-12xMYC-EST2 mex67::HIS+pmex67-5* (*mex67-5*, HKY1336) were grown to the logarithmic phase. Half of the cells were kept at 25°C and the other half were shifted to 37°C for 1 hour. The localisations of Est1 and Est2 in the cells were detected by using mouse anti-myc antibodies and AlexaFluor488 conjugated goat anti-mouse secondary antibodies.

The results (figure 4.1.7A) show a nuclear enrichment of Est1 and Est2 in wild type cells, representing the nuclear localisation of the telomerase components. In contrast, Est1 and Est2 are mislocalised to the cytoplasm in the absence of *TLC1*, indicating a failure of the telomerase assembly. Similarly, in the *TLC1* export defective mutant, *xpo1-1*, a significant

reduction of nuclear Est1 and Est2 distribution was observed under the non-permissive condition (37°C). Although there was nuclear signal remaining, it can be explained by the presence of the pre-existing telomerase. Similar to *xpo1-1*, the mRNA export defective mutants, *mex67-5*, *rat7-1* and *rat8-2*, also show a comparable distribution of the telomerase components in the cytosol compared to wild type at the non-permissive condition (37°C).

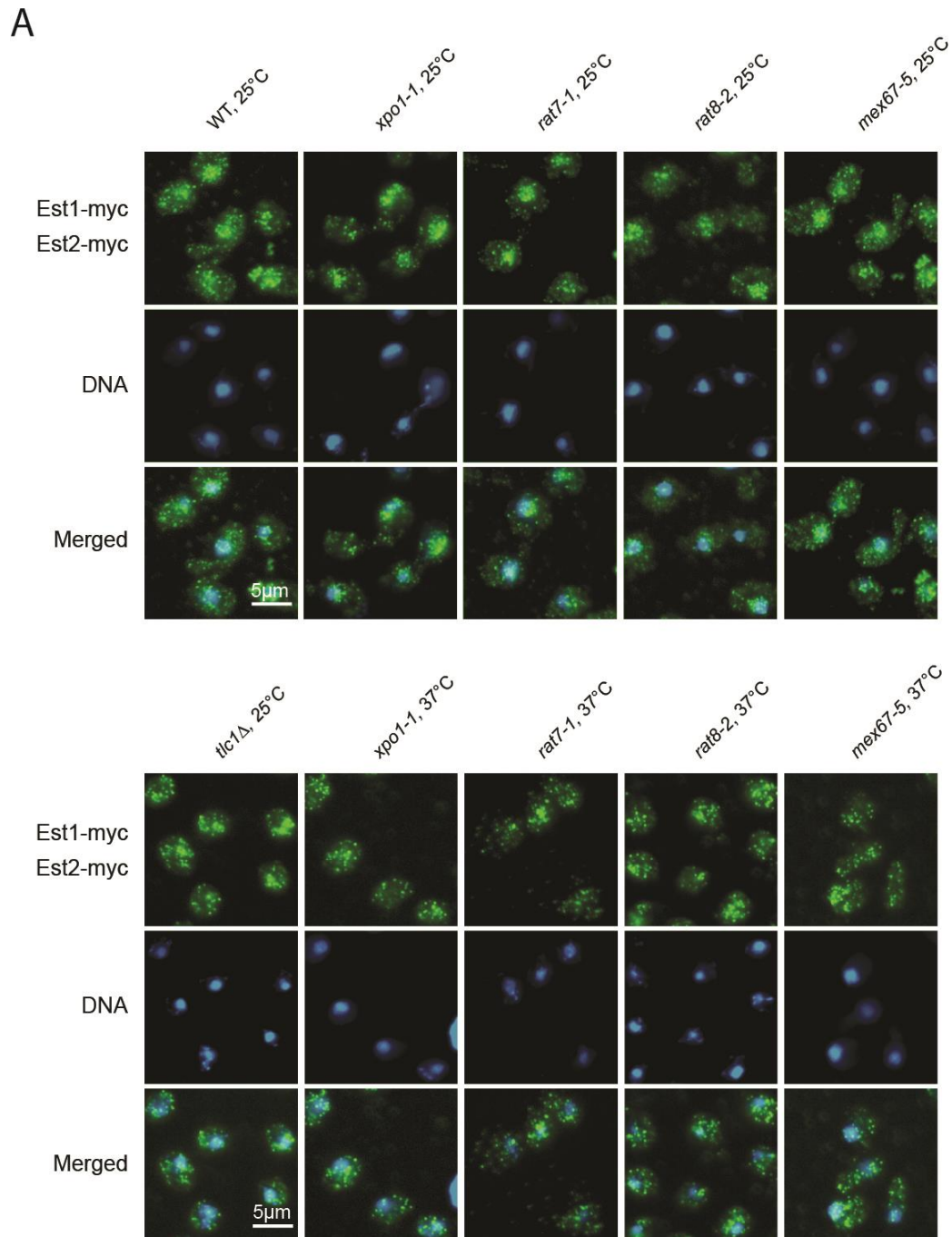
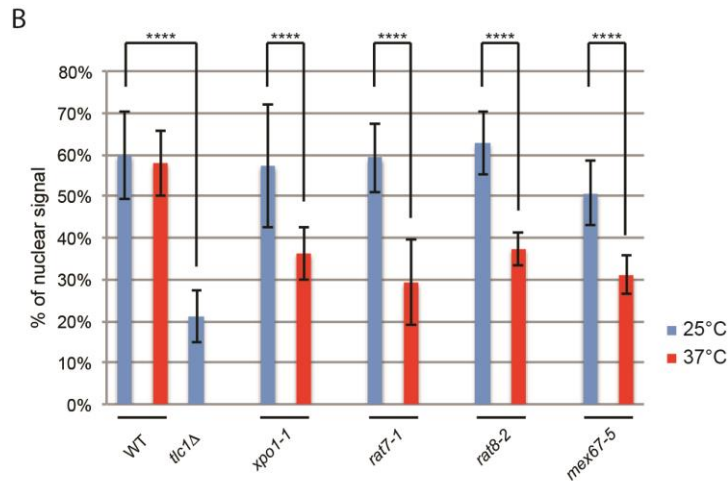


Figure legend see next page



**Figure 4.1.7 Telomerase components localisation is impaired due to *TLC1* export defects.**

All indicated strains were grown to the logarithmic phase. The cells were split into two equal portions. One portion was kept at 25°C and the other portion was shifted to 37°C for 1 hour. (A) Myc tagged Est1 and Est2 were detected by using mouse anti-myc antibodies and AlexaFluor488 anti-mouse antibodies (green). The nuclei were stained by hoechst33342 (blue). Scale bars: 5µm. (B) The ratios of the nuclear signal to total cell signal were shown in the diagram. For each condition the ratios of 20 cells were calculated. At least three independent experiments were done, one of which is shown in figure A. Error bars indicate the standard deviation. P-value was calculated using two-tailed, unpaired t-test (\*\*\*\*:  $p < 0.0001$ )

This suggests that due to the *TLC1* cytoplasmic deficiency in these mutants, the Est proteins are not imported into the nucleus. Signal quantification (figure 4.1.7B) reveals the change of the telomerase component localisation through calculating the ratio between the nuclear and total signal (N/T ratio) (figure 4.1.7B). Compared to the wild type (~60% N/T) and *tlc1Δ* (~21% N/T) strains, *mex67-5* (~29% N/T), *rat7-1* (~37% N/T) and *rat8-2* (~30% N/T) mutants show similar N/T ratios to *xpo1-1* (~36% N/T) at 37°C. Furthermore, comparing 25°C to 37°C in a given strain, the export mutants show an obvious reduction of the nuclear localisation of the telomerase components, e.g. *xpo1-1* (~21% N/T ratio reduction), *rat7-1* (~30% N/T ratio reduction), *rat8-2* (~26% N/T ratio reduction), and *mex67-5* (~20% N/T ratio reduction). Summed up, these results suggest that (1) Like Xpo1, the mRNA export factors also participate in transporting *TLC1*; (2) the model that the telomerase might be formed in the cytoplasm following the *TLC1* nuclear export is further supported; (3) the conclusion that Est1 nuclear re-import is independent of *TLC1* transport (Hawkins and Friedman, 2014) is however challenged.

Since Est1 and Est2 are mislocalised to the cytoplasm due to the *TLC1* nuclear export block in the mRNA export mutants, the amount of Est1 and Est2 in the cytoplasm might also be increased in this case. To obtain further evidence, cytoplasmic fractionation experiments were performed (figure 4.1.8).

Similar to the cell fractionation experiments in section 4.1.1.2, the strains mentioned above were fractionated and their cytoplasmic fractions were extracted. Zwf1 and Nop1, which were mentioned in section 4.1.1.2, were used as indicators to verify the fractionation experiments. As shown in the total cell lysates (T in figure 4.1.8), all Est1, Est2, Nop1 and Zwf1 were detectable; however, in the cytoplasmic fractions (C in figure 4.1.8), Nop1 was not detectable, suggesting the successful elimination of the nuclear fraction. Subsequently, the cytoplasmic amount of Est1+Est2 at 37°C was compared to that at 25°C and the ratios were set into relation to that of the wild type at 25°C (figure 4.1.8 bottom panel). In addition, the amount of the cytoplasmic Est1+Est2 in *tlc1Δ* at 25°C was also compared to that in wild type and the ratios were used as positive controls.

The experiments (figure 4.1.8) clearly show a cytoplasmic retention of the telomerase components once *TLC1* is unable to reach the cytoplasm to serve as the scaffold for the telomerase formation. The quantification indicates a dramatic cytoplasmic mislocalisation of the telomerase components in the absence of *TLC1* (~8 fold cytoplasmic enrichment comparing *tlc1Δ* to wild type). Moreover, in the *TLC1* nuclear export defective mutants, *xpo1-1* (~4 fold cytoplasmic enrichment comparing 37°C to 25°C), *mex67-5* (~3 fold cytoplasmic enrichment comparing 37°C to 25°C) as well as *rat8-2* (~4 fold cytoplasmic enrichment comparing 37°C to 25°C), show a comparable mislocalisation phenotype of the telomerase components, suggesting that the nuclear re-import of the telomerase components is dependent on *TLC1* nuclear export.

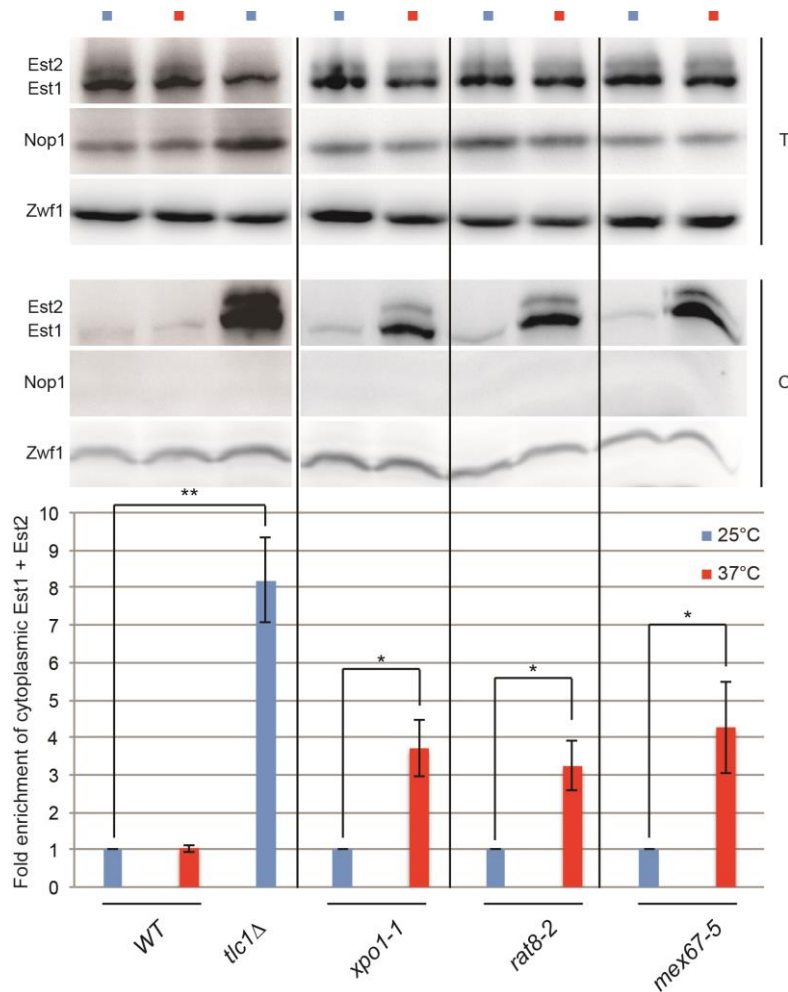


**Figure 4.1.8 *TLC1* cytoplasmic deficiency leads to the cytoplasmic enrichment of the telomerase components.** All indicated strains were grown to the logarithmic phase. Half of the cells were kept at 25°C and the other half were shifted to 37°C for 1 hour. Cells were fractionated and the cytoplasmic fractions were isolated. The total cell extracts (T) and the cytoplasmic fractions (C) were analysed through western blot analyses (upper panel). Est1-myc and Est2-myc were detected using anti-myc antibodies. Zwf1 and Nop1 were used as the cytoplasmic and nuclear indicators and were detected using rabbit anti-Zwf1 and anti-Nop1 antibodies, respectively. The amount of Est1+Est2 at 37°C was compared to that at 25°C. In addition, the amount of the cytoplasmic Est1 and Est2 in *tlc1Δ* was compared to that in wild type. The ratios are shown in the diagram (lower panel). At least three independent experiments were done, one of which is shown in the upper panel. Error bars indicate the standard deviation. P-value was calculated using two-tailed, paired t-test (\*:  $0.01 \leq p \leq 0.05$ ; \*\*:  $0.001 \leq p \leq 0.01$ ).

#### 4.1.2.2 Less *TLC1*-Est2 interactions are formed due to the *TLC1* nuclear retention

Since the results above show a mislocalisation of the telomerase components, which could be due to the reduction of the cytoplasmic presence of *TLC1*, a reduced physical interaction between *TLC1* and the telomerase components would be expected. RNA co-immunoprecipitation experiments were performed to determine the association of *TLC1* to the telomerase component in the cytoplasm (figure 4.1.9).

The strains (HKY1292, HKY1302, HKY1332, HKY1334 and HKY1336) that were used in section 4.1.2.1 were also used in these experiments. The cells were grown to the logarithmic phase at 25°C. The cells were either retained at 25°C or shifted to 37°C for 1 hour. Est2 was precipitated by using anti-FLAG antibodies. The Est2 bound RNA was subsequently eluted from the precipitated proteins and the total RNA was extracted from the whole cell lysates. *TLC1* was quantified through qRT-PCR by using the specific *TLC1* primer pair (HK1385+HK1386). The Est2 bound *TLC1* in a given strain was first compared to the total *TLC1*. This ratios at 37°C was further compared to that at 25°C in this strain. The ratios were finally set into relation to the wild type.

The results show that the interactions between *TLC1* and Est2 are reduced not only in *xpo1-1* (~34% reduced), but also in the mRNA export mutants (~36% in *rat7-1*, ~33% in *rat8-2* and ~41% in *mex67-5*). These results support the potential role of mRNA export factors in *TLC1* nuclear export and the model of cytoplasmic assembly of the telomerase complex (Ferrezuelo et al., 2002).

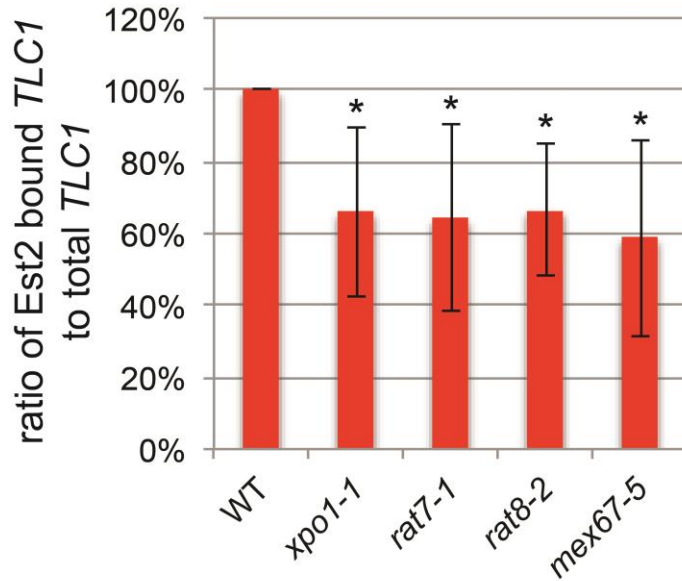


**Figure 4.1.9 RNA co-immunoprecipitation experiments show a reduced association of *TLC1* to Est2 in the export defective mutants.** All indicated strains were grown to the logarithmic phase. Half of the cells were kept at 25°C and the other half were shifted to 37°C for 1 hour. FLAG tagged Est2 was precipitated by using mouse anti-FLAG antibodies. RNA bound to Est2 the total RNA was extracted. *TLC1* was quantified through qRT-PCR by using the specific *TLC1* primer pair (HK1385+HK1386). The bound *TLC1* was compared to the total *TLC1*. This ratio at 37°C was further compared to that at 25°C. They were finally set into relation with that of wild type. At least three independent experiments were done. Error bars indicate the standard deviation. The p-value was calculated using two-tailed, paired t-test (\*:  $0.01 \leq p \leq 0.05$ ).



### 4.1.2.3 Reduction of the *TLC1* cytoplasmic presence affects the interaction between the telomerase components

The interaction between Est1 and Est2 is indirect and mediated by *TLC1* (Lubin et al., 2012). Due to the scaffold function of *TLC1* on composition of the telomerase complex, the components are not able to be assembled to build up the telomerase complex without *TLC1*. Therefore, since it has been concluded that telomerase formation might occur in the cytoplasm and this constitution needs cytoplasmic *TLC1* presence, the decreased *TLC1* nuclear export might reduce the efficiency of telomerase assembly. Co-immunoprecipitation experiments were performed to examine the interaction between telomerase components, Est1 and Est2, to identify the telomerase assembly (figure 4.1.10).

The strains (HKY1292, HKY1294, HKY1302, HKY1332, HKY1334 and HKY1336) that were used in section 4.1.2.1 were also used in these experiments. All strains were grown to the logarithmic phase and were either retained at 25°C or shifted to 37°C for 1 hour. FLAG tagged Est2 was precipitated with anti-FLAG antibodies. In addition, one of the wild type sample was treated with RNaseA (final concentration: 0.1mg/ml) to remove *TLC1* and its mediated Est1-Est2 interaction. Both Est1 and Est2 were detected by using the anti-myc antibodies through western blot analyses. Besides, the total cell lysates were used as input controls and Hem15, a mitochondrial inner membrane protein, was used as loading control. Hem15 was detected by anti-Hem15 antibodies. The interactions between Est1 and Est2 were evaluated through calculating the ratios of the amount of Est2 to Est1. These ratios at 37°C were further set into relation to those at 25°C in a given strain. The protein levels of Est1 and Est2 were evaluated through comparing the amount of Est1+Est2 from the input control to that of Hem15 from the loading control. These ratios were also set into relation to that of wild type. Apparently, decreased interactions of the telomerase components are observed in the *TLC1* export mutants (figure 4.1.10A). The quantification of the interactions (figure 4.1.10B) shows that ~89% of the interaction between Est1 and Est2 is reduced if *TLC1* is not present in *tlc1Δ* strains. In wild type cells upon RNase treatment, ~65% of the interaction is also reduced. Since Est1 and Est2 interact through *TLC1*, incomplete destruction of Est1-Est2 interaction

from this RNase treatment might be probably due to the compact clustering of the telomerase complex reported previously (Gallardo et al., 2011). Interestingly, the *TLC1* export defective mutants show only ~53%, ~58%, ~64% and ~67% of the Est1-Est2 interactions remaining in *xpo1-1*, *rat7-1*, *rat8-2* and *mex67-5*, respectively. In addition, the protein levels of Est1 and Est2 were also quantified to identify the effect of the RNA export defects on gene expression (figure 4.1.10C). Interestingly, stronger defect on producing of the telomerase components, especially Est2, is found in *tlc1Δ* and this is coincident to previous findings showing only 50% *EST2* expression level in the *tlc1Δ* strain (Taggart et al.,

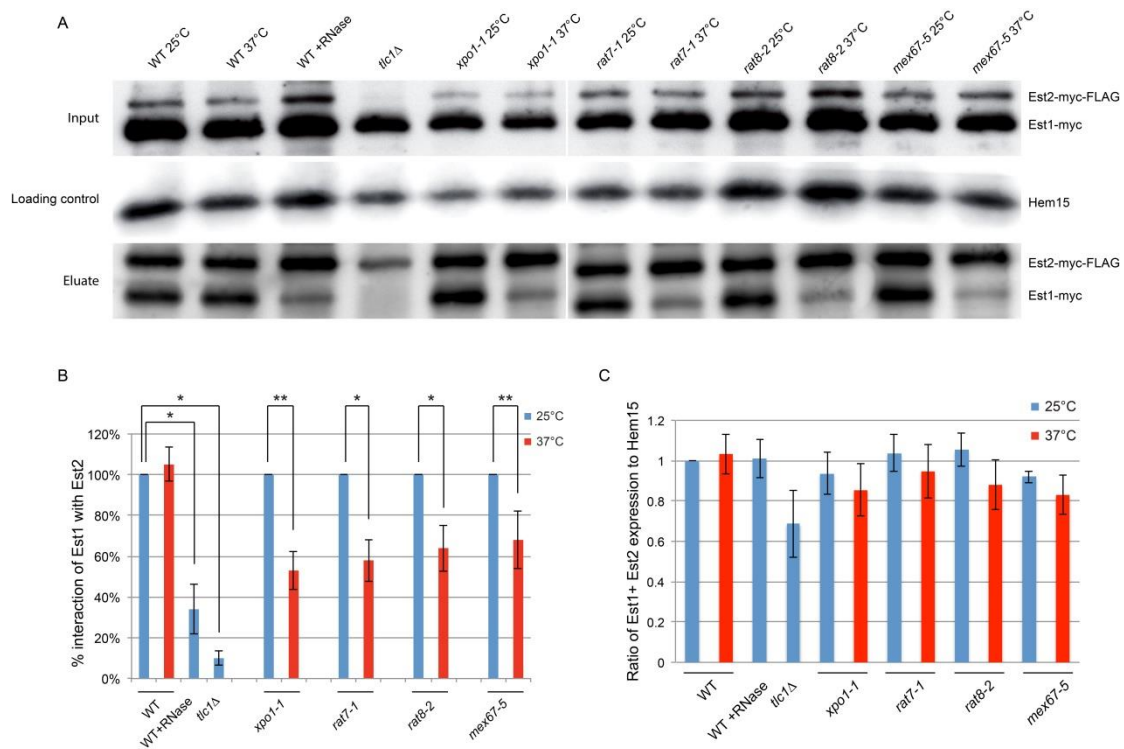


**Figure 4.1.10 The interactions between Est1 and Est2 are impaired in the export mutants.** All indicated strains were grown to the logarithmic phase. Half of the cells were kept at 25°C and the other half were shifted to 37°C for 1 hour. One additional portion of the wild type sample was treated with RNaseA (final concentration: 0.1mg/ml). To precipitate FLAG tagged Est2, mouse anti-FLAG antibodies were used. (A) Precipitated Est2 and its interacted Est1 were detected through western blot analyses by using rabbit anti-myc antibodies. The whole cell lysates were used as input controls. Hem15 was used as loading control and was detected by using anti-Hem15 antibodies. (B) The Est1-Est2 interactions were evaluated through calculating the ratios between the amount of Est2 and Est1. The ratios at 37°C were further set into relation to that at 25°C. The P-value is calculated using two-tailed, paired t-test (\*:0.01≤p≤0.05; \*\*:0.001≤p≤0.01). (C) The protein levels of the telomerase components were reflected by calculating the ratios of the total amount of Est1 and Est2 to Hem15. Error bars indicate the standard deviation. At least three independent experiments were done, one of which is shown in figure A.

2002). Why the expression level of telomerase components is dependent on *TLC1* is still poorly understood and is supposed to be a consequence of an accelerated degradation of the unbound telomerase components.

Furthermore, since the Ku-complex is related to *TLC1* nuclear import (Gallardo et al., 2008) and to the recruitment of the telomerase onto telomeres (Fisher et al., 2004), the improper *TLC1* localisation, which leads to a defect in telomerase formation, is proposed to reduce the binding of the telomerase components to the Ku components. This hypothesis was tested by performing co-immunoprecipitation experiments to identify the interaction between Est2 and Yku70 (figure 4.1.11).

All strains (HKY1292, HKY1294, HKY1302, HKY1332, HKY1334 and HKY1336) used above were grown to the logarithmic phase and were either retained at 25°C or shifted to 37°C for 1 hour. Est2 was precipitated by using anti-FLAG antibodies and Yku70 was detected through western blot analyses by using anti-Yku70 antibodies. Additionally, the total cell lysates were used as input controls; Zwf1 was used as loading control and was detected by using anti-Zwf1 antibodies. The ratio of Yku70 to Est2 at 37°C were primarily compared to that at 25°C and subsequently set into relation with that of wild type.

The result shows that, in the case of no *TLC1* export defect, the interaction of Est2 with Yku70 is similar in the export defective mutants and the wild type at 25°C. However, this interaction is reduced upon a temperature shift (~60% in *xpo1-1*, ~41% in *rat8-2* and ~59% in *mex67-5*, respectively) suggesting that the *TLC1* cytoplasmic deficiency leads to an impairment of the telomerase assembly in *xpo1-1* and the mRNA export mutants.

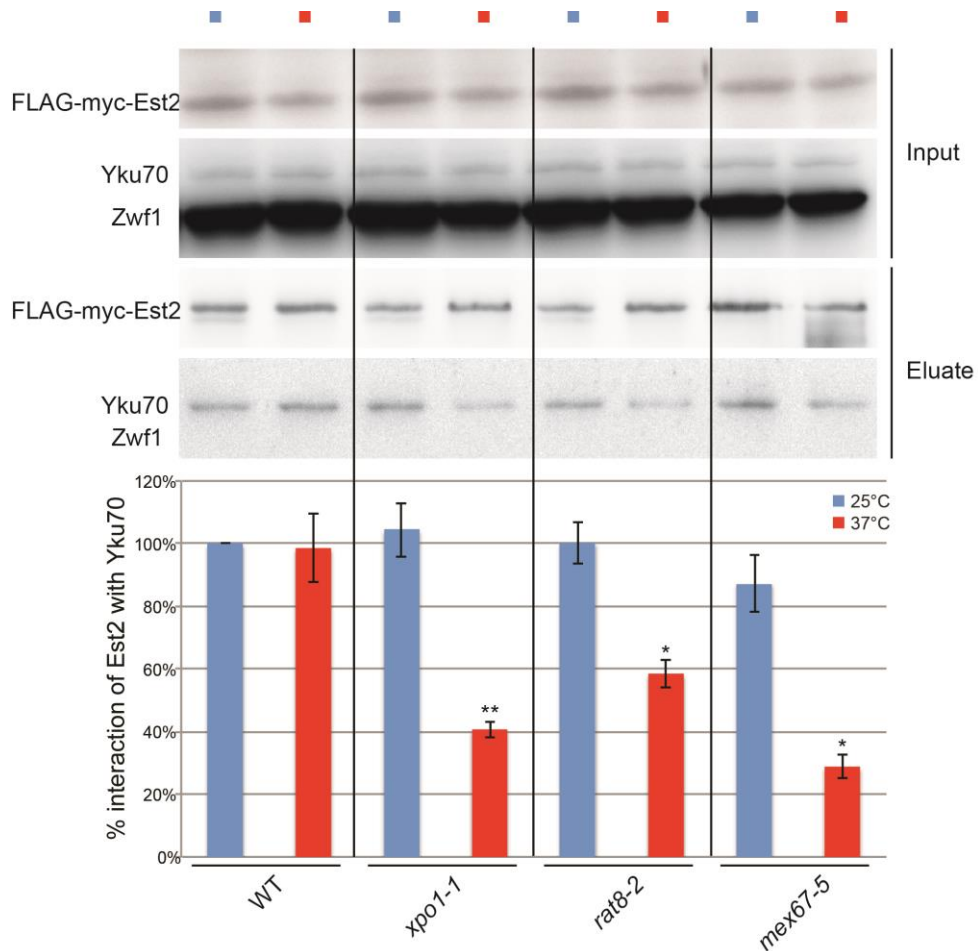


**Figure 4.1.11 The interactions between Est2 and Yku70 are reduced due to the *TLC1* nuclear export block.** All indicated strains were grown to the logarithmic phase and were either retained at 25°C or shifted to 37°C for 1 hour. Est2 was precipitated through mouse anti-FLAG antibodies. Est2 and its interacted Yku70 were analysed via western blot analyses (upper panel). Est2 was detected by anti-FLAG antibodies and Yku70 was detected by anti-Yku70 antibodies. Total cell lysates were used as input controls. Zwf1 was detected by anti-Zwf1 antibodies and was used as the loading control. The amount of Est2 was compared to that of Yku70. These ratios were set into relation to that of the wild type and were shown in the diagram (lower panel). At least three independent experiments were done, one of which is shown in the upper panel. The error bars indicate the standard deviation. P-value was calculated using two-tailed, paired t-test (\*:  $0.01 \leq p \leq 0.05$ ; \*\*:  $0.001 \leq p \leq 0.01$ )

### **4.1.3 Analyses of the *mex67-5 xpo1-1* double mutant on *TLC1* nuclear export**

#### **4.1.3.1 The *mex67-5 xpo1-1* double mutant shows a stronger *TLC1* nuclear accumulation and an increased rate of *TLC1* processing**

Since both of Crm1/Xpo1 and Mex67 were identified to mediate *TLC1* nuclear export, an enhancement of the *TLC1* nuclear export block would be expected if both pathways were simultaneously mutated. Fluorescent *in situ* hybridisation experiments were performed to identify the localisation of *TLC1* in the *mex67-5 xpo1-1* double mutant (figure 4.1.12). In addition, to distinguish the export block from an increased nuclear import of *TLC1*, the *yku70Δ* background mentioned in section 4.1.1.1 was also used in these experiments.

All strains wild type (HKY381), *yku70Δ* (HKY1073), *xpo1-1 yku70Δ* (HKY1444), *mex67-5 yku70Δ* (HKY1397) and *xpo1-1 mex67-5 yku70Δ* (HKY1445) were grown to the logarithmic phase at 25 °C before they were shifted to 37°C for 1 hour. *TLC1* was detected by using Cy3 labelled specific *TLC1* oligo probe (HK1761, HK1789 and HK1790). The nuclear/total signal ratios (N/T) were calculated through comparing the nuclear signals to the total cellular signals of *TLC1* and the ratios were subsequently set into relation to that of *yku70Δ*.

Strikingly, in the double mutant an increased level of *TLC1* nuclear accumulation (~2.4 fold N/T signal ratio compared to *yku70Δ*) is observed in contrast to the mutant containing any defective single pathway (~1.8 fold N/T signal ratio compared to *yku70Δ* in *xpo1-1* and ~1.9 fold N/T signal ratio compared to *yku70Δ* in *mex67-5*) (figure 4.1.12). This result suggests a combined action of both factors on transporting *TLC1*.

Furthermore, as mentioned in 4.1.1.4, although the *TLC1* nuclear export block does not alter the procedure of the *TLC1* processing, it changes the rate of the processing of *TLC1*. In the *TLC1* export mutants, more *TLC1* undergoes processing than in wild type. Therefore, an even higher rate of the processing of *TLC1* would be expected in the double mutant *xpo1-1*

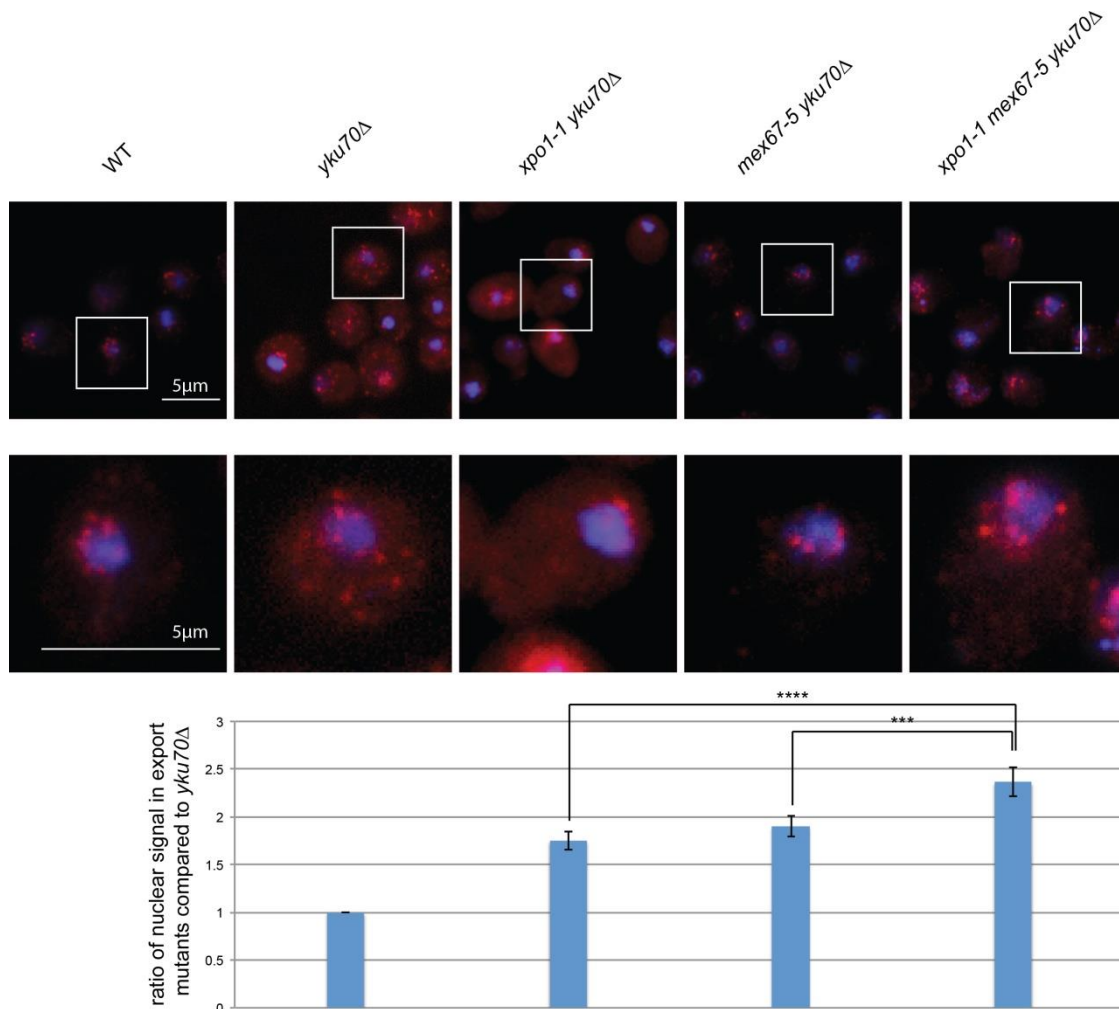


**Figure 4.1.12** Fluorescent *in situ* hybridisation experiments show an increased nuclear mislocalisation of *TLC1* in the double mutant *xpo1-1 mex67-5*. The indicated strains were grown to the logarithmic phase and were shifted to 37°C for 1 hour. *TLC1* was detected by specific Cy3 labeled oligo *TLC1* probes (HK1761, HK1789, HK1790) (red) (top panel). The nuclei were stained with hoehchst33342 (blue). The ratios between nuclear *TLC1* signal and total *TLC1* signal were calculated. The ratios were set into relation to that of *yku70Δ* and were showed in the diagram (bottom panel). At least 20 cells were quantified for each condition. At least three independent experiments were done, one of which is shown in the upper panel. Error bars indicate the standard deviation. The P-value was calculated using two-tailed, unpaired t-test (\*\*\*: 0.0001 ≤ p < 0.001; \*\*\*\*: p < 0.0001).

*mex67-5* than in the single mutants. To test this, qRT-PCR analyses were performed to examine the effect of the double mutant *xpo1-1 mex67-5* on the processing of *TLC1* (figure 4.1.13).

All strains, wild type (HKY381), *xpo1-1* (HKY206), *mex67-5* (HKY644) and *xpo1-1 mex67-5* (HKY1353) were grown to the logarithmic phase and shifted to 37°C for 1 hour. RNA was extracted from the whole cell lysates. The total *TLC1* and the unprocessed *TLC1* were

quantified by qRT-PCR with specific primer pairs HK1385+HK1386 and HK1382+HK1384 as mentioned in section 4.1.1.4. Furthermore, as the reference, the U6 snRNAs were quantified by using the primer pair HK1404+HK1405. To evaluate the transcription levels of the total *TLC1*, the amount of the total *TLC1* was compared to that of the U6 snRNA and the ratios were set into relation to that of the wild type (figure 4.1.13A). The processing of *TLC1* was evaluated by comparing the amount of the unprocessed *TLC1* to that of the total *TLC1* and the ratios were also set into relation to that of wild type (figure 4.1.13B).

The results (figure 4.1.13) indicate that in the *mex67-5 xpo1-1* double mutant, the amount of the total *TLC1* was slightly reduced (~82% of the wild type amount). Nevertheless, the ratio of the unprocessed *TLC1* to the total *TLC1* is dramatically reduced (~3% of the wild type level) in contrast to any one of the single mutants (~17% in *xpo1-1* and ~30% in *mex67-5*, of the wild type level) (figure 4.1.13B). Considering that in wild type only 5-10% of the unprocessed *TLC1* exists in the total *TLC1*, ~3% unprocessed *TLC1* of the wild type level in *xpo1-1 mex67-5* indicates that the vast majority of *TLC1* (more than 99%) undergoes processing in the *xpo1-1 mex67-5* double mutants. These results point out that the *xpo1-1 mex67-5* double mutant shows a similar but even stronger phenotype on *TLC1* processing than the single mutants, *xpo1-1* or *mex67-5*. These results also suggest that the processing of *TLC1* occurs prior to its nuclear export.

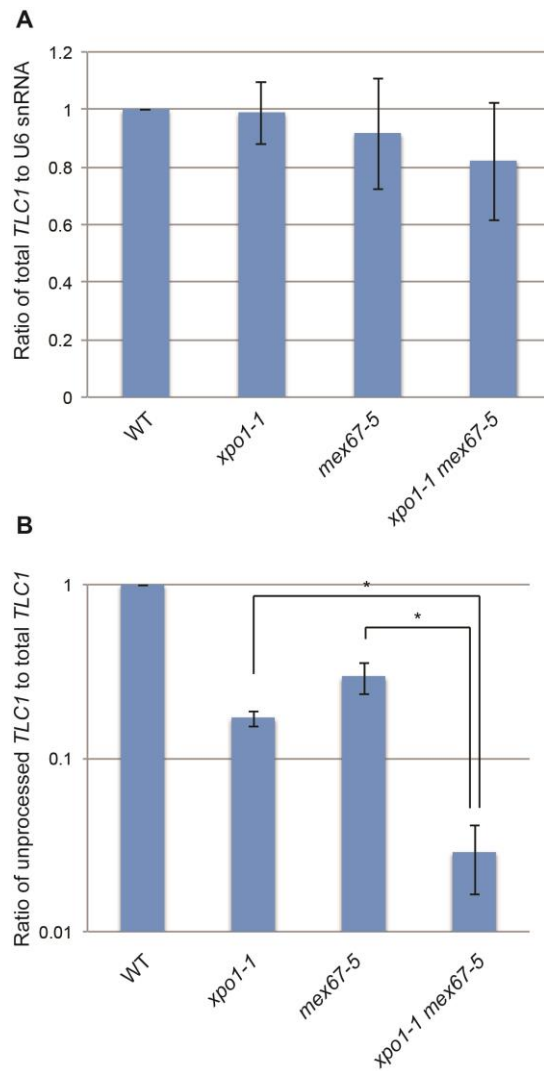


**Figure 4.1.13 The *xpo1-1 mex67-5* double mutant shows a higher *TLC1* processing rate than the single mutants, *xpo1-1* and *mex67-5*.** All indicated strains were grown to the logarithmic phase and shifted to 37°C for 1 hour. The total *TLC1* and the unprocessed *TLC1* were quantified with specific primer pairs (HK1385+HK1386 for total *TLC1*, HK1382+HK1384 for unprocessed *TLC1*) through qRT-PCR. The U6 snRNA was quantified as reference by using the primer pair HK1404+HK1405. (A) The transcription levels of the total *TLC1* were calculated through comparing the amount of the total *TLC1* to that of the U6 snRNA. The ratios were set into relation to that of the wild type. (B) The *TLC1* processing rates were calculated through comparing the amount of the unprocessed *TLC1* to that of the total *TLC1*. The ratios were set into relation to that of the wild type. At least three independent experiments were done. Error bars indicate the standard deviation. P-value was calculated using two-tailed, paired t-test (\*:  $0.01 \leq p \leq 0.05$ )



#### **4.1.3.2 The cytoplasmic mislocalisation of a telomerase component is increased in the *xpo1-1 mex67-5* double mutant**

Since *TLC1* export defect leads to cytoplasmic mislocalisation of the telomerase components, a stronger mislocalisation would be expected in the *xpo1-1 mex67-5* double mutant. To test this hypothesis, immunofluorescence experiments were performed to examine the localisation of the telomerase component, Est1 (figure 4.1.14).

All strains *EST1-3xMYC* (wild type, HKY1463), *EST1-3xMYC xpo1-1* (HKY1464), *EST1-3xMYC mex67-5* (HKY1465) and *EST1-3xMYC xpo1-1 mex67-5* (HKY1466) were grown to the logarithmic phase and were subsequently either retained at 25°C or shifted to 37°C for 1 hour. Myc tagged Est1 was detected by mouse anti-myc antibodies and sheep anti-mouse-AlexFluor488 secondary antibodies. In addition to the immunofluorescence experiments, the cells were imaged through 6-10 z-stacks (0.2µm/stack) followed by deconvolution to acquire sharper and more focussed images .

The results show that the Est1 proteins are localised to the nucleus at 25°C and 37°C in the wild type. In contrast to that, in *xpo1-1*, *mex67-5* as well as the *xpo1-1 mex67-5* double mutant, the Est1 proteins are distributed in the cytoplasm upon a temperature shift to 37°C. Furthermore, in contrast to ~34% and ~37% nuclear signal reduction in *xpo1-1* and *mex67-5*, respectively, an increased reduction (~58%) is found in the *xpo1-1 mex67-5* double mutant upon the temperature shift to 37°C. This suggests an increased mislocalisation of the telomerase component in this double mutant.

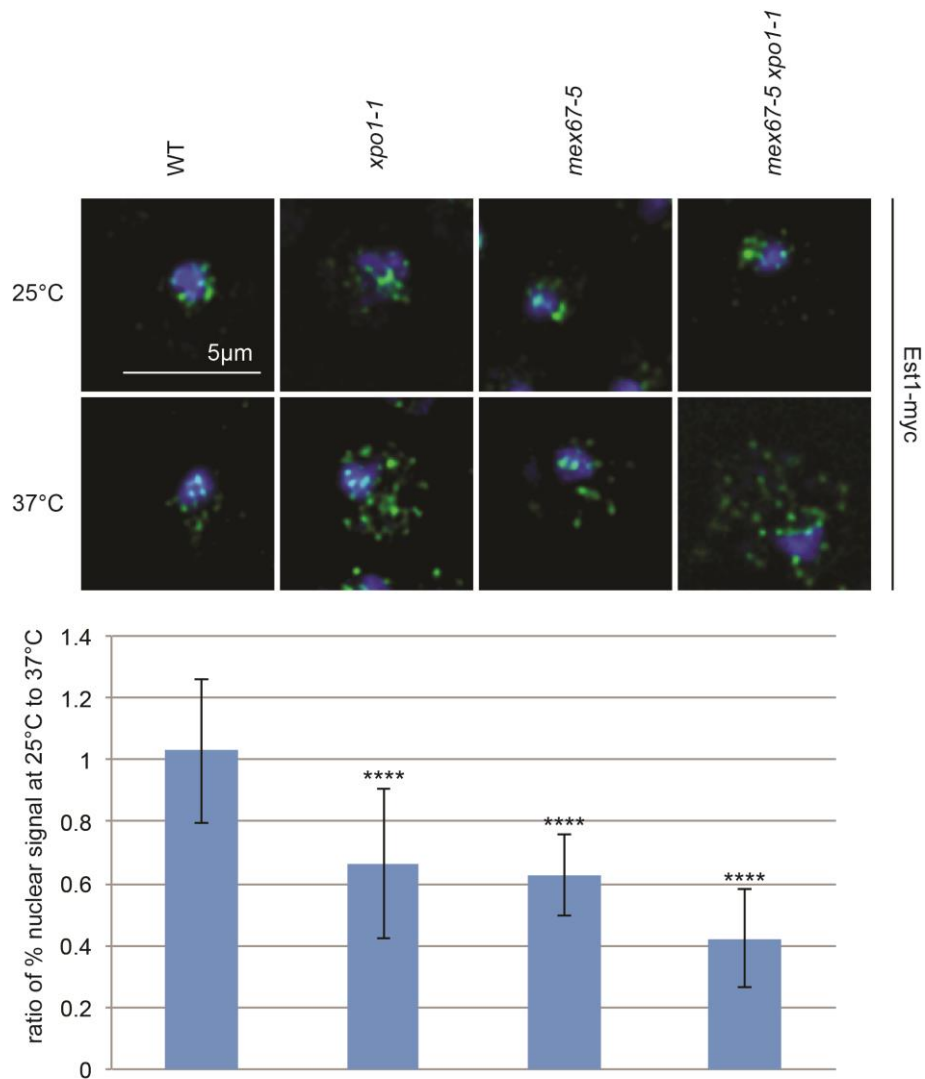


**Figure 4.1.14 The *xpo1-1 mex67-5* double mutant shows stronger cytoplasmic mislocalisation of the telomerase component than the single mutants.** All indicated strain were grown to the logarithmic phase and were either retained at 25°C or shifted to 37°C for 1 hour. With immunofluorescence experiments (top panel), Est1-myc was detected by using mouse anti-myc antibodies and AlexFluor488 anti-mouse antibodies (green). The nuclei were stained with hoechst33342 (blue). The cells were imaged through 6-10 stacks (0.2μm/stack) followed by deconvolution. To calculate the ratio of the nuclear signal of Est1, the nuclear Est1 signal was compared to that of the total Est1 signals. These ratios at 37°C was further compared to those at 25°C in a given strains and were showed in the diagram (bottom panel). For each condition at least 20 cells were calculated. At least three independent experiments were done, one of which is shown in the upper panel. Error bars indicate the standard deviation. P-value was calculated according to two-tailed, unpaired t-test (\*\*\*\*:  $p \leq 0.0001$ ).

### 4.1.3.3 Telomere maintenance is impaired in the double mutant *xpo1-1 mex67-5*

All of the findings shown above indicate that the *xpo1-1 mex67-5* double mutant shows a stronger *TLC1* nuclear export defect and an increased mislocalisation of the telomerase component. On the other side, these results additionally suggest a function of the mRNA export factor on *TLC1* nuclear export. These results also support a coordination between the mRNA export pathway and the Crm1/Xpo1 pathway on *TLC1* nuclear export. Although all these results support that *TLC1* nuclear export utilises both the mRNA export and the Xpo1/Crm1 pathways, there is no telomere shortening found in any of the mutants of these export factors alone. Since the *xpo1-1 mex67-5* double mutant shows a very strong *TLC1* export defect, it would be expected that telomere maintenance would also be impaired in this mutant. To test this hypothesis, southern blot experiments were performed to detect telomere length in this mutant (figure 4.1.15).

The strains wild type (HKY381), *yku70Δ* (HKY1073), *xpo1-1* (HKY206), *mex67-5* (HKY644) and *xpo1-1 mex67-5* (HKY1353) were used for the southern blot experiments. Importantly, the temperature sensitive mutants expose their phenotypes only under non-permissive conditions, which are lethal. Therefore, the semi-permissive temperature of 32°C, which was the highest temperature that allowed growth of the *xpo1-1, mex67-5* double mutants, was used for cultivating the strains. Cells were initially grown at 25°C to the concentration of  $1 \times 10^8$  cells/ml and were regarded as the 0th generations. The cells were diluted 1:1000 into fresh media and grown again to the concentration of  $1 \times 10^8$  cells/ml at 32°C. These cells were regarded as the cells that were grown for 10 generations. The cells were grown at 32°C for 0, 30, 60 generations. The genomic DNA was extracted from the cells prior to an XhoI digestion. The digested genomic DNA was separated on 1.2% agarose gels and transferred onto nylon membranes. The telomeric DNA was hybridised to a specific DIG labelled telomeric probe (HK1539) and detected by using DIG-High Prime DNA Labeling and Detection Starter Kit II from Roche.

Furthermore, to exclude the possibility that the telomere shortening phenotype in these

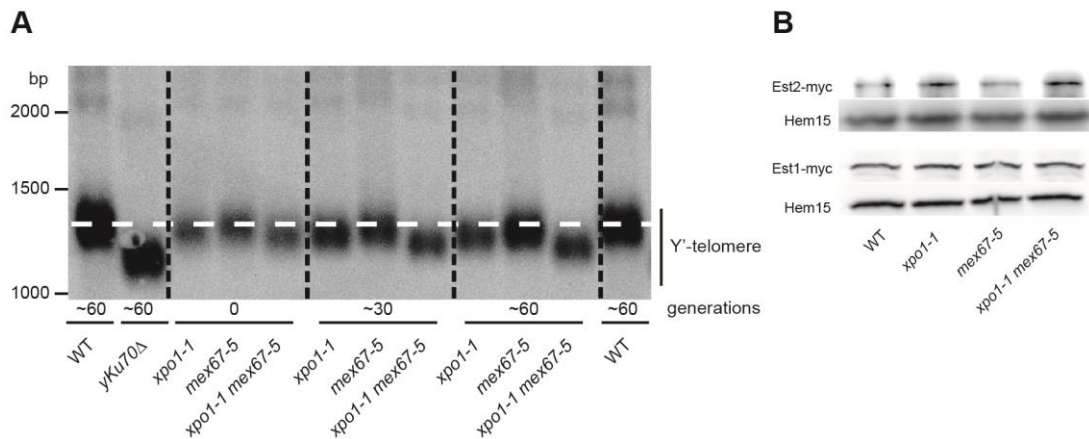


**Figure 4.1.15 The *xpo1-1 mex67-5* double mutant shows an impaired telomere maintenance at 32°C.** (A) The indicated strains were used for the southern blot experiments. Cells that were grown to the concentration of  $1 \times 10^8$  cells/ml were diluted 1:1000 into fresh media and grown again to the concentration of  $1 \times 10^8$  cells/ml at 32°C. These cells were regarded as the cells that were grown for 10 generations. The cells were grown at 32°C for 0, 30, 60 generations. The genomic DNA was extracted and XhoI digested. With southern blot experiments, the DNA that was hybridised to the DIG labeled telomeric oligo probes (HK1539) was detected by anti-DIG-AP antibodies and CSPD (Roche). The figure shows telomeres containing Y'-subtelomeres. (B) The indicated strains were grown to the logarithmic phase at 32°C. The protein levels of Est1 and Est2 were detected by using mouse anti-myc antibodies and anti-mouse-Hrp antibodies. Hem15 was used as loading control and was detected by using anti-Hem15 antibodies. At least three independent experiments were done, one of which is shown here.

mutants might be caused by expression defects of the telomerase components, western analyses was carried out to examine the protein levels of the telomerase components. For western analyses, the strains *EST1-3xMYC* (wild type, HKY1463), *EST1-3xMYC xpo1-1* (HKY1464), *EST1-3xMYC mex67-5* (HKY1465) and *EST1-3xMYC xpo1-1 mex67-5* (HKY1466) were used for examining the protein levels of Est1. The strains *EST2-3xMYC* (wild type, HKY1467), *EST2-3xMYC xpo1-1* (HKY1468), *EST2-3xMYC mex67-5* (HKY1469) and *EST2-3xMYC xpo1-1 mex67-5* (HKY1470) were used to examine the protein levels of Est2. All strains were grown to the logarithmic phase at 32°C. The protein levels of Est1 and Est2 were detected by using mouse anti-myc antibodies and anti-mouse-HRP antibodies. Hem15 that was also used in section 4.2.1.3 served as the reference and detect by rabbit anti-Hem15 antibodies and anti-rabbit-HRP antibodies.

Strikingly, the southern blot experiments indicate that the *xpo1-1, mex67-5* double mutant shows a clear telomere shortening after growing for about 30 generations at 32°C and this

shortening is even enhanced after around 60 generations (figure 4.1.15A). In contrast to that, the *mex67-5* mutant shows no telomere shortening and the *xpo1-1* mutant shows very mild telomere shortening. Besides, the western blot experiments show that Est1 and Est2 are not degraded at 32°C in all strains (figure 4.1.15B). In addition, a stable *TLC1* transcription level at 32°C was also identified (Daniel Becker and Heike Krebber). These results indicate that the *TLC1* export defects lead to defective telomere maintenance. From these experiments, genetic evidence is also obtained, supporting that the mRNA export pathway cooperates with Crm1/Xpo1 to mediate the nuclear export of *TLC1*.

#### 4.1.3.4 Xpo1/Crm1 is directly involved in *TLC1* nuclear export

Since *xpo1-1* indirectly leads to mRNA nuclear export defect (AskjaerStade et al., 1997), whether *xpo1-1* leading to *TLC1* nuclear accumulation is direct remains unclear. To answer this question, fluorescent *in situ* hybridisation and southern blot experiments were performed (figure 4.1.16).

Overexpression of *DBP5/RAT8* is able to rescue the mRNA export defect of *xpo1-1* (Hodge et al., 1999). To identify the role of Xpo1/Crm1 on transporting *TLC1*, an overexpression plasmid of *DBP5/RAT8* was used to rescue the mRNA nuclear export in *xpo1-1*. This plasmid contained the *DBP5/RAT8* gene under control of a galactose promoter (*pGAL1-RAT8-MYC*, 2 $\mu$ , *URA3*, pHK649) and was used for transforming the strains wild type (HKY381), *yku70 $\Delta$*  (HKY1073), *xpo1-1 yku70 $\Delta$*  (HKY1444), *mex67-5 yku70 $\Delta$*  (HKY1397) and *xpo1-1 mex67-5 yku70 $\Delta$*  (HKY1445). Fluorescent *in situ* hybridisation experiments were performed in the transformed strains (figure 4.1.16A). All strains were initially inoculated in raffinose containing media. Galactose or glucose is used as carbon source and for inducing or repressing the overexpression of *DBP5/RAT8* from the plasmid, respectively. The induced or repressed strains were grown overnight to the logarithmic phase and shifted to 37°C for 1 hour. Poly(A)<sup>+</sup> RNA or *TLC1* molecules were detected by using a Cy3-oligo(dT)<sub>50</sub> probe (Biospring) or Cy3 labelled specific *TLC1* oligo probes (HK1761, HK1789, HK1790).

In addition, southern blot experiments were carried out to identify the length of the telomeres in the double mutant *xpo1-1 mex67-5* in the presence of overexpressed *DBP5/RAT8* (figure 4.1.16B). All strains wild type (HKY381), *yku70 $\Delta$*  (HKY1073), *xpo1-1* (HKY206), *mex67-5* (HKY644) and *xpo1-1 mex67-5* (HKY1353) were transformed with the plasmid pHK649 (*pGAL1-RAT8-MYC*, 2 $\mu$ , *URA3*). Transformed strains were grown at 32 °C with addition of either glucose or galactose for about 60 generations. The cells were harvested and the southern blot experiments were performed as mentioned in section 4.1.3.3.

The fluorescent *in situ* experiments show that although defect of poly(A)<sup>+</sup> RNA export is rescued in *xpo1-1* by overexpression of *DBP5/RAT8*, the *TLC1* nuclear mislocalisation still

remains, indicating that the defect of *TLC1* translocation in *xpo1-1* is due to its impaired Crm1/Xpo1 function rather than the improper regulation of mRNA export. The southern blot experiments show that suppression of the *xpo1-1* phenotype does not rescue the defect in telomere maintenance caused by the *xpo1-1, mex67-5* double mutants. These findings further provide evidence that unlike mRNA nuclear export, Crm1/Xpo1 is directly involved in *TLC1* nuclear export.

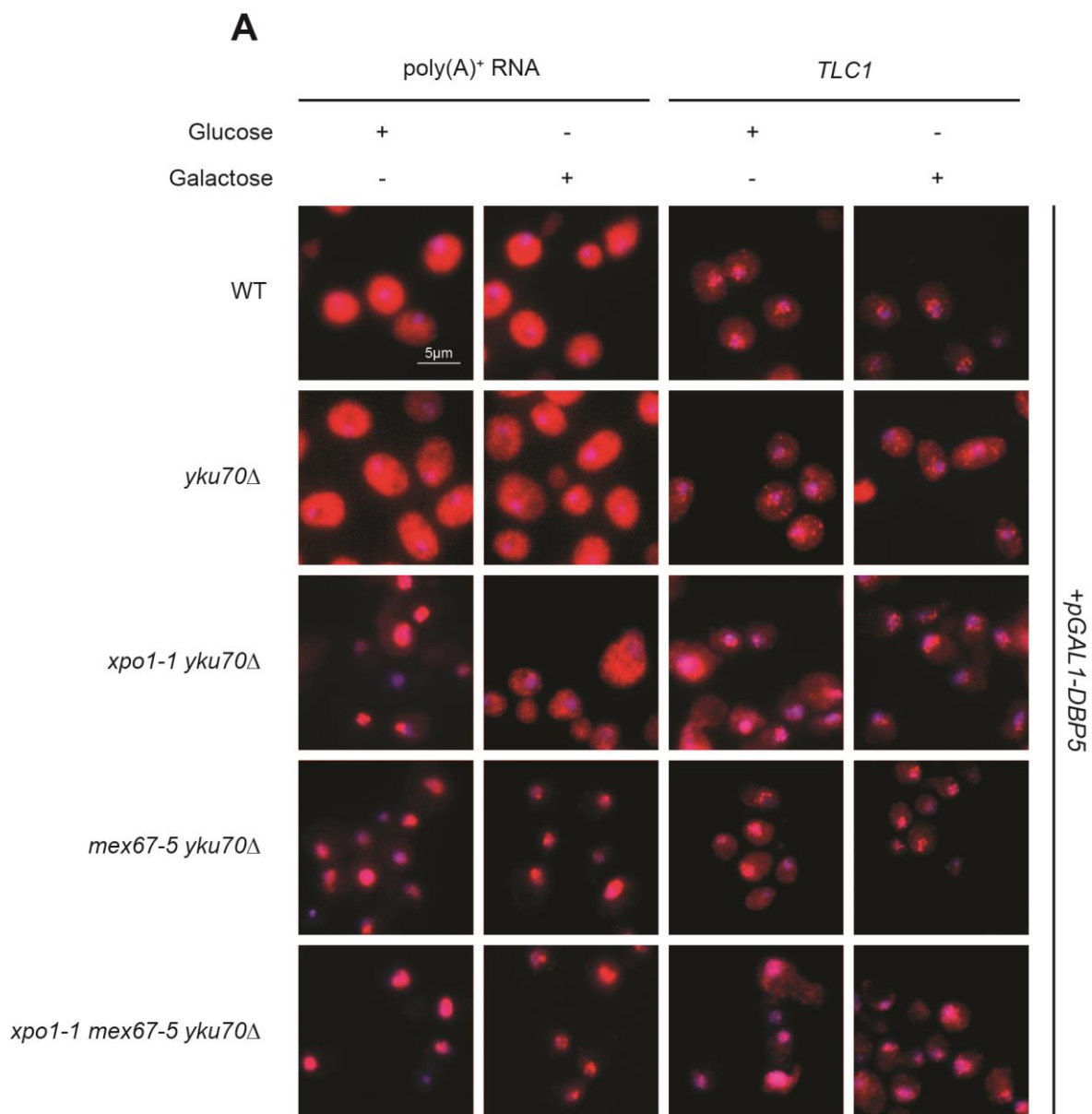
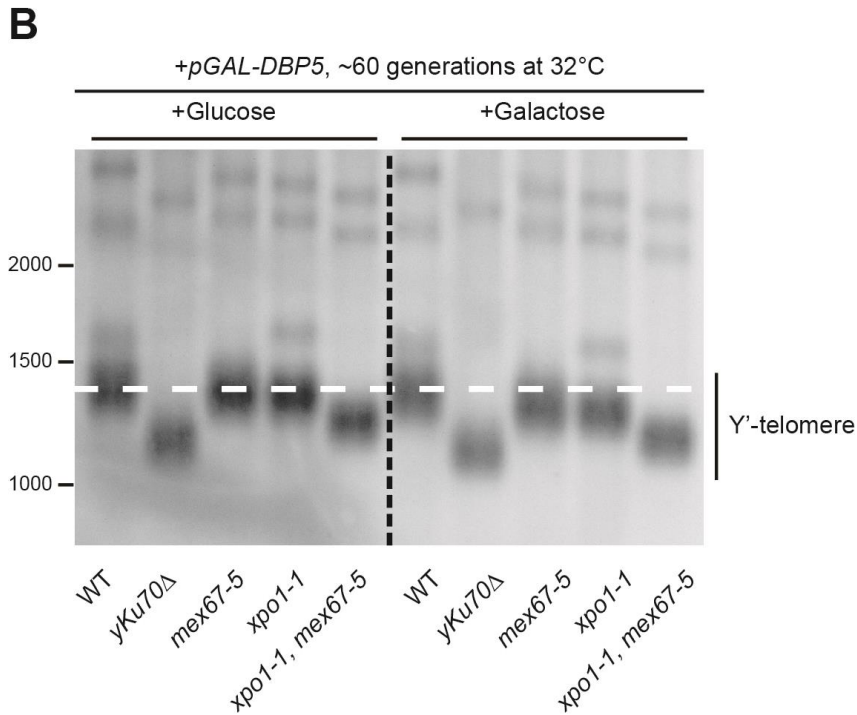


Figure legend see next page



**Figure 4.1.16 Overexpression of *DBP5/RAT8* does not rescue the *TLC1* nuclear accumulation in *xpo1-1* and the telomere shortening in the *xpo1-1 mex67-5* double mutants.** (A) All indicated strains were transformed with the plasmid pHK649 (*pGAL1-RAT8-MYC*,  $2\mu$ , *URA3*). Fluorescent *in situ* hybridisation experiments were performed in the transformed strains. All strains were initially inoculated in raffinose containing media. Overexpression of *DBP5/RAT8* was either induced or repressed in all strains overnight by adding galactose or glucose, respectively. The strains were grown to the logarithmic phase and shifted to 37°C for 1 hour. Poly(A)<sup>+</sup> RNA or *TLC1* molecules (red) were detected by using Cy3-oligo(dT)<sub>50</sub> probe (Biospring) or Cy3 labelled specific *TLC1* oligo probes (HK1761, HK1789, HK1790). The nuclei were stained with hoechst33342 (blue). (B) The cells were grown at 32 °C in the presence of either glucose or galactose for about 60 generations. The genomic DNA was extracted and *Xho*I digested. With southern blot the DNA that was hybridised to the DIG labeled telomeric oligo probes (HK1539) was detected by anti-DIG-AP antibodies and CSPD (Roche). Figure shows telomeres containing Y'-subtelomeres. At least three independent experiments were done, one of which is shown here.



## 4.2 The processing of *TLC1*

### 4.2.1 The transcription and processing defects of *TLC1* in the *mtr10Δ* strain is not due to its effect on *TLC1* transport

Mtr10 is a nuclear import receptor that mediates *TLC1* nuclear import (Ferrezuelo et al., 2002). Previous investigation showed that the transcription level of *TLC1* was greatly reduced in *mtr10Δ* (Ferrezuelo et al., 2002), suggesting a feedback effect of the nuclear import of *TLC1* might regulate its transcription. To test this hypothesis, qRT-PCR experiments were performed in the *TLC1* mislocalisation mutants (figure 4.2.1).

In addition to the *mtr10Δ* strain, other knockout strains that showed cytoplasmic mislocalisation of *TLC1* (Ferrezuelo et al., 2002; Gallardo et al., 2008) were also used in the experiments. All strains wild type (HKY381), *est2Δ* (HKY1072), *yku70Δ* (HKY1073), *tel1Δ* (HKY1075), *mre11Δ* (HKY1077), *mtr10Δ* (HKY82) and *pdr6Δ* (HKY209) were grown to the

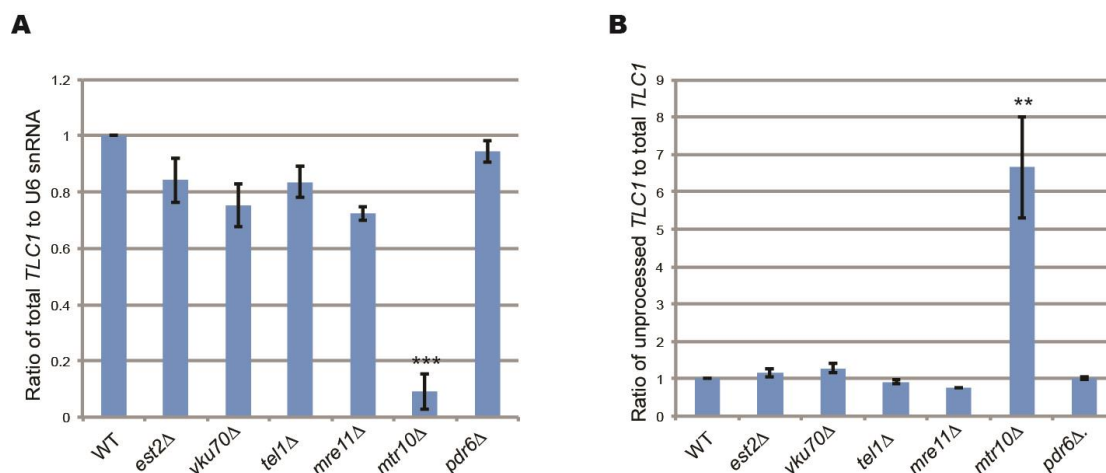


**Figure 4.2.1 Quantification of *TLC1* transcription and processing in the mutants that show a cytoplasmic mislocalisation of *TLC1*.** All indicated strains were grown to the logarithmic phase and the total RNAs were extracted. The amounts of the total *TLC1*, the unprocessed *TLC1* and the U6 snRNA were measured via qRT-PCR by using specific primer pairs HK1385+HK1386, HK1382+HK1384 and HK1404+HK1405 respectively. (A) To evaluate the *TLC1* transcription level, the amount of the total *TLC1* was compared to that of the U6 snRNA and the ratios were set into relation with that of the wild type. (B) To evaluate *TLC1* processing rates, the amount of the unprocessed *TLC1* was compared to that of the total *TLC1* and the ratios were set into relation with that of the wild type. At least three independent experiments were done. Error bars indicate the standard deviation. P-value was calculated according to two-tailed, paired t-test (\*\*:  $0.001 \leq p \leq 0.01$ ; \*\*\*:  $0.0001 \leq p \leq 0.001$ ).

logarithmic phase and the total RNA was extracted from the cells. The amount of the total *TLC1* and unprocessed *TLC1* was quantified by using qRT-PCR with the primer pair HK1385+HK1386 and HK1382+HK1384, respectively. The U6 snRNA was quantified as a transcription control by using the primer pair HK1404+HK1405 as mentioned in section 4.1.1.4. To evaluate the transcription levels of *TLC1*, the amount of the total *TLC1* were compared to that of the snRNA U6 and the ratios were set into relation to that of the wild type. To evaluate the processing of *TLC1*, the amount of unprocessed *TLC1* was compared to that of the total *TLC1* and the ratios were set into relation to that of the wild type.

Unexpectedly, the experiments show that although all these factors are involved in the *TLC1* nuclear import, Mtr10 is the only factor that affects the transcription of *TLC1*. Besides, the *mtr10Δ* strain possesses not only a *TLC1* transcription level reduction, but also an impaired *TLC1* processing. These defects are not found in the other mutants that affect *TLC1* localisation. Therefore, this result suggests a unique function of Mtr10 in *TLC1* transcription and processing within these factors. Since Mtr10 is known as a nuclear import receptor (Senger et al., 1998), it can be proposed that unlike the other factors, Mtr10 might import not only the telomerase complex, but also factors necessary for *TLC1* transcription and processing, into the nucleus.

## 4.2.2 The factors involved in *TLC1* processing are identified by qRT-PCR analyses

The results from section 4.1.1.4 and 4.1.3.1 suggest that *TLC1* maturation might be completed in the nucleus. Therefore, it can also be concluded that *TLC1* maturation is mediated by the nuclear RNA processing factors. To identify which factors mediate *TLC1* processing, qRT-PCR analyses were performed (figure 4.2.2).

The experiments were performed by using the mutants of the nuclear RNA processing factors, e.g. components of the ribonuclease, components of the TRAMP complex and the splicing factors, etc. After all strains were grown to the logarithmic phase, wild type (HKY381)

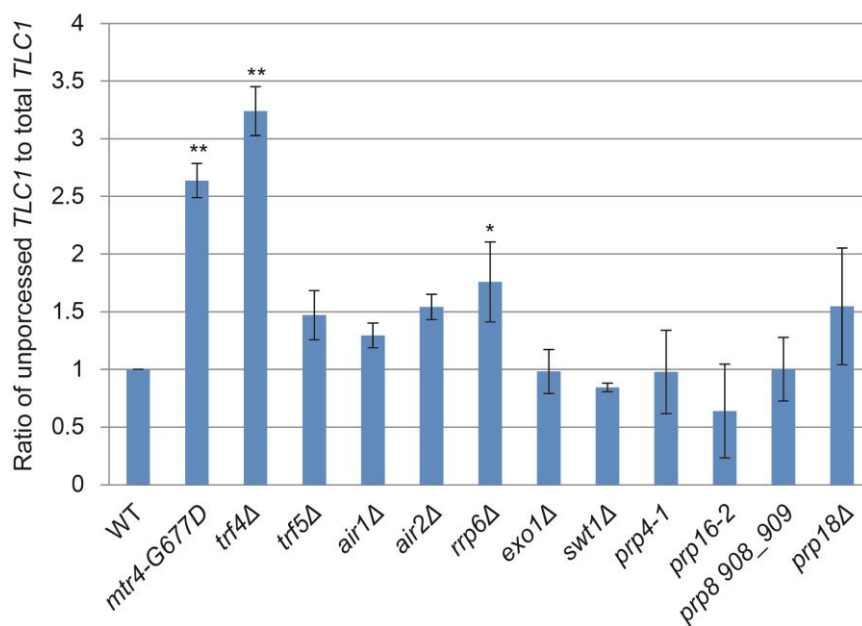


**Figure 4.2.2 Potential *TLC1* processing factors are identified by using qRT-PCR experiments.**

All indicated strains were grown to the logarithmic phase. Wild type (HKY381), *mtr4-G677D* (HKY428), *prp4-1* (HKY305), *prp16-2* (HKY306), *prp8 908\_909* (HKY1008) were shift to 37°C for 1 hour and *rrp6Δ* (HKY1028), *trf4Δ* (HKY1112), *trf5Δ* (HKY1236), *air1Δ* (HKY1237), *air2Δ* (HKY1038), *exo1Δ* (HKY1094), *swt1Δ* (HKY1111) were incubated at 25°C. The total RNAs were extracted from the cells. The qRT-PCR analyses were performed to measure the amount of total *TLC1* and unprocessed *TLC1* with the primer pairs HK1385+HK1386 and HK1382+HK1384, respectively. To evaluate *TLC1* processing, the amounts of unprocessed *TLC1* were compared to those of the total *TLC1* and the ratios were set into relation to the wild type. At least three independent experiments were done. Error bars indicate the standard deviation. P-value was calculated according to two-tailed, paired t-test (\*:  $0.01 \leq p \leq 0.05$ ; \*\*:  $0.001 \leq p \leq 0.01$ ).

and the temperature sensitive mutants *mtr4-G677D* (HKY428), *prp4-1* (HKY305), *prp16-2* (HKY306) and *prp8 908\_909* (HKY1008) were shifted to 37°C for 1 hour. The knockout strains *rrp6Δ* (HKY1028), *trf4Δ* (HKY1112), *trf5Δ* (HKY1236), *air1Δ* (HKY1237), *air2Δ* (HKY1038), *exo1Δ* (HKY1094), *swt1Δ* (HKY1111) and *prp18Δ* (HKY948) were incubated at 25°C. Total RNA was extracted from these strains and further used for the qRT-PCR analyses. In qRT-PCR, the primer pair HK1385+HK1386 was used to measure the total *TLC1* and the primer pair HK1382+HK1384 was used to measure the unprocessed *TLC1*. To evaluate the processing of *TLC1*, the amount of the unprocessed *TLC1* was compared to that of the total *TLC1* and the ratios were set into relation to that of the wild type.

The results indicate that unlike telomerase RNA in *Schizosaccharomyces pombe* (Box et al., 2008) and *Trypanosoma brucei* (Sandhu et al., 2013), *TLC1* does not undergo splicing in *S. cerevisiae*. In addition, *Swt1*, an RNA endonuclease involved in RNA turnover in the nucleus (Skruzny et al., 2009), and *Exo1*, an exonuclease mainly responsible for DNA recombination (Fiorentini et al., 1997; Tran et al., 2002), show no influence on the processing of *TLC1*. In contrast, clear defects of the processing of *TLC1* are shown in the TRAMP component mutants (*mtr4-G677D*, *trf4Δ*) as well as the nuclear exosome component knockout strain (*rrp6Δ*). Consistently, recent published data also show that *Rrp6* and *Lrp1* are involved in the processing of *TLC1* (Coy et al., 2013).

The yeast nuclear exosome is composed of the exo-10 core complex, *Rrp6* and *Lrp1* (Synowsky et al., 2009). So far, no data are available to show if the catalytic core component of the exo-10 complex, *Dis3* (Mitchell et al., 1997), is involved in the processing of *TLC1*. Besides, since *Dis3* possesses both endo- and exo-nuclease activities (Mitchell et al., 1997), it is also unclear which activity of *Dis3* could be responsible for the processing of *TLC1*. To answer these questions, qRT-PCR experiments were performed (figure 4.2.3).

Using the strain (*GAL::dis3*, HKY1290) in which the genomic *DIS3* promoter was replaced by a *GAL* promoter, expression of *DIS3* is able to be repressed by glucose (Schneider et al., 2009). The strain wild type (HKY381) and *GAL::dis3* (HKY1290) were initially inoculated in galactose containing media. The *GAL::dis3* culture was divided into two equal portions. One portion of the *GAL::dis3* culture and the wild type culture were kept in galactose containing media and

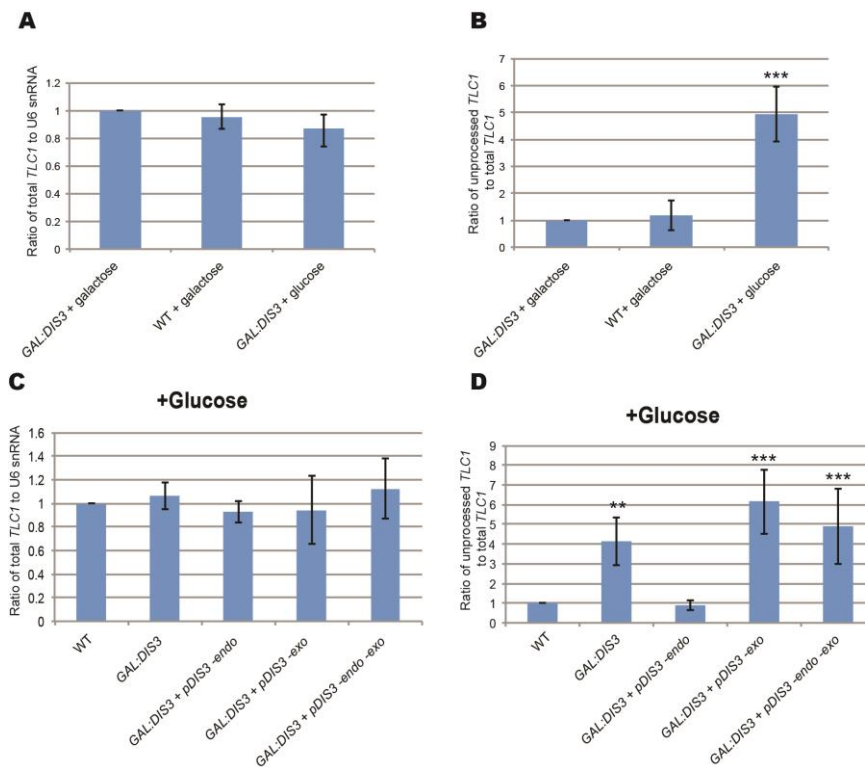


**Figure 4.2.3 Dis3 is involved in the processing of *TLC1* and this activity might be mainly from its exonuclease activity.** (A, B) The indicated strains were grown in galactose containing media. Half of the *GAL::dis3* cells and the wild type cells were kept in galactose containing media and grown for 24 hours to the logarithmic phase. The other half of the *GAL::dis3* cells were grown in glucose containing media for 24 hours to the logarithmic phase. Total *TLC1* and unprocessed *TLC1* were quantified by qRT-PCR with the primer pairs HK1385+HK1386 and HK1382+HK1384, respectively. The U6 snRNA was used as the reference RNA and quantified with the primer pair HK1404+HK1405. *TLC1* transcription levels were calculated through the ratios of the total *TLC1* to the U6 snRNAs (A). The processing of *TLC1* was evaluated through the ratios of the unprocessed *TLC1* to the total *TLC1* (B). (C, D) Wild type strain (HKY381) bearing empty vector (*pRS315-LEU2*, pHK87) and the strain *GAL::dis3* (HKY1290) bearing empty vector (pHK87), or one of the three plasmids (*pDIS3-exo*, pHK1353; *pDIS3-endo*, pHK1354; *pDIS3-exo-endo*, pHK1355) were cultivated in galactose containing media. Subsequently expression of wild-typic *DIS3* gene in *GAL::dis3* strains is repressed by adding glucose for 24 hours. *TLC1* transcription (C) and processing (D) were evaluated as mentioned above. At least three independent experiments were done. Error bars indicate the standard deviation. P-value was calculated according to two-tailed, paired t-test (\*\*: 0.001 ≤ p ≤ 0.01; \*\*\*: 0.0001 ≤ p ≤ 0.001).

grown for 24 hours to the logarithmic phase. Glucose was added to the other portion of the *GAL::dis3* culture and it was also grown for 24 hours to the logarithmic phase. Total RNA was extracted from the cells. Total *TLC1* and unprocessed *TLC1* were quantified by qRT-PCR with the primer pairs HK1385+HK1386 and HK1382+HK1384, respectively. The U6 snRNA was used as the reference RNA and quantified with the primer pair HK1404+HK1405. *TLC1*

transcription and processing were evaluated (figure 4.2.3 A,B) as mentioned in section 4.1.1.4.

Furthermore, three plasmids were used to identify the functional domain of Dis3 for the processing of *TLC1*. All three plasmids contain mutated *DIS3* genes. One plasmid (*pDIS3-endo*, *LEU2*, pHK1354) produces defective Dis3 proteins without its endo-nuclease activity; one plasmid (*pDIS3-exo*, *LEU2*, pHK1353) produces defective Dis3 proteins without its exo-nuclease activity; and the third plasmid (*pDIS3-exo-endo*, *LEU2*, pHK1355) produces defective Dis3 proteins without both endo- and exo-nuclease activities (Schneider et al., 2009). The wild type strain (HKY381) was transformed with the empty vector (*pRS315-LEU2*, *CEN*, pHK87) and the strain *GAL::dis3* (HKY1290) was transformed with the empty vector (pHK87), or one of the three plasmids (pHK1353, pHK1354, pHK1355). All these transformed strains were initially inoculated in galactose containing media. Subsequently glucose was added to the cultures to repress the expression of the wild-typic *DIS3* gene in the *GAL::dis3* strains. The strains were cultivated for 24 hours in this media and grown to the logarithmic phase. Total RNA was extracted from the cells. *TLC1* transcription and processing were evaluated (figure 4.2.3 C,D).

The qRT-PCR analyses show that the processing of *TLC1* is defective upon repression of *DIS3* expression, suggesting a role of Dis3 in the processing of *TLC1* (figure 4.2.3A, B). Furthermore, the results also indicate that only in the *DIS3-exo* mutants, the processing of *TLC1* is impaired, suggesting the involvement of the exonuclease activity of Dis3 in this procedure (figure 4.2.3C, D). In addition, the *DIS3-exo* mutant shows a similar level of impairment of the processing of *TLC1* as shown in the *DIS3-endo-exo* strain and the *DIS3* expression repressed strain (*GAL::dis3* in glucose containing media), further pointing out that the catalytic function of Dis3 on the processing of *TLC1* is specific from its exo-nuclease activity rather than the endo-nuclease activity.

### 4.2.3 The factors involved in the processing of *TLC1* are mis-localised in the *mtr10Δ* mutant

Previously published data (Coy et al., 2013) show that the nuclear exosome and the TRAMP complex might be involved in the processing of *TLC1*. This opinion is also supported by our results in section 4.2.2. Furthermore, the results from section 4.2.1 suggest that Mtr10 might transport factors that are necessary for the processing of *TLC1*. Therefore, immunofluorescence experiments were performed to identify the localisation of the nuclear exosome components and the TRAMP complex components in *mtr10Δ* (figure 4.2.13).

In the immunofluorescence experiments, wild type (HKY381) and *mtr10Δ* (HKY82) cells were

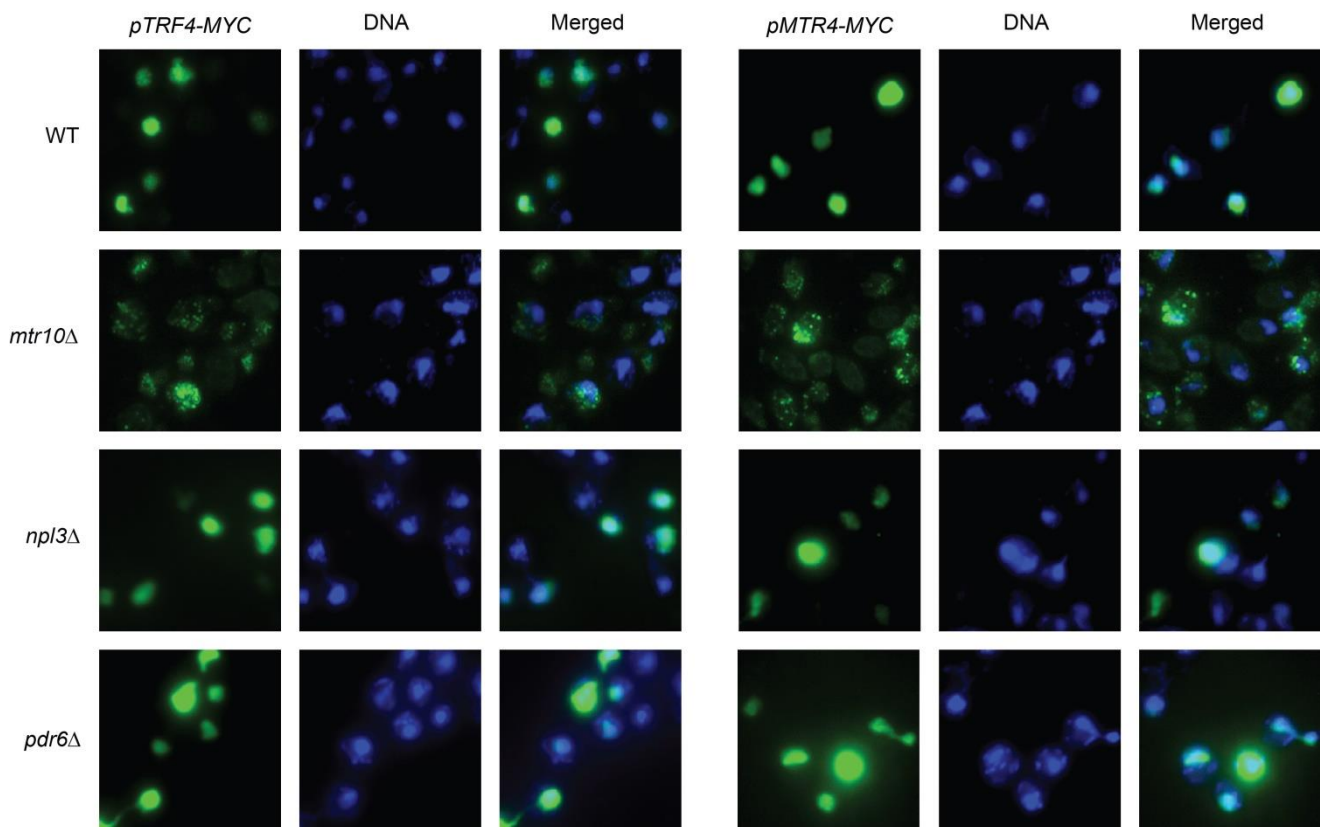


**Figure 4.2.4** Trf4 and Mtr4 are mis-localised in *mtr10Δ*. The strains wild type (HKY381), *mtr10Δ* (HKY82), *np13Δ* (HKY380) and *pdr6Δ* (HKY309) bearing the plasmid *pTRF4-MYC* (pHK1238) or *pMTR4-MYC* (pHK1240) were grown to the logarithmic phase. Myc tagged Trf4 or Mtr4 was detected by mouse anti-myc antibodies and AlexaFluor488 anti-mouse antibodies (green). The nuclei were stained with hoechst33342 (blue). Merged figures are used for co-localisation study. At least three independent experiments were done, one of which is shown here.

used. Besides, since Pdr6 is involved in *TLC1* nuclear import and Npl3 is one of the Mtr10 nuclear import targets, *pdr6* $\Delta$  (HKY309) and *npl3* $\Delta$  (HKY380) were also used in the experiments. The strains were transformed with *pTRF4-MYC* (pHK1238) or *pMTR4-MYC* (pHK1340) plasmids. Transformed strains were grown to the logarithmic phase. Myc tagged proteins were detected with mouse anti-myc antibodies and AlexaFluor488 sheep anti-mouse secondary antibodies. Nuclei were stained with hoechst33342.

The results show that in the wild type, Trf4 and Mtr4 are located to the nucleus, indicating that they are nuclear proteins. In contrast, in the *mtr10* $\Delta$  strain these factors are mislocalised to the cytoplasm, suggesting that Mtr10 mediates their nuclear import. Furthermore, this mislocalisation is unique for *mtr10* $\Delta$  since the other nuclear receptors, *e.g.* Pdr6, or the Mtr10 transport target, Npl3, do not cause this mislocalisation. In addition, mislocalisation of Dis3 in *mtr10* $\Delta$  was also identified (Lea Steffen and Heike Krebber). These findings indicate a unique function for Mtr10 in transporting the nuclear exosome components and the TRAMP complex components.



## 4.2.4 Mtr10 physically interacts with factors that are involved in the processing of *TLC1*

The studies of localisation of the TRAMP complex components and the nuclear exosome component show that these factors are mislocalised to the cytoplasm in *mtr10Δ*. This finding suggests potential physical interactions between Mtr10 and these factors. To identify the interactions, co-immunoprecipitation experiments were performed (figure 4.2.5).

The wild type strain (HKY381) and the *DIS3-GFP* (HKY1172) strain were transformed with the plasmids *pMTR10-TAP* (pHK413) and *pTRF4-MYC* (pHK1238). Transformed strains were grown to the logarithmic phase. Mtr10-TAP was precipitated using IgG coupled sepharose

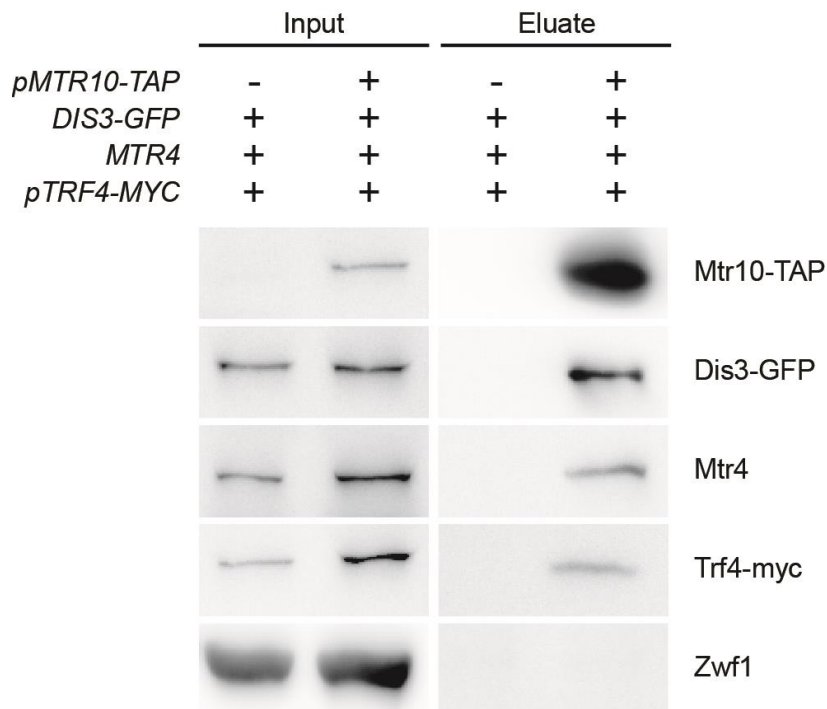


**Figure 4.2.5 Mtr10 interacts with the TRAMP complex components and an exosome component.** The strains wild type (HKY381) and *DIS3-GFP* (HKY1172) were transformed with the plasmids *pMTR10-TAP* (pHK413) and *pTRF4-MYC* (pHK1238). Mtr10-TAP was precipitated by using IgG coupled sepharose beads (GE Healthcare) in the presence of RNaseA (0.1mg/ml). Its interaction partners were analysed by western blots. The whole cell lysates were used as input controls. Dis3-GFP was detected by anti-GFP antibodies. Trf4-myc was detected by anti-myc antibodies. Mtr4 was detected by anti-Mtr4 antibodies. Mtr10 is detected by any of these antibodies. Zwf1 was used as loading and washing control and was detected by anti-Zwf1 antibodies. At least three independent experiments were done, one of which is shown here.

beads (GE Healthcare). RNaseA (final concentration: 0.1mg/ml) was used during the experiments to remove potential RNA mediated interactions. The eluates were analysed by western blots. Dis3 was detected by using anti-GFP antibodies and Trf4 was detected by using anti-myc antibodies and Mtr4 was detected by using anti-Mtr4 antibodies and Mtr10 is detected by any of these antibodies. Zwf1, a cytoplasmic protein used in section 4.1.1.2, was used as the loading control and detected by using anti-Zwf1 antibodies.

The results show physical interactions between Mtr10 and these exosome or TRAMP complex components. These findings support that both TRAMP complex components and an exosome component are transported via Mtr10. Moreover, these findings also indicate that the processing and transcription of *TLC1* in *mtr10Δ* could be due to the transport defects of the TRAMP components and the exosome component.

## 4.3 Conclusions

This thesis led to a better understanding of the life cycle of *TLC1*.

Fluorescent *in situ* hybridisation experiments identified that *TLC1* accumulates in the nucleus of the mRNA export mutants, suggesting that not only known Xpo1/Crm1, but also the mRNA export factors are involved in *TLC1* nuclear export. This finding is further supported by the cell fractionation experiments showing cytoplasmic *TLC1* deficiency in the mRNA export mutants and by the co-immunoprecipitation experiments showing physical interactions between *TLC1* and the mRNA export factors. Furthermore, the RNA co-immunoprecipitation and qRT-PCR analyses indicate that the processing of *TLC1* is completed in the nucleus and the subsequent nuclear export is mediated by the cooperation of Xpo1/Crm1 and the mRNA export factors. In addition, immunofluorescence and immunoprecipitation experiments show that the *TLC1* nuclear export defect impairs the formation of the telomerase complex and the localisation of the telomerase components. Moreover, the *xpo1-1 mex67-5* double mutant shows a stronger *TLC1* nuclear export defect, an increased *TLC1* processing rate and an enhanced mislocalisation of the telomerase components than in the single mutants, supporting a model in which Xpo1/Crm1 and the mRNA export factors cooperate to transport *TLC1*. In support of these findings, in the *xpo1-1 mex67-5* double mutant a telomere maintenance defect is observed confirming the genetic interaction between Xpo1/Crm1 and Mex67. Finally, the fluorescent *in situ* hybridisation and southern blot experiments show that Xpo1/Crm1 is directly involved in *TLC1* nuclear export.

Furthermore, qRT-PCR experiments reveal the transcription and processing defects of *TLC1* in *mtr10Δ* and propose that in addition to *TLC1* transport, Mtr10 might possess a unique function in the transcription and processing of *TLC1*. QRT-PCR experiments further show that mutations of the genes of the TRAMP complex components and the exosome component lead to defects in the processing of *TLC1*, suggesting involvements of these factors in the processing of *TLC1*. Further immunofluorescence experiments show cytoplasmic mislocalisations of the TRAMP complex components and the exosome component in *mtr10Δ*, logically connecting these proposals and suggesting a possibility of the transport of these

factors via Mtr10. In support of this hypothesis, the physical interaction studies reveal the interactions between Mtr10 and the TRAMP complex components or the exosome component.

Taken together, our knowledge about the transport and maturation of *TLC1* is extended and the model of the life cycle of *TLC1* is demonstrated in figure 4.3.1.

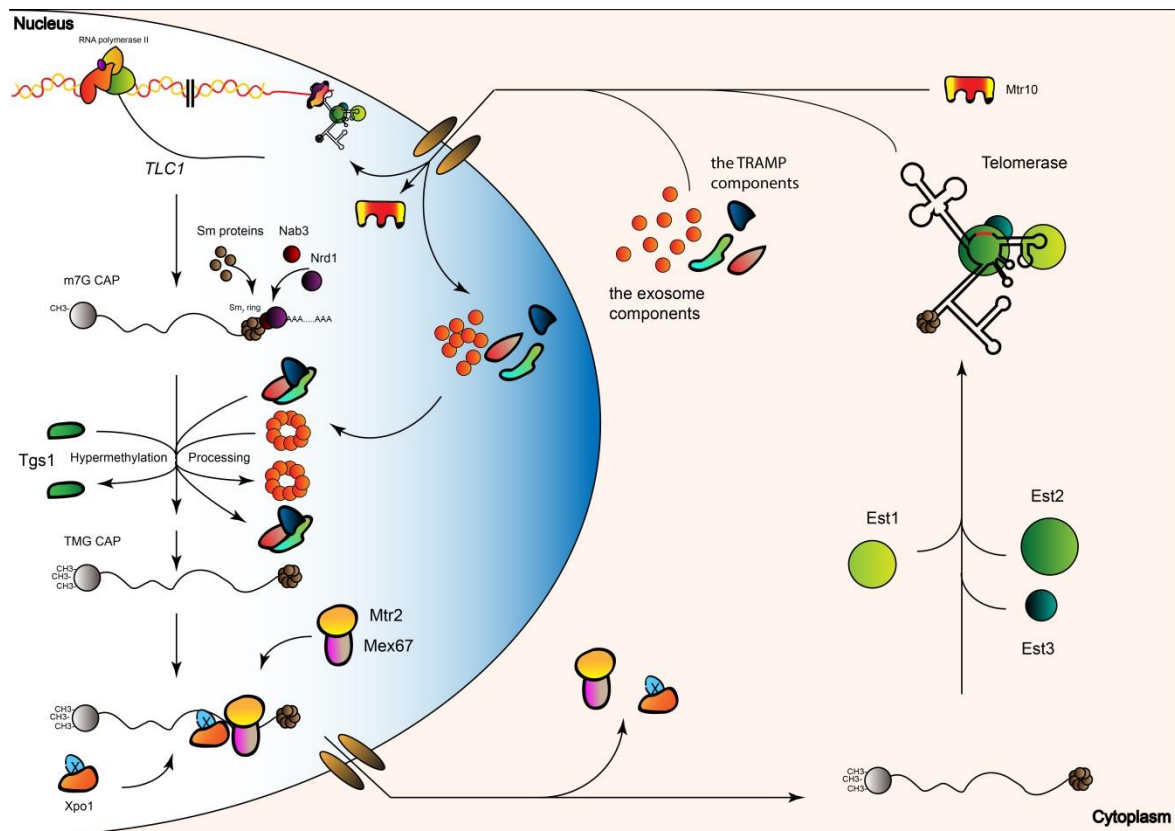


**Figure 4.3.1 Model of the transport and maturation of *TLC1*.** *TLC1* is generated by RNA polymerase II with a m<sup>7</sup>G cap structure and a poly(A)<sup>+</sup> tail. The binding of the Sm<sub>7</sub> Ring complex to its Sm binding site triggers the hypermethylation of the cap structure by Tgs1. Besides, the Sm<sub>7</sub> binding also leads to a 3'-end trimming performed through the combination of the Nrd1-Nab3 complex, the nuclear exosome and probably the TRAMP complex. After maturation, *TLC1* is exported to the cytoplasm via the combination of the Crm/Xpo1 and mRNA export factors. In the cytoplasm, *TLC1* assembles the telomerase components to form the telomerase complex. Telomerase is re-imported into the nucleus by Mtr10, which might also transport the factors necessary for *TLC1* maturation. Finally, in the nucleus, telomerase elongates the shortened telomeres to maintain their length and to avoid senescence.

## 5. Discussion and Perspective

### 5.1 The life cycle of the telomerase complex

The life cycle of the telomerase complex begins with the synthesis of the telomerase RNA *TLC1*. *TLC1* is generated by RNA polymerase II and polyadenylated like other RNA polymerase II products (reviewed in (Gallardo and Chartrand, 2008)). However, the association of the Sm<sub>7</sub> complex to its binding site on the 3' end leads to different processing events than those of the mRNAs (Seto et al., 1999). This Sm<sub>7</sub> ring complex binding triggers two events: Hypermethylation of the 5' cap structure of *TLC1* (Franke et al., 2008) and shortening of its 3' part through the Nab1-Nab3-Sen1 pathway (Noel et al., 2012). Our results have shown that mature *TLC1* accumulates in the nucleus upon an export block, suggesting that the complete maturation of the *TLC1* RNA occurs in the nucleus. Nevertheless, the sequential order of these two events remains unclear. The only deduction that can be made is that they do not occur simultaneously, since the hypermethylation factor, Tgs1, is located in the nucleolus (Mouaikel et al., 2002) while Nrd1 and Nab3 are located in the nucleus in *Saccharomyces cerevisiae* (Huh et al., 2003). Moreover, whether these two events are dependent on each other is also unknown. Measurement of the processing of *TLC1* with qRT-PCR in *tgs1Δ* strains would help to answer this question. The 3' processing of *TLC1* is performed through a pathway that contains a recognition system, which includes the Nab1-Nab3-Sen1 termination complex (Noel et al., 2012), and a degradation system, which contains the nuclear exosome (Coy et al., 2013). The boundary of the degradation is defined by the Sm<sub>7</sub> ring binding site (Coy et al., 2013). Although Dis3 is the only catalytic core component of the Exo-10, the remaining components in the Exo-9, are required to recognise the substrate (Das and Das, 2013). Which exact component is involved in this *TLC1* recognition is another interesting topic. Furthermore, the TRAMP complex component knockout strains show *TLC1* processing defects, suggesting that they might be involved in *TLC1* processing. This is consistent with the findings that the TRAMP complex interacts with the Nab1-Nab3-Sen1 pathway and is involved in the maturation and degradation of non-coding RNAs (Grzechnik

and Kufel, 2008; Tudek et al., 2014).

The nuclear export of *TLC1* is initiated after full maturation. *TLC1* export is mediated by the Crm1/Xpo1 pathway (Gallardo et al., 2008), and our results demonstrate that this nuclear export additionally requires the mRNA export pathway. Such coordination has also been reported in the transport of ribosomal subunits (Faza et al., 2012; Yao et al., 2007). Since Xpo1 interacts with proteins and needs adaptors to contact the RNA (reviewed in (Doye, 2014)), such an adaptor for *TLC1* nuclear export is unknown yet.

Upon arrival of mature *TLC1* in the cytoplasm, its secondary structure is recognised by the telomerase components. However, the serial events in formation of the telomerase holoenzyme remain unclear. A previous report has shown that the Est1-*TLC1* interaction is Est2 and Est3 independent and the nuclear localisation of Est1 is mediated by Srp1, a karyopherin alpha (Hawkins and Friedman, 2014). This is different for *TLC1*, which is transported by Mtr10 (Ferrezuelo et al., 2002; Gallardo et al., 2008). It is possible that Est1 and Est2-Est3-*TLC1* might be imported into the nucleus separately and are subsequently assembled to form the telomerase holoenzyme. This hypothesis is supported by the observation that in the early G1 phase of the cell cycle Yku80 recruits the Est2-*TLC1* premature telomerase without Est1 on the subtelomeric region (Fisher et al., 2004). However, Est2 is in this context inactive and does not elongate the telomeres (Fischer et al., 2004), suggesting that this could only be a way for retaining the telomerase components in the nucleus. Our result showing that both Est1 and Est2 mislocalise to the cytoplasm in absence of *TLC1* argues against this hypothesis and rather supports a model that formation of the telomerase holoenzyme might occur prior to the nuclear import. Certainly, there would be another possibility to explain that the Mtr10-independent nuclear localisation of Est1 is dependent on *TLC1*. Although Est1 is imported by Srp1, it needs bind to *TLC1* for its nuclear retention. This hypothesis is similar to our previous proposal that the Est2-*TLC1* complexes are anchored at chromosome ends in the G1 phase (Fischer et al., 2004) for their nuclear retention. The hypothesis can be examined by nucleo-cytoplasmic cell fractionation experiments. Two biogenesis models of telomerase have been proposed: 1) the shuttling model, in which *TLC1* would be transported to the cytoplasm to be assembled to the

telomerase with the telomerase components and is then re-imported into the nucleus; 2) the processing enzyme model, in which the necessary factors that are required for the maturation of *TLC1* and the telomerase complex are transported by Mtr10 (Ferrezuelo et al., 2002). Our results suggest a hypothesis combining these two models. On the one side, *TLC1* would be exported to the cytoplasm and form the telomerase complex with the protein components there, followed by its re-import into the nucleus via Mtr10. On the other side, the maturation of *TLC1* requires processing factors (the TRAMP complex, the nuclear exosome), some of which are imported into the nucleus by Mtr10.

Telomerase defects lead to telomere shortening. So far, the genome wide screens that identified factors involved in telomere shortening mostly identified non-essential genes (Askree et al., 2004). Here we have shown that under a particular condition, *e.g.* at semi-permissive temperature, the mutants of essential genes could also lead to telomere shortening. This result largely expands our view of the factors involved in telomere maintenance. A similar observation has also been reported recently that at the semi-permissive temperature a *SRP1* mutant, which encodes a defective karyopherin alpha, shows telomere shortening due to a failed nuclear import of Est1 (Hawkins and Friedman, 2014). These observations suggest that the senescence phenotypes could also be caused by defects of essential genes and there might be more factors that are involved in telomere maintenance than expected.

After elongation of the telomeres, it is still unclear how telomerase would be recycled. Telomerase RNA is one of the most stable transcripts in a given organism, *e.g.* the half-life of around 4 weeks in H1299 cells, which is currently the RNA with the longest lifetime identified so far (Bodnar et al., 1998; Yi et al., 1999). In *Saccharomyces cerevisiae*, the half-life of *TLC1* is longer than 60 minutes (Chapon et al., 1997). How the organism protects *TLC1* from the access of the degradation machinery is unclear. One explanation might be that since *TLC1* is the factor with the lowest abundance of all telomerase components (Mozdy and Cech, 2006), all RNA molecules are integrated into the telomerase complex and thus protected from degradation by the bound proteins.

## 5.2 RNA nuclear export

As identified in this study, *TLC1* utilises Xpo1/Crm1 and Mex67 for its export to the cytosol. However, why both factors contribute to the export remains unknown. Interestingly, Mex67 is also involved in transporting pre-60S (Yao et al., 2007) and pre-40S ribosomes (Faza et al., 2012) together with Xpo1/Crm1 (Ho et al., 2000; Johnson et al., 2002; Moy and Silver, 1999; Nissan et al., 2002). These observations suggest that cooperative use of Xpo1/Crm1 and Mex67 could be one of the ways for transporting certain RNAs.

For most spliceosomal snRNAs, it has been shown that in human cells they are transported into the cytoplasm for certain maturation steps including the binding of the Sm ring complex, 5' cap hypermethylation, as well as 3' trimming (reviewed in (Will and Luhrmann, 2001)). Nevertheless, in yeast these maturation steps mainly occur in the nucleus. However, yeast *TLC1*, as a non-coding RNA, requires the journey to the cytoplasm for the formation of the telomerase. In contrast, snRNAs are integrated into the spliceosomes in the nucleus (reviewed in (Will and Luhrmann, 2001)). Interestingly, a nucleo-cytoplasmic shuttling of some snRNAs and snoRNAs have nevertheless been observed in budding yeast by using heterokaryon assays, which has been suggested to be due to a global leakage or a molecular exchange between nuclei in this special cell type (Olson and Siliciano, 2003). Therefore, it will require further experiments to find out if these non-coding RNAs shuttle in yeast. Moreover, if this is the case, whether the nuclear export of the RNAs is also mediated by cooperation of Xpo1/Crm1 and Mex67 remains to be known.



### 5.3 Mtr10 and its cargoes

Mtr10 has been first identified in a screen of mRNA transport-defective (*mtr*) mutants (Kadowaki et al., 1994). Later investigations have shown that the mRNA transport defects in the *mtr10* mutant are probably not due to loss of the function of Mtr10 directly, but rather indirectly by mediating the nuclear re-import of the three mRNA adaptor proteins for Mex67-Mtr2, Hrb1, Gbp2 and Npl3 (Pemberton et al., 1997; Senger et al., 1998; Windgassen and Krebber, 2003). Here we have identified that, in addition to these mRNA-binding proteins, Mtr10 might transport the TRAMP complex components, Mtr4 and Trf4, and the exosome component, Dis3 (Lea Steffen and Heike Krebber), into the nucleus. These findings are also supported by the immunoprecipitation experiments that show a physical interaction between Mtr10 and these factors. Interestingly, several global analyses of protein complexes have uncovered the interaction of Srp1, a karyopherin alpha, with all of the exosome core components that supported a possible transport function for Srp1 (Collins et al., 2007; Gavin et al., 2002; Ho et al., 2002; Krogan et al., 2006; Peng et al., 2003; Synowsky et al., 2009). It still remains to be shown if indeed Srp1 participate in the Mtr10 mediated nuclear import of these factors. Interestingly, the telomerase component Est1 might be transported via Srp1 (Hawkins and Friedman, 2014) but another telomerase component *TLC1* is imported via Mtr10. Therefore, further experiments, including the investigation of a physical interaction and genetic interaction between Mtr10 and Srp1, would be necessary to verify this potential cooperation. In fact, although the deletion of *MTR10* is lethal at higher temperatures (e.g. 37°C), it shows only a strong growth defect at lower growth temperatures (23-30°C) (Pemberton et al., 1997; Senger et al., 1998). This suggests that although Mtr10 is an important karyopherin, it is not essential. Without Mtr10 its substrates are still transported, however with much lower efficiency. This is further supported by the observation that overexpression of *TLC1* in *mtr10Δ* cells leads to a rescue of the telomere shortening (Ferrezuelo et al., 2002).

Moreover, it is unclear if Mtr10 imports the exosome complex and the TRAMP complex components as single proteins or as a formed complex. This can be addressed by interaction

studies in *mtr10* mutants.

## 6. References

- Abou Elela, S., and Ares, M., Jr. (1998). Depletion of yeast RNase III blocks correct U2 3' end formation and results in polyadenylated but functional U2 snRNA. *The EMBO journal* *17*, 3738-3746.
- Allmang, C., Mitchell, P., Petfalski, E., and Tollervey, D. (2000). Degradation of ribosomal RNA precursors by the exosome. *Nucleic Acids Res* *28*, 1684-1691.
- Arigo, J.T., Eyler, D.E., Carroll, K.L., and Corden, J.L. (2006). Termination of cryptic unstable transcripts is directed by yeast RNA-binding proteins Nrd1 and Nab3. *Mol Cell* *23*, 841-851.
- AskjaerStade, K., Ford, C.S., Guthrie, C., and Weis, K. (1997). Exportin 1 (Crm1p) is an essential nuclear export factor. *Cell* *90*, 1041-1050.
- Askree, S.H., Yehuda, T., Smolikov, S., Gurevich, R., Hawk, J., Coker, C., Krauskopf, A., Kupiec, M., and McEachern, M.J. (2004). A genome-wide screen for *Saccharomyces cerevisiae* deletion mutants that affect telomere length. *Proceedings of the National Academy of Sciences of the United States of America* *101*, 8658-8663.
- Bachi, A., Braun, I.C., Rodrigues, J.P., Pante, N., Ribbeck, K., von Kobbe, C., Kutay, U., Wilm, M., Gorlich, D., Carmo-Fonseca, M., *et al.* (2000). The C-terminal domain of TAP interacts with the nuclear pore complex and promotes export of specific CTE-bearing RNA substrates. *RNA* *6*, 136-158.
- Bianchi, A., and Shore, D. (2007). Increased association of telomerase with short telomeres in yeast. *Genes Dev* *21*, 1726-1730.
- Bodnar, A.G., Ouellette, M., Frolkis, M., Holt, S.E., Chiu, C.P., Morin, G.B., Harley, C.B., Shay, J.W., Lichtsteiner, S., and Wright, W.E. (1998). Extension of life-span by introduction of telomerase into normal human cells. *Science* *279*, 349-352.
- Bonetti, D., Clerici, M., Anbalagan, S., Martina, M., Lucchini, G., and Longhese, M.P. (2010a). Shelterin-like proteins and Yku inhibit nucleolytic processing of *Saccharomyces cerevisiae* telomeres. *Plos Genet* *6*, e1000966.
- Bonetti, D., Clerici, M., Manfrini, N., Lucchini, G., and Longhese, M.P. (2010b). The MRX complex plays multiple functions in resection of Yku- and Rif2-protected DNA ends. *Plos One* *5*, e14142.
- Bosoy, D., Peng, Y., Mian, I.S., and Lue, N.F. (2003). Conserved N-terminal motifs of telomerase reverse transcriptase required for ribonucleoprotein assembly in vivo. *The Journal of biological chemistry* *278*, 3882-3890.
- Boulton, S.J., and Jackson, S.P. (1998). Components of the Ku-dependent non-homologous end-joining pathway are involved in telomeric length maintenance and telomeric silencing. *The EMBO journal* *17*, 1819-1828.
- Bourns, B.D., Alexander, M.K., Smith, A.M., and Zakian, V.A. (1998). Sir proteins, Rif proteins, and Cdc13p bind *Saccharomyces* telomeres in vivo. *Molecular and cellular biology* *18*, 5600-5608.
- Bousquet-Antonelli, C., Presutti, C., and Tollervey, D. (2000). Identification of a regulated pathway for nuclear pre-mRNA turnover. *Cell* *102*, 765-775.
- Box, J.A., Bunch, J.T., Tang, W., and Baumann, P. (2008). Spliceosomal cleavage generates the 3' end of telomerase RNA. *Nature* *456*, 910-914.
- Brune, C., Munchel, S.E., Fischer, N., Podtelejnikov, A.V., and Weis, K. (2005). Yeast poly(A)-binding protein Pab1 shuttles between the nucleus and the cytoplasm and functions in mRNA export. *Rna-a Publication of the Rna Society* *11*, 517-531.

- Burkard, K.T., and Butler, J.S. (2000). A nuclear 3'-5' exonuclease involved in mRNA degradation interacts with Poly(A) polymerase and the hnRNA protein Npl3p. *Molecular and cellular biology* 20, 604-616.
- Carroll, K.L., Pradhan, D.A., Granek, J.A., Clarke, N.D., and Corden, J.L. (2004). Identification of cis elements directing termination of yeast nonpolyadenylated snoRNA transcripts. *Molecular and cellular biology* 24, 6241-6252.
- Chan, A., Boule, J.B., and Zakian, V.A. (2008). Two pathways recruit telomerase to *Saccharomyces cerevisiae* telomeres. *Plos Genet* 4, e1000236.
- Chan, C.S., and Tye, B.K. (1983). Organization of DNA sequences and replication origins at yeast telomeres. *Cell* 33, 563-573.
- Chapon, C., Cech, T.R., and Zaug, A.J. (1997). Polyadenylation of telomerase RNA in budding yeast. *Rna-a Publication of the Rna Society* 3, 1337-1351.
- Cohn, M., and Blackburn, E.H. (1995). Telomerase in yeast. *Science* 269, 396-400.
- Collins, S.R., Kemmeren, P., Zhao, X.C., Greenblatt, J.F., Spencer, F., Holstege, F.C., Weissman, J.S., and Krogan, N.J. (2007). Toward a comprehensive atlas of the physical interactome of *Saccharomyces cerevisiae*. *Molecular & cellular proteomics : MCP* 6, 439-450.
- Conrad, M.N., Wright, J.H., Wolf, A.J., and Zakian, V.A. (1990). RAP1 protein interacts with yeast telomeres in vivo: overproduction alters telomere structure and decreases chromosome stability. *Cell* 63, 739-750.
- Coy, S., Volanakis, A., Shah, S., and Vasiljeva, L. (2013). The Sm Complex Is Required for the Processing of Non-Coding RNAs by the Exosome. *Plos One* 8.
- Creamer, T.J., Darby, M.M., Jamonnak, N., Schaughency, P., Hao, H., Wheelan, S.J., and Corden, J.L. (2011). Transcriptome-wide binding sites for components of the *Saccharomyces cerevisiae* non-poly(A) termination pathway: Nrd1, Nab3, and Sen1. *Plos Genet* 7, e1002329.
- Dandjinou, A.T., Levesque, N., Larose, S., Lucier, J.F., Abou Elela, S., and Wellinger, R.J. (2004). A phylogenetically based secondary structure for the yeast telomerase RNA. *Current biology : CB* 14, 1148-1158.
- Das, S., and Das, B. (2013). mRNA quality control pathways in *Saccharomyces cerevisiae*. *Journal of biosciences* 38, 615-640.
- de la Cruz, J., Kressler, D., and Linder, P. (1999). Unwinding RNA in *Saccharomyces cerevisiae*: DEAD-box proteins and related families. *Trends in biochemical sciences* 24, 192-198.
- de la Cruz, J., Kressler, D., Tollervey, D., and Linder, P. (1998). Dob1p (Mtr4p) is a putative ATP-dependent RNA helicase required for the 3' end formation of 5.8S rRNA in *Saccharomyces cerevisiae*. *The EMBO journal* 17, 1128-1140.
- de Vegvar, H.E., Lund, E., and Dahlberg, J.E. (1986). 3' end formation of U1 snRNA precursors is coupled to transcription from snRNA promoters. *Cell* 47, 259-266.
- Del Priore, V., Heath, C., Snay, C., MacMillan, A., Gorsch, L., Dagher, S., and Cole, C. (1997). A structure/function analysis of Rat7p/Nup159p, an essential nucleoporin of *Saccharomyces cerevisiae*. *Journal of cell science* 110 ( Pt 23), 2987-2999.
- Dewar, J.M., and Lydall, D. (2012). Similarities and differences between "uncapped" telomeres and DNA double-strand breaks. *Chromosoma* 121, 117-130.
- Dez, C., Dlakic, M., and Tollervey, D. (2007). Roles of the HEAT repeat proteins Utp10 and Utp20 in 40S ribosome maturation. *Rna-a Publication of the Rna Society* 13, 1516-1527.
- DeZwaan, D.C., and Freeman, B.C. (2009). The conserved Est1 protein stimulates telomerase DNA

- extension activity. *Proceedings of the National Academy of Sciences of the United States of America* *106*, 17337-17342.
- Doye, V. (2014). Preface. Nuclear pore complexes and nucleocytoplasmic transport-methods. *Methods in cell biology* *122*, xix-xx.
- Eckmann, C.R., Rammelt, C., and Wahle, E. (2011). Control of poly(A) tail length. *Wiley interdisciplinary reviews. RNA* *2*, 348-361.
- Egecioglu, D.E., Henras, A.K., and Chanfreau, G.F. (2006). Contributions of Trf4p- and Trf5p-dependent polyadenylation to the processing and degradative functions of the yeast nuclear exosome. *Rna-a Publication of the Rna Society* *12*, 26-32.
- Evans, S.K., and Lundblad, V. (1999). Est1 and Cdc13 as comediators of telomerase access. *Science* *286*, 117-120.
- Fasken, M.B., Leung, S.W., Banerjee, A., Kodani, M.O., Chavez, R., Bowman, E.A., Purohit, M.K., Rubinson, M.E., Rubinson, E.H., and Corbett, A.H. (2011). Air1 zinc knuckles 4 and 5 and a conserved IWRXY motif are critical for the function and integrity of the Trf4/5-Air1/2-Mtr4 polyadenylation (TRAMP) RNA quality control complex. *The Journal of biological chemistry* *286*, 37429-37445.
- Faza, M.B., Chang, Y., Occhipinti, L., Kemmler, S., and Panse, V.G. (2012). Role of Mex67-Mtr2 in the Nuclear Export of 40S Pre-Ribosomes. *Plos Genet* *8*.
- Ferrezuelo, F., Steiner, B., Aldea, M., and Fitcher, B. (2002). Biogenesis of yeast telomerase depends on the importin mtr10. *Molecular and cellular biology* *22*, 6046-6055.
- Fiorentini, P., Huang, K.N., Tishkoff, D.X., Kolodner, R.D., and Symington, L.S. (1997). Exonuclease I of *Saccharomyces cerevisiae* functions in mitotic recombination in vivo and in vitro. *Molecular and cellular biology* *17*, 2764-2773.
- Fischer, T., Rodriguez-Navarro, S., Pereira, G., Racz, A., Schiebel, E., and Hurt, E. (2004). Yeast centrin Cdc31 is linked to the nuclear mRNA export machinery. *Nature cell biology* *6*, 840-848.
- Fisher, T.S., Taggart, A.K., and Zakian, V.A. (2004). Cell cycle-dependent regulation of yeast telomerase by Ku. *Nat Struct Mol Biol* *11*, 1198-1205.
- Forstemann, K., and Lingner, J. (2001). Molecular basis for telomere repeat divergence in budding yeast. *Molecular and cellular biology* *21*, 7277-7286.
- Franke, J., Gehlen, J., and Ehrenhofer-Murray, A.E. (2008). Hypermethylation of yeast telomerase RNA by the snRNA and snoRNA methyltransferase Tgs1. *Journal of cell science* *121*, 3553-3560.
- Friedman, K.L., and Cech, T.R. (1999). Essential functions of amino-terminal domains in the yeast telomerase catalytic subunit revealed by selection for viable mutants. *Genes Dev* *13*, 2863-2874.
- Friedman, K.L., Heit, J.J., Long, D.M., and Cech, T.R. (2003). N-terminal domain of yeast telomerase reverse transcriptase: recruitment of Est3p to the telomerase complex. *Molecular biology of the cell* *14*, 1-13.
- Gadal, O., Strauss, D., Kessel, J., Trumpower, B., Tollervey, D., and Hurt, E. (2001). Nuclear export of 60s ribosomal subunits depends on Xpo1p and requires a nuclear export sequence-containing factor, Nmd3p, that associates with the large subunit protein Rpl10p. *Molecular and cellular biology* *21*, 3405-3415.
- Gallardo, F., and Chartrand, P. (2008). Telomerase biogenesis. *Rna Biol* *5*, 212-215.
- Gallardo, F., Laterreur, N., Cusanelli, E., Ouenzar, F., Querido, E., Wellinger, R.J., and Chartrand, P. (2011). Live cell imaging of telomerase RNA dynamics reveals cell cycle-dependent clustering of telomerase at elongating telomeres. *Mol Cell* *44*, 819-827.

- Gallardo, F., Olivier, C., Dandjinou, A.T., Wellinger, R.J., and Chartrand, P. (2008). TLC1 RNA nucleo-cytoplasmic trafficking links telomerase biogenesis to its recruitment to telomeres. *Embo J* 27, 748-757.
- Gauss, R., Trautwein, M., Sommer, T., and Spang, A. (2005). New modules for the repeated internal and N-terminal epitope tagging of genes in *Saccharomyces cerevisiae*. *Yeast* 22, 1-12.
- Gavin, A.C., Bosche, M., Krause, R., Grandi, P., Marzioch, M., Bauer, A., Schultz, J., Rick, J.M., Michon, A.M., Cruciat, C.M., *et al.* (2002). Functional organization of the yeast proteome by systematic analysis of protein complexes. *Nature* 415, 141-147.
- Gilson, E., Roberge, M., Giraldo, R., Rhodes, D., and Gasser, S.M. (1993). Distortion of the DNA double helix by RAP1 at silencers and multiple telomeric binding sites. *Journal of molecular biology* 231, 293-310.
- Gorsch, L.C., Dockendorff, T.C., and Cole, C.N. (1995). A conditional allele of the novel repeat-containing yeast nucleoporin RAT7/NUP159 causes both rapid cessation of mRNA export and reversible clustering of nuclear pore complexes. *The Journal of cell biology* 129, 939-955.
- Gottschling, D.E., Aparicio, O.M., Billington, B.L., and Zakian, V.A. (1990). Position effect at *S. cerevisiae* telomeres: reversible repression of Pol II transcription. *Cell* 63, 751-762.
- Grant, R.P., Hurt, E., Neuhaus, D., and Stewart, M. (2002). Structure of the C-terminal FG-nucleoporin binding domain of Tap/NXF1. *Nature structural biology* 9, 247-251.
- Gravel, S., Larrivee, M., Labrecque, P., and Wellinger, R.J. (1998). Yeast Ku as a regulator of chromosomal DNA end structure. *Science* 280, 741-744.
- Grzechnik, P., and Kufel, J. (2008). Polyadenylation linked to transcription termination directs the processing of snoRNA precursors in yeast. *Mol Cell* 32, 247-258.
- Gudipati, R.K., Xu, Z., Lebreton, A., Seraphin, B., Steinmetz, L.M., Jacquier, A., and Libri, D. (2012). Extensive degradation of RNA precursors by the exosome in wild-type cells. *Mol Cell* 48, 409-421.
- Gwizdek, C., Iglesias, N., Rodriguez, M.S., Ossareh-Nazari, B., Hobeika, M., Divita, G., Stutz, F., and Dargemont, C. (2006). Ubiquitin-associated domain of Mex67 synchronizes recruitment of the mRNA export machinery with transcription. *Proceedings of the National Academy of Sciences of the United States of America* 103, 16376-16381.
- Hamill, S., Wolin, S.L., and Reinisch, K.M. (2010). Structure and function of the polymerase core of TRAMP, a RNA surveillance complex. *Proceedings of the National Academy of Sciences of the United States of America* 107, 15045-15050.
- Hamm, J., and Mattaj, I.W. (1990). Monomethylated cap structures facilitate RNA export from the nucleus. *Cell* 63, 109-118.
- Hardy, C.F., Balderes, D., and Shore, D. (1992a). Dissection of a carboxy-terminal region of the yeast regulatory protein RAP1 with effects on both transcriptional activation and silencing. *Molecular and cellular biology* 12, 1209-1217.
- Hardy, C.F., Sussel, L., and Shore, D. (1992b). A RAP1-interacting protein involved in transcriptional silencing and telomere length regulation. *Genes Dev* 6, 801-814.
- Harley, C.B., Futcher, A.B., and Greider, C.W. (1990). Telomeres shorten during ageing of human fibroblasts. *Nature* 345, 458-460.
- Hawkins, C., and Friedman, K.L. (2014). Normal Telomere Length Maintenance in Yeast Requires Nuclear Import of the Ever Shorter Telomeres 1 (Est1) Protein via the Importin Alpha Pathway. *Eukaryotic cell*.
- Hayflick, L. (1979). Cell biology of aging. *Fed Proc* 38, 1847-1850.

- Hector, R.E., Shtofman, R.L., Ray, A., Chen, B.R., Nyun, T., Berkner, K.L., and Runge, K.W. (2007). Tel1p preferentially associates with short telomeres to stimulate their elongation. *Mol Cell* 27, 851-858.
- Hernandez, N., and Weiner, A.M. (1986). Formation of the 3' end of U1 snRNA requires compatible snRNA promoter elements. *Cell* 47, 249-258.
- Ho, J.H., Kallstrom, G., and Johnson, A.W. (2000). Nmd3p is a Crm1p-dependent adapter protein for nuclear export of the large ribosomal subunit. *The Journal of cell biology* 151, 1057-1066.
- Ho, Y., Gruhler, A., Heilbut, A., Bader, G.D., Moore, L., Adams, S.L., Millar, A., Taylor, P., Bennett, K., Boutilier, K., *et al.* (2002). Systematic identification of protein complexes in *Saccharomyces cerevisiae* by mass spectrometry. *Nature* 415, 180-183.
- Hobeika, M., Brockmann, C., Gruessing, F., Neuhaus, D., Divita, G., Stewart, M., and Dargemont, C. (2009). Structural requirements for the ubiquitin-associated domain of the mRNA export factor Mex67 to bind its specific targets, the transcription elongation THO complex component Hpr1 and nucleoporin FXFG repeats. *The Journal of biological chemistry* 284, 17575-17583.
- Hodge, C.A., Colot, H.V., Stafford, P., and Cole, C.N. (1999). Rat8p/Dbp5p is a shuttling transport factor that interacts with Rat7p/Nup159p and Gle1p and suppresses the mRNA export defect of xpo1-1 cells. *The EMBO journal* 18, 5778-5788.
- Holub, P., Lalakova, J., Cerna, H., Pasulka, J., Sarazova, M., Hrazdilova, K., Arce, M.S., Hobor, F., Stefl, R., and Vanacova, S. (2012). Air2p is critical for the assembly and RNA-binding of the TRAMP complex and the KOW domain of Mtr4p is crucial for exosome activation. *Nucleic acids research* 40, 5679-5693.
- Hopper, A.K. (2006). Cellular dynamics of small RNAs. *Critical reviews in biochemistry and molecular biology* 41, 3-19.
- Houseley, J., and Tollervey, D. (2006). Yeast Trf5p is a nuclear poly(A) polymerase. *Embo Rep* 7, 205-211.
- Hughes, T.R., Evans, S.K., Weilbaecher, R.G., and Lundblad, V. (2000a). The Est3 protein is a subunit of yeast telomerase. *Current biology : CB* 10, 809-812.
- Hughes, T.R., Weilbaecher, R.G., Walterscheid, M., and Lundblad, V. (2000b). Identification of the single-strand telomeric DNA binding domain of the *Saccharomyces cerevisiae* Cdc13 protein. *Proceedings of the National Academy of Sciences of the United States of America* 97, 6457-6462.
- Huh, W.K., Falvo, J.V., Gerke, L.C., Carroll, A.S., Howson, R.W., Weissman, J.S., and O'Shea, E.K. (2003). Global analysis of protein localization in budding yeast. *Nature* 425, 686-691.
- Hurt, E., Hannus, S., Schmelzl, B., Lau, D., Tollervey, D., and Simos, G. (1999). A novel in vivo assay reveals inhibition of ribosomal nuclear export in ran-cycle and nucleoporin mutants. *The Journal of cell biology* 144, 389-401.
- Izaurralde, E., Lewis, J., Gamberi, C., Jarmolowski, A., McGuigan, C., and Mattaj, I.W. (1995). A cap-binding protein complex mediating U snRNA export. *Nature* 376, 709-712.
- Jackson, R.N., Klauer, A.A., Hintze, B.J., Robinson, H., van Hoof, A., and Johnson, S.J. (2010). The crystal structure of Mtr4 reveals a novel arch domain required for rRNA processing. *The EMBO journal* 29, 2205-2216.
- Jia, H., Wang, X., Liu, F., Guenther, U.P., Srinivasan, S., Anderson, J.T., and Jankowsky, E. (2011). The RNA helicase Mtr4p modulates polyadenylation in the TRAMP complex. *Cell* 145, 890-901.
- Johnson, A.W., Lund, E., and Dahlberg, J. (2002). Nuclear export of ribosomal subunits. *Trends in biochemical sciences* 27, 580-585.
- Kadaba, S., Krueger, A., Trice, T., Krecic, A.M., Hinnebusch, A.G., and Anderson, J. (2004). Nuclear

- surveillance and degradation of hypomodified initiator tRNA(Met) in *S-cerevisiae*. *Gene Dev* *18*, 1227-1240.
- Kadaba, S., Wang, X.Y., and Anderson, J.T. (2006). Nuclear RNA surveillance in *Saccharomyces cerevisiae*: Trf4p-dependent polyadenylation of nascent hypomethylated tRNA and an aberrant form of 5S rRNA. *Rna-a Publication of the Rna Society* *12*, 508-521.
- Kadowaki, T., Chen, S., Hitomi, M., Jacobs, E., Kumagai, C., Liang, S., Schneiter, R., Singleton, D., Wisniewska, J., and Tartakoff, A.M. (1994). Isolation and characterization of *Saccharomyces cerevisiae* mRNA transport-defective (mtr) mutants. *The Journal of cell biology* *126*, 649-659.
- Kang, Y., and Cullen, B.R. (1999). The human Tap protein is a nuclear mRNA export factor that contains novel RNA-binding and nucleocytoplasmic transport sequences. *Genes Dev* *13*, 1126-1139.
- Katahira, J., Strasser, K., Podtelejnikov, A., Mann, M., Jung, J.U., and Hurt, E. (1999). The Mex67p-mediated nuclear mRNA export pathway is conserved from yeast to human. *The EMBO journal* *18*, 2593-2609.
- Kironmai, K.M., and Muniyappa, K. (1997). Alteration of telomeric sequences and senescence caused by mutations in RAD50 of *Saccharomyces cerevisiae*. *Genes to cells : devoted to molecular & cellular mechanisms* *2*, 443-455.
- Knop, M., Siegers, K., Pereira, G., Zachariae, W., Winsor, B., Nasmyth, K., and Schiebel, E. (1999). Epitope tagging of yeast genes using a PCR-based strategy: More tags and improved practical routines. *Yeast* *15*, 963-972.
- Kohler, A., and Hurt, E. (2007). Exporting RNA from the nucleus to the cytoplasm. *Nat Rev Mol Cell Bio* *8*, 761-773.
- Krogan, N.J., Cagney, G., Yu, H., Zhong, G., Guo, X., Ignatchenko, A., Li, J., Pu, S., Datta, N., Tikuisis, A.P., et al. (2006). Global landscape of protein complexes in the yeast *Saccharomyces cerevisiae*. *Nature* *440*, 637-643.
- Kufel, J., Bousquet-Antonelli, C., Beggs, J.D., and Tollervey, D. (2004). Nuclear pre-mRNA decapping and 5' degradation in yeast require the Lsm2-8p complex. *Molecular and cellular biology* *24*, 9646-9657.
- Kupiec, M. (2014). Biology of telomeres: lessons from budding yeast. *FEMS microbiology reviews* *38*, 144-171.
- LaCava, J., Houseley, J., Saveanu, C., Petfalski, E., Thompson, E., Jacquier, A., and Tollervey, D. (2005). RNA degradation by the exosome is promoted by a nuclear polyadenylation complex. *Cell* *121*, 713-724.
- Larrivee, M., LeBel, C., and Wellinger, R.J. (2004). The generation of proper constitutive G-tails on yeast telomeres is dependent on the MRX complex. *Genes Dev* *18*, 1391-1396.
- Libri, D., Dower, K., Boulay, J., Thomsen, R., Rosbash, M., and Jensen, T.H. (2002). Interactions between mRNA export commitment, 3'-end quality control, and nuclear degradation. *Molecular and cellular biology* *22*, 8254-8266.
- Liker, E., Fernandez, E., Izaurralde, E., and Conti, E. (2000). The structure of the mRNA export factor TAP reveals a cis arrangement of a non-canonical RNP domain and an LRR domain. *The EMBO journal* *19*, 5587-5598.
- Lin, J., Ly, H., Hussain, A., Abraham, M., Pearl, S., Tzfati, Y., Parslow, T.G., and Blackburn, E.H. (2004). A universal telomerase RNA core structure includes structured motifs required for binding the telomerase reverse transcriptase protein. *Proceedings of the National Academy of Sciences of the United States of America* *101*, 14713-14718.



- Lin, J.J., and Zakian, V.A. (1996). The *Saccharomyces* CDC13 protein is a single-strand TG1-3 telomeric DNA-binding protein in vitro that affects telomere behavior in vivo. *Proceedings of the National Academy of Sciences of the United States of America* *93*, 13760-13765.
- Lingner, J., Cooper, J.P., and Cech, T.R. (1995). Telomerase and DNA end replication: no longer a lagging strand problem? *Science* *269*, 1533-1534.
- Lingner, J., Hughes, T.R., Shevchenko, A., Mann, M., Lundblad, V., and Cech, T.R. (1997). Reverse transcriptase motifs in the catalytic subunit of telomerase. *Science* *276*, 561-567.
- Liu, Q., Greimann, J.C., and Lima, C.D. (2006). Reconstitution, activities, and structure of the eukaryotic RNA exosome. *Cell* *127*, 1223-1237.
- Liu, Y., Guo, W., Tartakoff, P.Y., and Tartakoff, A.M. (1999). A Crm1p-independent nuclear export path for the mRNA-associated protein, Npl3p/Mtr13p. *Proceedings of the National Academy of Sciences of the United States of America* *96*, 6739-6744.
- Livengood, A.J., Zaug, A.J., and Cech, T.R. (2002). Essential regions of *Saccharomyces cerevisiae* telomerase RNA: separate elements for Est1p and Est2p interaction. *Molecular and cellular biology* *22*, 2366-2374.
- Louis, E.J., Naumova, E.S., Lee, A., Naumov, G., and Haber, J.E. (1994). The chromosome end in yeast: its mosaic nature and influence on recombinational dynamics. *Genetics* *136*, 789-802.
- Lubin, J.W., Tucey, T.M., and Lundblad, V. (2012). The interaction between the yeast telomerase RNA and the Est1 protein requires three structural elements. *Rna-a Publication of the Rna Society* *18*, 1597-1604.
- Lundblad, V., and Szostak, J.W. (1989). A Mutant with a Defect in Telomere Elongation Leads to Senescence in Yeast. *Cell* *57*, 633-643.
- Lustig, A.J., Kurtz, S., and Shore, D. (1990). Involvement of the silencer and UAS binding protein RAP1 in regulation of telomere length. *Science* *250*, 549-553.
- Mantiero, D., Clerici, M., Lucchini, G., and Longhese, M.P. (2007). Dual role for *Saccharomyces cerevisiae* Tel1 in the checkpoint response to double-strand breaks. *Embo Rep* *8*, 380-387.
- Martin, S.G., Laroche, T., Suka, N., Grunstein, M., and Gasser, S.M. (1999). Relocalization of telomeric Ku and SIR proteins in response to DNA strand breaks in yeast. *Cell* *97*, 621-633.
- Matera, A.G., Terns, R.M., and Terns, M.P. (2007). Non-coding RNAs: lessons from the small nuclear and small nucleolar RNAs. *Nature reviews. Molecular cell biology* *8*, 209-220.
- Mitchell, P., Petfalski, E., Shevchenko, A., Mann, M., and Tollervey, D. (1997). The exosome: A conserved eukaryotic RNA processing complex containing multiple 3'->5' exoribonucleases. *Cell* *91*, 457-466.
- Mitton-Fry, R.M., Anderson, E.M., Hughes, T.R., Lundblad, V., and Wuttke, D.S. (2002). Conserved structure for single-stranded telomeric DNA recognition. *Science* *296*, 145-147.
- Mitton-Fry, R.M., Anderson, E.M., Theobald, D.L., Glustrom, L.W., and Wuttke, D.S. (2004). Structural basis for telomeric single-stranded DNA recognition by yeast Cdc13. *Journal of molecular biology* *338*, 241-255.
- Moretti, P., Freeman, K., Coodly, L., and Shore, D. (1994). Evidence that a complex of SIR proteins interacts with the silencer and telomere-binding protein RAP1. *Genes Dev* *8*, 2257-2269.
- Morlando, M., Greco, P., Dichtl, B., Fatica, A., Keller, W., and Bozzoni, I. (2002). Functional analysis of yeast snoRNA and snRNA 3'-end formation mediated by uncoupling of cleavage and polyadenylation. *Molecular and cellular biology* *22*, 1379-1389.
- Morris, D.K., and Lundblad, V. (1997). Programmed translational frameshifting in a gene required for

- yeast telomere replication. *Current biology* : CB 7, 969-976.
- Mouaikel, J., Verheggen, C., Bertrand, E., Tazi, J., and Bordonne, R. (2002). Hypermethylation of the cap structure of both yeast snRNAs and snoRNAs requires a conserved methyltransferase that is localized to the nucleolus. *Mol Cell* 9, 891-901.
- Moy, T.I., and Silver, P.A. (1999). Nuclear export of the small ribosomal subunit requires the ran-GTPase cycle and certain nucleoporins. *Genes Dev* 13, 2118-2133.
- Mozdy, A.D., and Cech, T.R. (2006). Low abundance of telomerase in yeast: implications for telomerase haploinsufficiency. *RNA* 12, 1721-1737.
- Nakada, D., Matsumoto, K., and Sugimoto, K. (2003). ATM-related Tel1 associates with double-strand breaks through an Xrs2-dependent mechanism. *Genes Dev* 17, 1957-1962.
- Neville, M., Stutz, F., Lee, L., Davis, L.I., and Rosbash, M. (1997). The importin-beta family member Crm1p bridges the interaction between Rev and the nuclear pore complex during nuclear export. *Current biology* : CB 7, 767-775.
- Nissan, T.A., Bassler, J., Petfalski, E., Tollervey, D., and Hurt, E. (2002). 60S pre-ribosome formation viewed from assembly in the nucleolus until export to the cytoplasm. *The EMBO journal* 21, 5539-5547.
- Noel, J.F., Larose, S., Abou Elela, S., and Wellinger, R.J. (2012). Budding yeast telomerase RNA transcription termination is dictated by the Nrd1/Nab3 non-coding RNA termination pathway. *Nucleic acids research* 40, 5625-5636.
- Nugent, C.I., Hughes, T.R., Lue, N.F., and Lundblad, V. (1996). Cdc13p: a single-strand telomeric DNA-binding protein with a dual role in yeast telomere maintenance. *Science* 274, 249-252.
- Ohno, M., Segref, A., Bachi, A., Wilm, M., and Mattaj, I.W. (2000). PHAX, a mediator of U snRNA nuclear export whose activity is regulated by phosphorylation. *Cell* 101, 187-198.
- Olovnikov, A.M. (1971). [Principle of marginotomy in template synthesis of polynucleotides]. *Doklady Akademii nauk SSSR* 201, 1496-1499.
- Olson, B.L., and Siliciano, P.G. (2003). A diverse set of nuclear RNAs transfer between nuclei of yeast heterokaryons. *Yeast* 20, 893-903.
- Osterhage, J.L., Talley, J.M., and Friedman, K.L. (2006). Proteasome-dependent degradation of Est1p regulates the cell cycle-restricted assembly of telomerase in *Saccharomyces cerevisiae*. *Nat Struct Mol Biol* 13, 720-728.
- Palladino, F., Laroche, T., Gilson, E., Axelrod, A., Pillus, L., and Gasser, S.M. (1993). SIR3 and SIR4 proteins are required for the positioning and integrity of yeast telomeres. *Cell* 75, 543-555.
- Paolo, S.S., Vanacova, S., Schenk, L., Scherrer, T., Blank, D., Keller, W., and Gerber, A.P. (2009). Distinct Roles of Non-Canonical Poly(A) Polymerases in RNA Metabolism. *Plos Genet* 5.
- Pemberton, L.F., Rosenblum, J.S., and Blobel, G. (1997). A distinct and parallel pathway for the nuclear import of an mRNA-binding protein. *The Journal of cell biology* 139, 1645-1653.
- Peng, W.T., Robinson, M.D., Mnaimneh, S., Krogan, N.J., Cagney, G., Morris, Q., Davierwala, A.P., Grigull, J., Yang, X., Zhang, W., *et al.* (2003). A panoramic view of yeast noncoding RNA processing. *Cell* 113, 919-933.
- Pennock, E., Buckley, K., and Lundblad, V. (2001). Cdc13 delivers separate complexes to the telomere for end protection and replication. *Cell* 104, 387-396.
- Pfingsten, J.S., Goodrich, K.J., Taabazuing, C., Ouenzar, F., Chartrand, P., and Cech, T.R. (2012). Mutually exclusive binding of telomerase RNA and DNA by Ku alters telomerase recruitment model. *Cell* 148, 922-932.

- Porter, S.E., Greenwell, P.W., Ritchie, K.B., and Petes, T.D. (1996). The DNA-binding protein Hdf1p (a putative Ku homologue) is required for maintaining normal telomere length in *Saccharomyces cerevisiae*. *Nucleic acids research* *24*, 582-585.
- Pryde, F.E., and Louis, E.J. (1999). Limitations of silencing at native yeast telomeres. *The EMBO journal* *18*, 2538-2550.
- Puig, O., Caspary, F., Rigaut, G., Rutz, B., Bouveret, E., Bragado-Nilsson, E., Wilm, M., and Seraphin, B. (2001). The tandem affinity purification (TAP) method: a general procedure of protein complex purification. *Methods* *24*, 218-229.
- Qi, H., and Zakian, V.A. (2000). The *Saccharomyces* telomere-binding protein Cdc13p interacts with both the catalytic subunit of DNA polymerase alpha and the telomerase-associated est1 protein. *Genes Dev* *14*, 1777-1788.
- Qiao, F., and Cech, T.R. (2008). Triple-helix structure in telomerase RNA contributes to catalysis. *Nat Struct Mol Biol* *15*, 634-640.
- Raghuraman, M.K., Winzeler, E.A., Collingwood, D., Hunt, S., Wodicka, L., Conway, A., Lockhart, D.J., Davis, R.W., Brewer, B.J., and Fangman, W.L. (2001). Replication dynamics of the yeast genome. *Science* *294*, 115-121.
- Rathmell, W.K., and Chu, G. (1994). Involvement of the Ku autoantigen in the cellular response to DNA double-strand breaks. *Proceedings of the National Academy of Sciences of the United States of America* *91*, 7623-7627.
- Ray, A., and Runge, K.W. (1999a). Varying the number of telomere-bound proteins does not alter telomere length in tel1Delta cells. *Proceedings of the National Academy of Sciences of the United States of America* *96*, 15044-15049.
- Ray, A., and Runge, K.W. (1999b). The yeast telomere length counting machinery is sensitive to sequences at the telomere-nontelomere junction. *Molecular and cellular biology* *19*, 31-45.
- Ribeyre, C., and Shore, D. (2012). Anticheckpoint pathways at telomeres in yeast. *Nat Struct Mol Biol* *19*, 307-U364.
- Richard, P., and Manley, J.L. (2009). Transcription termination by nuclear RNA polymerases. *Genes Dev* *23*, 1247-1269.
- Roy, R., Meier, B., McAinsh, A.D., Feldmann, H.M., and Jackson, S.P. (2004). Separation-of-function mutants of yeast Ku80 reveal a Yku80p-Sir4p interaction involved in telomeric silencing. *The Journal of biological chemistry* *279*, 86-94.
- Sabourin, M., Tuzon, C.T., and Zakian, V.A. (2007). Telomerase and Tel1p preferentially associate with short telomeres in *S. cerevisiae*. *Mol Cell* *27*, 550-561.
- Sandhu, R., Sanford, S., Basu, S., Park, M., Pandya, U.M., Li, B., and Chakrabarti, K. (2013). A trans-spliced telomerase RNA dictates telomere synthesis in *Trypanosoma brucei*. *Cell research* *23*, 537-551.
- Schneider, C., Kudla, G., Wlotzka, W., Tuck, A., and Tollervey, D. (2012). Transcriptome-wide analysis of exosome targets. *Mol Cell* *48*, 422-433.
- Schneider, C., Leung, E., Brown, J., and Tollervey, D. (2009). The N-terminal PIN domain of the exosome subunit Rrp44 harbors endonuclease activity and tethers Rrp44 to the yeast core exosome. *Nucleic Acids Res* *37*, 1127-1140.
- Segref, A., Sharma, K., Doye, V., Hellwig, A., Huber, J., Luhrmann, R., and Hurt, E. (1997). Mex67p, a novel factor for nuclear mRNA export, binds to both poly(A)(+) RNA and nuclear pores. *Embo J* *16*, 3256-3271.

- Seipelt, R.L., Zheng, B., Asuru, A., and Rymond, B.C. (1999). U1 snRNA is cleaved by RNase III and processed through an Sm site-dependent pathway. *Nucleic acids research* 27, 587-595.
- Senger, B., Simos, G., Bischoff, F.R., Podtelejnikov, A., Mann, M., and Hurt, E. (1998). Mtr10p functions as a nuclear import receptor for the mRNA-binding protein Npl3p. *The EMBO journal* 17, 2196-2207.
- Seto, A.G., Livengood, A.J., Tzfati, Y., Blackburn, E.H., and Cech, T.R. (2002). A bulged stem tethers Est1p to telomerase RNA in budding yeast. *Genes Dev* 16, 2800-2812.
- Seto, A.G., Zaug, A.J., Sobel, S.G., Wolin, S.L., and Cech, T.R. (1999). *Saccharomyces cerevisiae* telomerase is an Sm small nuclear ribonucleoprotein particle. *Nature* 401, 177-180.
- Shampay, J., Szostak, J.W., and Blackburn, E.H. (1984). DNA sequences of telomeres maintained in yeast. *Nature* 310, 154-157.
- Shima, H., Suzuki, M., and Shinohara, M. (2005). Isolation and characterization of novel xrs2 mutations in *Saccharomyces cerevisiae*. *Genetics* 170, 71-85.
- Sikorski, R.S., and Hieter, P. (1989). A System of Shuttle Vectors and Yeast Host Strains Designed for Efficient Manipulation of DNA in *Saccharomyces-Cerevisiae*. *Genetics* 122, 19-27.
- Singer, M.S., and Gottschling, D.E. (1994). TLC1: template RNA component of *Saccharomyces cerevisiae* telomerase. *Science* 266, 404-409.
- Skruzny, M., Schneider, C., Racz, A., Weng, J., Tollervey, D., and Hurt, E. (2009). An endoribonuclease functionally linked to perinuclear mRNP quality control associates with the nuclear pore complexes. *Plos Biol* 7, e8.
- Slomovic, S., and Schuster, G. (2011). Exonucleases and endonucleases involved in polyadenylation-assisted RNA decay. *Wiley interdisciplinary reviews. RNA* 2, 106-123.
- Snay-Hodge, C.A., Colot, H.V., Goldstein, A.L., and Cole, C.N. (1998). Dbp5p/Rat8p is a yeast nuclear pore-associated DEAD-box protein essential for RNA export. *The EMBO journal* 17, 2663-2676.
- Stade, K., Ford, C.S., Guthrie, C., and Weis, K. (1997). Exportin 1 (Crm1p) is an essential nuclear export factor. *Cell* 90, 1041-1050.
- Stage-Zimmermann, T., Schmidt, U., and Silver, P.A. (2000). Factors affecting nuclear export of the 60S ribosomal subunit in vivo. *Molecular biology of the cell* 11, 3777-3789.
- Stansfield, I., Kushnirov, V.V., Jones, K.M., and Tuite, M.F. (1997). A conditional-lethal translation termination defect in a sup45 mutant of the yeast *Saccharomyces cerevisiae*. *European journal of biochemistry / FEBS* 245, 557-563.
- Steinmetz, E.J., Conrad, N.K., Brow, D.A., and Corden, J.L. (2001). RNA-binding protein Nrd1 directs poly(A)-independent 3'-end formation of RNA polymerase II transcripts. *Nature* 413, 327-331.
- Stellwagen, A.E., Haimberger, Z.W., Veatch, J.R., and Gottschling, D.E. (2003). Ku interacts with telomerase RNA to promote telomere addition at native and broken chromosome ends. *Genes Dev* 17, 2384-2395.
- Suyama, M., Doerks, T., Braun, I.C., Sattler, M., Izaurralde, E., and Bork, P. (2000). Prediction of structural domains of TAP reveals details of its interaction with p15 and nucleoporins. *Embo Rep* 1, 53-58.
- Synowsky, S.A., van Wijk, M., Raijmakers, R., and Heck, A.J.R. (2009). Comparative Multiplexed Mass Spectrometric Analyses of Endogenously Expressed Yeast Nuclear and Cytoplasmic Exosomes. *J Mol Biol* 385, 1300-1313.
- Szostak, J.W., and Blackburn, E.H. (1982). Cloning yeast telomeres on linear plasmid vectors. *Cell* 29, 245-255.

- Taccioli, G.E., Gottlieb, T.M., Blunt, T., Priestley, A., Demengeot, J., Mizuta, R., Lehmann, A.R., Alt, F.W., Jackson, S.P., and Jeggo, P.A. (1994). Ku80: product of the XRCC5 gene and its role in DNA repair and V(D)J recombination. *Science* 265, 1442-1445.
- Taggart, A.K., Teng, S.C., and Zakian, V.A. (2002). Est1p as a cell cycle-regulated activator of telomere-bound telomerase. *Science* 297, 1023-1026.
- Talley, J.M., DeZwaan, D.C., Maness, L.D., Freeman, B.C., and Friedman, K.L. (2011). Stimulation of yeast telomerase activity by the ever shorter telomere 3 (Est3) subunit is dependent on direct interaction with the catalytic protein Est2. *The Journal of biological chemistry* 286, 26431-26439.
- Taura, T., Krebber, H., and Silver, P.A. (1998). A member of the Ran-binding protein family, Yrb2p, is involved in nuclear protein export. *Proceedings of the National Academy of Sciences of the United States of America* 95, 7427-7432.
- Tieg, B., and Krebber, H. (2013). Dbp5 - from nuclear export to translation. *Biochimica et biophysica acta* 1829, 791-798.
- Torchet, C., Bousquet-Antonelli, C., Milligan, L., Thompson, E., Kufel, J., and Tollervy, D. (2002). Processing of 3'-extended read-through transcripts by the exosome can generate functional mRNAs. *Mol Cell* 9, 1285-1296.
- Tran, P.T., Erdeniz, N., Dudley, S., and Liskay, R.M. (2002). Characterization of nuclease-dependent functions of Exo1p in *Saccharomyces cerevisiae*. *DNA repair* 1, 895-912.
- Tsukamoto, Y., Taggart, A.K., and Zakian, V.A. (2001). The role of the Mre11-Rad50-Xrs2 complex in telomerase-mediated lengthening of *Saccharomyces cerevisiae* telomeres. *Current biology : CB* 11, 1328-1335.
- Tudek, A., Porrua, O., Kabzinski, T., Lidschreiber, M., Kubicek, K., Fortova, A., Lacroute, F., Vanacova, S., Cramer, P., Stefl, R., *et al.* (2014). Molecular basis for coordinating transcription termination with noncoding RNA degradation. *Mol Cell* 55, 467-481.
- Tuzon, C.T., Wu, Y., Chan, A., and Zakian, V.A. (2011). The *Saccharomyces cerevisiae* telomerase subunit Est3 binds telomeres in a cell cycle- and Est1-dependent manner and interacts directly with Est1 in vitro. *Plos Genet* 7, e1002060.
- Van Hoof, A., Lennertz, P., and Parker, R. (2000a). Yeast exosome mutants accumulate 3'-extended polyadenylated forms of U4 small nuclear RNA and small nucleolar RNAs. *Mol Cell Biol* 20, 441-452.
- van Hoof, A., Staples, R.R., Baker, R.E., and Parker, R. (2000b). Function of the Ski4p (Csl4p) and Ski7p proteins in 3'-to-5' degradation of mRNA. *Mol Cell Biol* 20, 8230-8243.
- Vanacova, S., Wolf, J., Martin, G., Blank, D., Dettwiler, S., Friedlein, A., Langen, H., Keith, G., and Keller, W. (2005). A new yeast poly(A) polymerase complex involved in RNA quality control. *Plos Biol* 3, 986-997.
- Vasiljeva, L., Kim, M., Mutschler, H., Buratowski, S., and Meinhart, A. (2008). The Nrd1-Nab3-Sen1 termination complex interacts with the Ser5-phosphorylated RNA polymerase II C-terminal domain. *Nat Struct Mol Biol* 15, 795-804.
- Vega, L.R., Phillips, J.A., Thornton, B.R., Benanti, J.A., Onigbanjo, M.T., Toczyski, D.P., and Zakian, V.A. (2007). Sensitivity of yeast strains with long G-tails to levels of telomere-bound telomerase. *Plos Genet* 3, e105.
- Virta-Pearlman, V., Morris, D.K., and Lundblad, V. (1996). Est1 has the properties of a single-stranded telomere end-binding protein. *Genes Dev* 10, 3094-3104.
- Vodenicharov, M.D., and Wellinger, R.J. (2007). The cell division cycle puts up with unprotected

- telomeres: cell cycle regulated telomere uncapping as a means to achieve telomere homeostasis. *Cell Cycle* **6**, 1161-1167.
- Wang, S.S., and Zakian, V.A. (1990). Sequencing of *Saccharomyces* telomeres cloned using T4 DNA polymerase reveals two domains. *Molecular and cellular biology* **10**, 4415-4419.
- Watson, J.D. (1972). Origin of Concatemeric T7 DNA. *Nature-New Biol* **239**, 197-&.
- Weir, J.R., Bonneau, F., Hentschel, J., and Conti, E. (2010). Structural analysis reveals the characteristic features of Mtr4, a DExH helicase involved in nuclear RNA processing and surveillance. *Proceedings of the National Academy of Sciences of the United States of America* **107**, 12139-12144.
- Weirich, C.S., Erzberger, J.P., Berger, J.M., and Weis, K. (2004). The N-terminal domain of Nup159 forms a beta-propeller that functions in mRNA export by tethering the helicase Dbp5 to the nuclear pore. *Mol Cell* **16**, 749-760.
- Wellinger, R.J., Wolf, A.J., and Zakian, V.A. (1993a). Origin activation and formation of single-strand TG1-3 tails occur sequentially in late S phase on a yeast linear plasmid. *Molecular and cellular biology* **13**, 4057-4065.
- Wellinger, R.J., Wolf, A.J., and Zakian, V.A. (1993b). *Saccharomyces* telomeres acquire single-strand TG1-3 tails late in S phase. *Cell* **72**, 51-60.
- Wellinger, R.J., and Zakian, V.A. (2012). Everything you ever wanted to know about *Saccharomyces cerevisiae* telomeres: beginning to end. *Genetics* **191**, 1073-1105.
- Will, C.L., and Luhrmann, R. (2001). Spliceosomal UsnRNP biogenesis, structure and function. *Current opinion in cell biology* **13**, 290-301.
- Windgassen, M., and Krebber, H. (2003). Identification of Gbp2 as a novel poly(A)<sup>+</sup> RNA-binding protein involved in the cytoplasmic delivery of messenger RNAs in yeast. *Embo Rep* **4**, 278-283.
- Winston, F., Dollard, C., and Ricupero, S.L. (1995). Construction of a Set of Convenient *Saccharomyces-Cerevisiae* Strains That Are Isogenic to S288c. *Yeast* **11**, 53-55.
- Wotton, D., and Shore, D. (1997). A novel Rap1p-interacting factor, Rif2p, cooperates with Rif1p to regulate telomere length in *Saccharomyces cerevisiae*. *Genes Dev* **11**, 748-760.
- Wright, J.H., and Zakian, V.A. (1995). Protein-DNA interactions in soluble telosomes from *Saccharomyces cerevisiae*. *Nucleic acids research* **23**, 1454-1460.
- Wu, Y., and Zakian, V.A. (2011). The telomeric Cdc13 protein interacts directly with the telomerase subunit Est1 to bring it to telomeric DNA ends in vitro. *Proceedings of the National Academy of Sciences of the United States of America* **108**, 20362-20369.
- Wyers, F., Rougemaille, M., Badis, G., Rousselle, J.C., Dufour, M.E., Boulay, J., Regnault, B., Devaux, F., Namane, A., Seraphin, B., *et al.* (2005). Cryptic Pol II transcripts are degraded by a nuclear quality control pathway involving a new poly(A) polymerase. *Cell* **121**, 725-737.
- Yao, W., Roser, D., Kohler, A., Bradatsch, B., Bassler, J., and Hurt, E. (2007). Nuclear export of ribosomal 60S subunits by the general mRNA export receptor Mex67-Mtr2. *Mol Cell* **26**, 51-62.
- Yi, X., Tesmer, V.M., Savre-Train, I., Shay, J.W., and Wright, W.E. (1999). Both transcriptional and posttranscriptional mechanisms regulate human telomerase template RNA levels. *Molecular and cellular biology* **19**, 3989-3997.
- Zappulla, D.C., and Cech, T.R. (2004). Yeast telomerase RNA: a flexible scaffold for protein subunits. *Proceedings of the National Academy of Sciences of the United States of America* **101**, 10024-10029.
- Zappulla, D.C., Goodrich, K., and Cech, T.R. (2005). A miniature yeast telomerase RNA functions in vivo

- and reconstitutes activity in vitro. *Nat Struct Mol Biol* 12, 1072-1077.
- Zenklusen, D., Vinciguerra, P., Strahm, Y., and Stutz, F. (2001). The yeast hnRNP-Like proteins Yra1p and Yra2p participate in mRNA export through interaction with Mex67p. *Molecular and cellular biology* 21, 4219-4232.
- Zenklusen, D., Vinciguerra, P., Wyss, J.C., and Stutz, F. (2002). Stable mRNP formation and export require cotranscriptional recruitment of the mRNA export factors Yra1p and Sub2p by Hpr1p. *Molecular and cellular biology* 22, 8241-8253.

# Acknowledgments

Filling in the last word in this thesis is ending of a stage of my life. Experiences during these years will be a precious gift which will lead me and accompany with me. Countless thanks to those people, who instruct me, encourage me and move me.

I would like to send my greatest gratefulness to Prof. Dr. Heike Krebber, for guiding me into a new world and for always inspiring me on the way of this beautiful exploration.

I would also like to express my sincere gratitude to PD Dr. Wilfried Kramer, for sharing his excellent and exhaustive minds on the aspects of both science and life.

I would like to thank Prof. Dr. Holger Bastians for his heartfelt support on my future investigation.

I would like to thank Prof. Dr. Gerhard Braus, Prof. Dr. Ralf Ficner, Prof. Dr. Stefanie Pöggeler, Prof. Dr. Kai Heimel for spending time on evaluating my work.

I would like to thank Dr. Alexandra Hackmann, Daniel Becker and Ulla-Maria Schneider for their helpful collaborations and selfless contributions to my work.

I would like to thank all of my dear lab colleagues, Dr. Claudia Baierlein, Lysann Henker, Bettina Tieg, Gesa Zander, Lena Oldehaver, Angelika Löffers and Angela Bindseil for sharing our emotions, for treating me like a real family member and for bringing me endless happy memories.

I am also grateful to those, who have ever helped me and encouraged me: members of group of Prof. Dr. Holger Bastians, Dr. Norman Ertych, Dr. Aline Stolz, Dr. Phillip Kaestner, Dr. Makus Becker, Sina Lüddecke and Katharina Berger.

I would also like to express lots of gratitude but also apologies to my parents and my in-laws, Fengming Ma, Guoping Wu, Tang Li and Li Li, for their unconditional love and support even by disappointment only, for being not able to fulfill my duty as a son for too long time and for never doing enough to repay them.

The last, but not the least part is dedicated to my wife, Sangmeng Li. There are many thanks beyond words to her for only encouraging me but never pressing me. It is the luckiest thing to meet her and know her in my life and it is the happiest thing to share the rest of my life with her.



# ***Curriculum Vitae***

- Year2011-2015      Georg-August-University Göttingen, Germany  
Dept. Molecular Genetics, Institute of Microbiology and Genetics  
Ph.D. Candidate in group of Prof. Dr. Heike Krebber
- Year2009-2011      Philipps-University Marburg, Germany  
IMT (Institute of Molecular Biology and Tumor Research)  
Ph.D. Candidate in group of Prof. Dr. Heike Krebber
- Year2003-2009      Eberhard-Karls University Tübingen, Germany  
Diploma Biologie (Dipl.-Biol.)
- Year2008-2009      The Max Planck Institute for Developmental Biology, Tübingen Germany  
Diploma thesis in group of Prof. Dr. Ingrid Lohmann
- Year1996-2000      Huazhong Agriculture University in Wuhan, Hubei province, China  
Bachelor of Science (B.Sc) in microbiology
- Year1984-1996      Basic Education in Shuiguohu School in Wuhan, Hubei province, China